

# GRADIENT-NORMALIZED SMOOTHNESS FOR OPTIMIZATION WITH APPROXIMATE HESSIANS

000  
001  
002  
003  
004  
005 **Anonymous authors**  
006 Paper under double-blind review  
007  
008  
009  
010

## ABSTRACT

011 In this work, we develop new optimization algorithms that use approximate second-  
012 order information combined with the gradient regularization technique to achieve  
013 fast global convergence rates for both convex and non-convex objectives. The key  
014 innovation of our analysis is a novel notion called Gradient-Normalized Smooth-  
015 ness, which characterizes the maximum radius of a ball around the current point that  
016 yields a good relative approximation of the gradient field. Our theory establishes a  
017 natural intrinsic connection between Hessian approximation and the linearization  
018 of the gradient. Importantly, Gradient-Normalized Smoothness does not depend on  
019 the specific problem class of the objective functions, while effectively translating  
020 local information about the gradient field and Hessian approximation into the global  
021 behavior of the method. This new concept equips approximate second-order algo-  
022 rithms with universal global convergence guarantees, recovering state-of-the-art  
023 rates for functions with Hölder-continuous Hessians and third derivatives, Quasi-  
024 Self-Concordant functions, as well as smooth classes in first-order optimization.  
025 These rates are achieved automatically and extend to broader classes, such as  
026 generalized self-concordant functions. We demonstrate direct applications of our  
027 results for global linear rates in logistic regression and softmax problems with  
028 approximate Hessians, as well as in non-convex optimization using Fisher and  
029 Gauss-Newton approximations.  
030

## 1 INTRODUCTION

031 **Motivation.** Numerical optimization methods that use *preconditioning* or *second-order* information—  
032 such as Newton-type methods—are extensively applied in machine learning, artificial intelligence,  
033 and scientific computing. While gradient-based methods—such as Gradient Descent—form a solid  
034 foundation for many large-scale applications due to their low per-iteration cost and well-established  
035 convergence theory, second-order methods are known to significantly accelerate convergence by  
036 taking into account the curvature information of the objective function. However, although the  
037 modern theory of second-order optimization establishes strong complexity guarantees for the Newton  
038 method with appropriate regularization techniques (Nesterov, 2018; Nesterov & Polyak, 2006; Cartis  
039 et al., 2011a; Doikov et al., 2024a), the theory for *inexact Hessians* is usually much more limited,  
040 suggesting that errors coming from the Hessian inexactness might drastically slow down convergence,  
041 causing the method to converge as slowly as Gradient Descent (Agafonov et al., 2024; Chayti et al.,  
042 2023). In this work, we aim to develop a new convergence theory for second-order methods with  
043 approximate Hessians, that matches state-of-the-art rates for the exact Newton method and bridges  
044 the geometry of the objective function with conditions on the Hessian approximation. The form of  
045 our method is very simple. For unconstrained minimization of the function  $f$ , using the standard  
046 Euclidean norm, we perform:

$$047 \quad \mathbf{x}_{k+1} = \mathbf{x}_k - \left( \mathbf{H}_k + \frac{\|\nabla f(\mathbf{x}_k)\|}{\gamma_k} \mathbf{I} \right)^{-1} \nabla f(\mathbf{x}_k), \quad k \geq 0, \quad (1)$$

048 where  $\mathbf{H}_k \succeq \mathbf{0}$  is a Hessian approximation matrix, and  $\gamma_k > 0$  is a (second-order) step-size. This  
049 parametrization ensures that each step is bounded,  $\|\mathbf{x}_{k+1} - \mathbf{x}_k\| \leq \gamma_k$ , and for  $\mathbf{H}_k = \mathbf{0}$  we obtain  
050 iterations of the normalized gradient descent (Nesterov, 2024). Moreover, in the case of the exact  
051 Hessians,  $\mathbf{H}_k = \nabla^2 f(\mathbf{x}_k)$ , the gradient regularization (1) was shown to achieve both very fast  
052 *quadratic local convergence*, as for the classical Newton method (Polyak, 2007), and strong global  
053 rates for a wide range of convex problem classes (Polyak, 2009; Doikov et al., 2024a; Doikov, 2023).  
054 In this paper, we relax  $\mathbf{H}_k \approx \nabla^2 f(\mathbf{x}_k)$  to be a Hessian approximation in (1). We consider the

054 following condition for our method:  
 055

$$056 \quad \|\nabla^2 f(\mathbf{x}_k) - \mathbf{H}_k\| \leq \mathbf{C}_1 + \mathbf{C}_2 \|\nabla f(\mathbf{x}_k)\|^{1-\beta}, \quad 0 \leq \beta \leq 1, \quad (2)$$

057 for certain  $\mathbf{C}_1, \mathbf{C}_2 \geq 0$ , and  $\beta$  is a fixed *approximation degree*. This condition appears to be  
 058 essentially satisfied by many natural approximations of the Hessian, such as Fisher or Gauss-Newton  
 059 approximations. For example, for the finite-sum structure of the objective  $f(\mathbf{x}) = \sum_{i=1}^n f_i(\mathbf{x})$ , that  
 060 is popular in applications from machine learning and statistics, one can take the Fisher approximation,  
 061

$$062 \quad \mathbf{H}_k := \sum_{i=1}^n \nabla f_i(\mathbf{x}_k) \nabla f_i(\mathbf{x}_k)^\top. \quad (3)$$

063 For simplicity, we consider here all gradients computed at the same point  $\mathbf{x}_k$ , while in practice the  
 064 gradients can be taken from the past (Frantar et al., 2021) (see also (Martens, 2020) and (Kunstner  
 065 et al., 2019) for an in-depth analysis of the Natural Gradient Descent and its variants). It appears  
 066 that this approximation (3), e.g., for the logistic regression problem or softmax with linear models  
 067 (Examples 6, 8) satisfies (2) with  $\beta = 0$ , and  $\mathbf{C}_1 = f^*$  (the global optimum), which can be small or  
 068 even zero for the well-separable data.

069 As a direct consequence of our new theory, we show that method (1), using the approximate  
 070 Hessian (3), exhibits the *global linear rate*, as soon as  $f^*$  is sufficiently small. This stands in stark  
 071 contrast to classical gradient methods, which typically achieve only sublinear convergence rates,  
 072 unless additional assumptions—such as strong or uniform convexity—are imposed. Notably, our  
 073 method remains formally first-order, relying solely on access to the first-order oracle.

074 Other examples include nonconvex problems with nonlinear operators, which satisfy (2) even with  
 075  $\mathbf{C}_1 = 0$  and  $\beta = 0$ , where  $\mathbf{H}_k$  is a specific combinations of Gauss-Newton and Fisher matrices  
 076 (see Examples 7, 8). We show that in these cases, when the degree  $\beta$  of Hessian approximation is  
 077 smaller than the degree of smoothness  $\alpha$  (see the formal definition in Section 4), the errors coming  
 078 from Taylor’s approximation dominate the Hessian inexactness. In these situation ( $\mathbf{C}_1 \approx 0$ ,  $\mathbf{C}_2 > 0$ ,  
 079 and  $\alpha \geq \beta$ ), our method with inexact Hessians has the *same global rate* as the full Newton method  
 080 ( $\mathbf{C}_1 = \mathbf{C}_2 = 0$ ), see Figure 1.

081 **Contributions.** In this work, we develop a new frame-  
 082 work for describing the global behavior of second-order  
 083 methods using a universal (problem-class free) local char-  
 084 acterization of the objective’s gradient field and Hessian  
 085 approximation, called *Gradient-Normalized Smoothness*  
 086 (Section 2). We propose a unified treatment for the er-  
 087 rors coming from both Hessian inexactness and Taylor’s  
 088 approximation, thereby showing an intrinsic connection  
 089 between them. Our theory provides method (1) with a  
 090 universal step-size rule for  $\gamma_k$ , which adapts automatically  
 091 to the right problem class (which is described by the *de-  
 092 gree of smoothness*,  $0 \leq \alpha \leq 1$ , introduced in Section 4)  
 093 and the Hessian approximation error (2). See Table 1  
 094 for the summary of the complexity results covered by our  
 095 Gradient-Normalized Smoothness, for particular problem  
 096 classes.

097 **(I) For the case of Exact Newton**,  $\mathbf{H}_k = \nabla^2 f(\mathbf{x}_k)$ , we ultimately recover the state-of-the-art rates  
 098 obtained in (Doikov et al., 2024a; Doikov, 2023) for functions with Hölder continuous Hessian  
 099 ( $\frac{1}{2} \leq \alpha \leq 1$ ), Hölder continuous third derivative ( $\frac{1}{3} \leq \alpha \leq \frac{1}{2}$ ), and Quasi-Self-Concordant functions  
 100 ( $\alpha = 0$ ). Our theory also extends to generalized Self-Concordant functions (Sun & Tran-Dinh, 2018),  
 101 which correspond to  $0 \leq \alpha \leq \frac{1}{2}$ , establishing novel global rates in this range. Beyond that, the  
 102 Gradient-Normalized Smoothness framework allows us to treat  $(L_0, L_1)$ -smooth functions (Zhang  
 103 et al., 2019; Xie et al., 2024) from both first-order and second-order optimization (see examples in  
 104 Section 2). Our convergence theory works both in convex and nonconvex cases (Theorems 1,2).

105 **(II) For the Inexact Hessian**, we use condition (2) to control the approximation errors, which is  
 106 automatically covered by our notion of Gradient-Normalized Smoothness and provides us with the  
 107 corresponding convergence rates. An interesting observation from our theory is that, in the regime  
 108  $\alpha \geq \beta$  and  $\mathbf{C}_1 \approx 0$ , *the smoothness class of the objective dominates the Hessian approximation*,  
 109 and we recover the same rates as for the exact Hessian (see Fig. 1). As a by-product, we establish

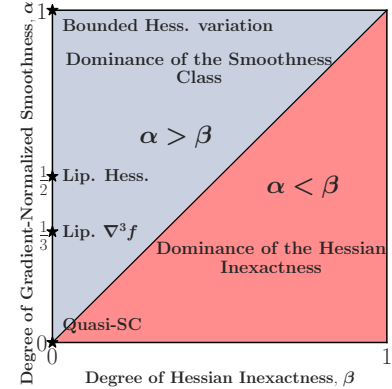


Figure 1: **Global Convergence Diagram for Algorithm 1.** We see that, for  $\alpha \geq \beta$ , the problem class of  $f$  dominates the Hessian inexactness, and our method achieves the same rate as full Newton.

Problem class	Exact Case ( $\mathbf{C}_1 = \mathbf{C}_2 = 0$ )	Inexact Hess. (ours)
Bounded Hess. variation	$O\left(\frac{M_0 D^2}{\varepsilon}\right)$ (Nesterov, 2018)	$O\left(\frac{(M_0 + \mathbf{C}_2) D^2}{\varepsilon} + \frac{\mathbf{C}_1 D^2}{\varepsilon}\right)$
Lip. Hess.	$O\left(\frac{M_{1/2} D^{3/2}}{\varepsilon^{1/2}}\right)$ (Nesterov & Polyak, 2006)	$O\left(\frac{(M_{1/2} + \mathbf{C}_2) D^{3/2}}{\varepsilon^{1/2}} + \frac{\mathbf{C}_1 D^2}{\varepsilon}\right)$
Lip. $\nabla^3 f$	$O\left(\frac{M_{1/3} D^{4/3}}{\varepsilon^{1/3}}\right)$ (Doikov et al., 2024a)	$O\left(\frac{(M_{1/3} + \mathbf{C}_2) D^{4/3}}{\varepsilon^{1/3}} + \frac{\mathbf{C}_1 D^2}{\varepsilon}\right)$
Gen.-SC, $0 < \alpha \leq 1/2$	$O\left(\frac{M_{1-\alpha} D^{1+\alpha}}{\varepsilon^\alpha}\right)$ (ours)	$O\left(\frac{(M_{1-\alpha} + \mathbf{C}_2) D^{1+\alpha}}{\varepsilon^\alpha} + \frac{\mathbf{C}_1 D^2}{\varepsilon}\right)$
Quasi-SC, $\alpha = 0$	$\tilde{O}(M_1 D)$ (Doikov, 2023)	$\tilde{O}\left((M_1 + \mathbf{C}_2) D + \frac{\mathbf{C}_1 D^2}{\varepsilon}\right)$

**Table 1: Global complexities for our Algorithm 1 on different problem classes with convex objectives and using inexact Hessian.** We show the number of iterations  $K$  required to find  $\varepsilon$ -solution to our problem:  $f(\mathbf{x}_K) - f^* \leq \varepsilon$ . Note that we recover state-of-the-art rates for the exact Newton ( $\mathbf{C}_1 = \mathbf{C}_2 = 0$ ) in all particular cases, and extend them to the inexact Hessians. The global rates for the Generalized Self-Concordant (Gen.-SC) functions, introduced in (Sun & Tran-Dinh, 2018), are also novel in the exact case.

new global convergence rates for several practical problems (see Section 5) particularly when using approximate Hessian information, such as Fisher and Gauss-Newton matrices, which are popular in machine learning.

**(III) Numerical experiments** (Section 6 and Appendix B) illustrate our theory and confirm excellent performance of method (2) with our step-size selection and Hessian approximations.

**Related Work.** Using a scalable approximation of the Hessian matrix in Newton’s method remains an attractive and popular approach to addressing the ill-conditioning of the function by better capturing the problem’s geometry. Various examples include: low-rank approximations of the Hessian or quasi-Newton methods (Dennis & Moré, 1977; Jorge & Stephen, 2006; Rodomanov & Nesterov, 2021; Rodomanov, 2022; Jin & Mokhtari, 2023), spectral preconditioning (Ma et al., 2023; Zhang et al., 2023; Doikov et al., 2024b), first- and zeroth-order approximations (Cartis et al., 2012; Grapiglia et al., 2022; Doikov & Grapiglia, 2025), the Fisher and Gauss-Newton approximations (Nesterov, 2007; Kunstner et al., 2019; Arbel et al., 2023), stochastic subspaces or sketches (Cartis & Scheinberg, 2018; Gower et al., 2019; Fuji et al., 2022; Zhao et al., 2025; Hanzely, 2025), and many others. Modern techniques to globalize Newton’s method, include the cubic regularization (Griewank, 1981; Nesterov & Polyak, 2006; Cartis et al., 2011a;b) and gradient regularization (Polyak, 2009; Mishchenko, 2023; Doikov & Nesterov, 2023; Doikov et al., 2024a; Doikov, 2023), that constitute the main basis of our work. Another popular approach consists in trust-region methods (Conn et al., 2000; Jiang et al., 2023; Xie et al., 2024), the notion Hessian stability (Karimireddy et al., 2018), and quasi-Newton methods with global convergence (Kamzolov et al., 2023; Scieur, 2024; Rodomanov, 2024; Jin et al., 2024). In recent years, we have seen more and more interesting deviations from the classical picture of complexity theory (Nemirovski & Yudin, 1983), with new important problem classes emerging from modern applications. These include the notion of *relative smoothness* (Bauschke et al., 2017; Lu et al., 2018), or  $(L_0, L_1)$ -smoothness (see (Zhang et al., 2019; Koloskova et al., 2023; Gorbunov et al., 2024; Vankov et al., 2024) and references therein), especially motivated by empirical smoothness properties of neural networks. While each of these new problem classes typically requires special attention—designing a new method and establishing the corresponding convergence theory—it is becoming increasingly evident that *the most natural optimization schemes are universal*, in the sense that they can automatically adapt to the appropriate degree of smoothness without requiring knowledge of any specific parameters (Nesterov, 2015; 2024).

**Notation.** Let us consider unconstrained minimization problem,

$$\min_{\mathbf{x} \in \mathbb{R}^n} f(\mathbf{x}), \quad (4)$$

where  $f : \mathbb{R}^n \rightarrow \mathbb{R}$  is a differentiable function, that can be *non-convex*. Let  $f^* := \inf_{\mathbf{x} \in \mathbb{R}^n} f(\mathbf{x})$ , which we assume to be finite:  $f^* > -\infty$ . We denote by  $\nabla f(\mathbf{x}) \in \mathbb{R}^n$  the gradient vector at point  $\mathbf{x} \in \mathbb{R}^n$  and by  $\nabla^2 f(\mathbf{x}) \in \mathbb{R}^{n \times n}$  the Hessian, which is a symmetric matrix. The third derivative,  $\nabla^3 f(\mathbf{x})$ , is a tri-linear symmetric form. We denote by  $\nabla^3 f(\mathbf{x})[\mathbf{h}_1, \mathbf{h}_2, \mathbf{h}_3] \in \mathbb{R}$  its action onto arbitrary directions  $\mathbf{h}_1, \mathbf{h}_2, \mathbf{h}_3 \in \mathbb{R}^n$ . Let us fix a symmetric positive-definite matrix  $\mathbf{B} \succ 0$ , which we use to define a pair of *global* Euclidean norms in our space:

$$\|\mathbf{h}\| := \langle \mathbf{B}\mathbf{h}, \mathbf{h} \rangle^{1/2}, \quad \|\mathbf{s}\|_* := \langle \mathbf{s}, \mathbf{B}^{-1}\mathbf{s} \rangle^{1/2}, \quad \mathbf{h}, \mathbf{s} \in \mathbb{R}^n,$$

which satisfy the Cauchy-Schwarz inequality:  $|\langle \mathbf{s}, \mathbf{h} \rangle| \leq \|\mathbf{s}\|_* \|\mathbf{h}\|$ . We use the dual norm to measure the size of the gradients. In the simplest case, we can set  $\mathbf{B} := \mathbf{I}$  (identity matrix), which gives the

162 classical Euclidean norm, while, in some cases, the use of a specific  $\mathbf{B}$  can significantly improve the  
 163 global geometry and convergence of our methods (see Section 5 for examples). Correspondingly, we  
 164 use the induced spectral norm for symmetric matrices and multi-linear forms, e.g.

$$165 \|\nabla^2 f(\mathbf{x})\| := \max_{\mathbf{h}: \|\mathbf{h}\| \leq 1} |\langle \nabla f(\mathbf{x}) \mathbf{h}, \mathbf{h} \rangle|, \quad \|\nabla^3 f(\mathbf{x})\| := \max_{\mathbf{h}: \|\mathbf{h}\| \leq 1} \nabla^3 f(\mathbf{x})[\mathbf{h}, \mathbf{h}, \mathbf{h}].$$

167 Along with the global norm in our space, we can also define the following *local norm* (Nesterov &  
 168 Nemirovski, 1994), which is induced by the Hessian of the objective, for any  $\mathbf{x} \in \mathbb{R}^n$ :  $\|\mathbf{h}\|_{\mathbf{x}}^2 :=$   
 169  $\langle \nabla^2 f(\mathbf{x}) \mathbf{h}, \mathbf{h} \rangle$ ,  $\mathbf{h} \in \mathbb{R}^n$ . Note that we use this notion even for points where the Hessian is not  
 170 positive definite. However,  $\|\cdot\|_{\mathbf{x}}$  is a well-defined norm for  $\mathbf{x}$  where  $\nabla^2 f(\mathbf{x}) \succ 0$ , which holds for  
 171 strictly convex functions.

## 172 2 GRADIENT-NORMALIZED SMOOTHNESS

174 Our aim is to characterize and approximate the behavior of the gradient field  $\nabla f(\cdot)$ , induced by  
 175 our objective. Along with it, we denote by  $\mathbf{H}(\cdot) \in \mathbb{R}^{n \times n}$ , the *matrix field* which assigns to every  
 176 point  $\mathbf{x} \in \mathbb{R}^n$  a symmetric positive-semidefinite matrix which serves as our Hessian approximation,  
 177  $\mathbf{H}(\mathbf{x}) \approx \nabla^2 f(\mathbf{x})$ . We will use this matrix directly in our algorithms (see Section 3 and corresponding  
 178 examples). We would like to use it for the following *linear approximation* of the gradient field in a  
 179 neighbourhood of the current point:

$$180 \nabla f(\mathbf{x} + \mathbf{h}) \approx \nabla f(\mathbf{x}) + \mathbf{H}(\mathbf{x}) \mathbf{h}. \quad (5)$$

181 The examples include:  $\mathbf{H} \equiv \nabla^2 f$ , exact Hessian, which provides us with the Newton approximation  
 182 in (5), or  $\mathbf{H} \equiv \mathbf{0}$ , zero matrix. The latter case corresponds to first-order methods.

184 **Definitions.** For a given  $\gamma > 0$ , we denote the ball  $B_{\gamma} := \{\mathbf{h} : \|\mathbf{h}\| \leq \gamma\}$ . Moreover, employing  
 185 the local norm, we define the following *local region*, at point  $\mathbf{x}$  and for an arbitrary direction  $\mathbf{g} \in \mathbb{R}^n$ :

$$186 \mathcal{O}_{\mathbf{x}, \mathbf{g}} := \{\mathbf{h} : \|\mathbf{h}\|_{\mathbf{x}}^2 + \langle \mathbf{g}, \mathbf{h} \rangle \leq 0\}. \quad (6)$$

188 Note that for  $\nabla^2 f(\mathbf{x}) \succ 0$  this set is an ellipsoid centered around the Newton direction:  $\mathcal{O}_{\mathbf{x}, \mathbf{g}} =$   
 189  $\{\mathbf{h} : \|\mathbf{h} + \frac{1}{2} \nabla^2 f(\mathbf{x})^{-1} \mathbf{g}\|_{\mathbf{x}}^2 \leq \frac{1}{4} \|\mathbf{g}\|_{\mathbf{x},*}^2 := \frac{1}{4} \langle \mathbf{g}, \nabla^2 f(\mathbf{x})^{-1} \mathbf{g} \rangle\}$ , and its geometry depends on the  
 190 properties of the objective. For non-convex functions,  $\mathcal{O}_{\mathbf{x}, \mathbf{g}}$  can be unbounded. Nevertheless, we  
 191 always intersect it with the Euclidean ball  $B_{\gamma}$ , thus working solely with bounded directions. Using  
 192 our local regions, we introduce new characteristic, called the *Gradient-Normalized Smoothness*:

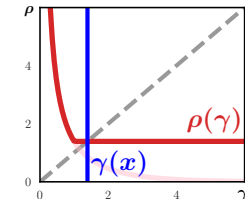
193 **Definition 1.** For any  $\mathbf{x} \in \mathbb{R}^n$  and direction  $\mathbf{g} \in \mathbb{R}^n$ , denote

$$195 \gamma(\mathbf{x}, \mathbf{g}) := \max \{\gamma \geq 0 : \|\nabla f(\mathbf{x} + \mathbf{h}) - \nabla f(\mathbf{x}) - \mathbf{H}(\mathbf{x}) \mathbf{h}\|_* \leq \frac{\|\mathbf{g}\|_* \|\mathbf{h}\|}{\gamma}, \forall \mathbf{h} \in B_{\gamma} \cap \mathcal{O}_{\mathbf{x}, \mathbf{g}}\}.$$

197 Thus, quantity  $\gamma(\mathbf{x}, \mathbf{g})$  describes the maximal radius of the Euclidean ball around point  $\mathbf{x}$ , within  
 198 which the error of linear approximation of the gradient field (5) is relatively small across all feasible  
 199 directions  $\mathbf{h}$ . Note that the local region  $\mathcal{O}_{\mathbf{x}, \mathbf{g}}$  only restricts the set of possible directions, and hence it  
 200 can only improve  $\gamma(\mathbf{x}, \mathbf{g})$ . It appears that including set  $\mathcal{O}_{\mathbf{x}, \mathbf{g}}$  in the definition is crucial to make the  
 201 modulus of smoothness  $\gamma(\cdot)$  large enough, for second-order problem classes that we present below.

202 In order to better understand the definition, let us introduce the following univariate function, at a given point  $\mathbf{x} \in \mathbb{R}^n$ :  $\rho(\gamma) :=$   
 203  $\min_{\mathbf{h} \in B_{\gamma} \cap \mathcal{O}_{\mathbf{x}, \mathbf{g}}} \{\|\nabla f(\mathbf{x} + \mathbf{h}) - \nabla f(\mathbf{x}) - \mathbf{H}(\mathbf{x}) \mathbf{h}\|_*^{-1} \|\mathbf{g}\|_* \|\mathbf{h}\|\}$ , where  
 204  $\gamma \geq 0$ . Clearly,  $\rho(\cdot)$  is monotonically decreasing, starting from some  
 205 large limit<sup>1</sup> value  $\rho(0)$ . Its graph is shown in Fig. 2. Then, the value of  
 206  $\gamma(\mathbf{x}, \mathbf{g})$  is the intersection of  $\rho(\cdot)$  with the main diagonal. These obser-  
 207 vations also demonstrate *monotonicity in  $\gamma$* : if the inequality from the  
 208 definition holds for some  $\gamma \geq 0$ , then it also holds for all  $0 \leq \gamma' \leq \gamma$ ,  
 209 and, by definition,  $\gamma(\mathbf{x}, \mathbf{g})$  is the *maximal possible* radius. Among all  
 210 possible directions at  $\mathbf{x}$ , the most important is  $\mathbf{g} = \nabla f(\mathbf{x})$ . For that, we  
 211 naturally define:

$$213 \gamma(\mathbf{x}) := \gamma(\mathbf{x}, \nabla f(\mathbf{x})).$$



214 **Figure 2:** The plot of  $\rho(\cdot)$  for  
 215  $f(x) = e^x$ . In this case,  $\gamma(x) \equiv$   
 $(e - 2)^{-1} \approx 1.39$  for all  $x \in \mathbb{R}$ .

<sup>1</sup>The limit always exists when  $f$  is sufficiently smooth at  $\mathbf{x}$ .

As we will see in Section 3,  $\gamma(\mathbf{x})$  provides us with the right *step-size* in our algorithm, that *automatically adjusts* to the best problem class and the degree of the Hessian approximation  $\nabla^2 f(\mathbf{x}) \approx \mathbf{H}(\mathbf{x})$  at the current point. It is possible to generalize our results to Composite Optimization Problems (Appendix C), which includes constrained optimization and non-smooth regularizers. In this case, we need to use for  $\mathbf{g}$  a *perturbed gradient direction*, that depends on the composite component.

**Basic Properties.** First, let us consider a stationary point  $\mathbf{x}^*$  which is a *strict local minimum*, so it holds:  $\nabla f(\mathbf{x}^*) = \mathbf{0}$  and  $\nabla^2 f(\mathbf{x}^*) \succ \mathbf{0}$ . Then, by our definition we have  $\gamma(\mathbf{x}^*) = +\infty$ , which means *no regularization* in our method. This implies that being in a neighborhood of the solution, the algorithm will switch to pure Newton steps, which confirms the intuition that the classical Newton's method has the best local behavior. Note that for quadratic functions and setting  $\mathbf{H} := \nabla^2 f$ , the linearization (5) is exact, and we also have  $\gamma \equiv +\infty$ . At the same time, when  $\gamma(\mathbf{x})$  is small, it indicates a need for regularization.

Now, we can state how the Gradient-Normalized Smoothness  $\gamma(\cdot)$  changes under simple operations <sup>2</sup>

1. *Scale-invariance.* Let  $\gamma_f(\mathbf{x})$  be the Gradient-Normalized Smoothness for function  $f$  and let  $\mathbf{g} := c \cdot \mathbf{f}$  for some  $c > 0$ . Accordingly, we set  $\mathbf{H}_g := c\mathbf{H}_f$ . Then,  $\gamma_g(\mathbf{x}) \equiv \gamma_f(\mathbf{x})$ .
2. *Affine substitution.* Let  $\mathbf{g}(\mathbf{x}) := f(\mathbf{A}\mathbf{x} + \mathbf{b})$  for some invertible  $\mathbf{A} \in \mathbb{R}^{n \times n}$  and  $\mathbf{b} \in \mathbb{R}^n$ . Set  $\mathbf{H}_g(\mathbf{x}) := \mathbf{A}^\top \mathbf{H}_f(\mathbf{A}\mathbf{x} + \mathbf{b})\mathbf{A}$ . Then,  $\gamma_g(\mathbf{x}) \geq \gamma_f(\mathbf{x}) \cdot \|\mathbf{A}\|^{-1}$ .
3. *Sum of functions.* Let  $f := \sum_{i=1}^d f_i$ . Then,  $\gamma_f$  is bounded by the Harmonic mean:

$$\gamma_f(\mathbf{x}, \mathbf{g}) \geq \left( \sum_{i=1}^d \gamma_{f_i}(\mathbf{x}, \mathbf{g})^{-1} \right)^{-1}, \quad \mathbf{x}, \mathbf{g} \in \mathbb{R}^n.$$

4. *Hessian inexactness.* Let  $\gamma_1(\mathbf{x})$  be the Gradient-Normalized Smoothness of  $f$  when using matrix field  $\mathbf{H}_1$ . Let  $\mathbf{H}_2$  be such that  $\|\mathbf{H}_1(\mathbf{x}) - \mathbf{H}_2(\mathbf{x})\| \leq \|\nabla f(\mathbf{x})\| \cdot \gamma_{12}(\mathbf{x})^{-1}$ , for a certain function  $\gamma_{12}$ . Then, the Gradient-Normalized Smoothness of  $f$  when using  $\mathbf{H}_2$  is bounded by the Harmonic mean:  $\gamma_2(\mathbf{x}) \geq [\gamma_1(\mathbf{x})^{-1} + \gamma_{12}(\mathbf{x})^{-1}]^{-1}$ .

**Examples.** Let us study the behavior of  $\gamma(\cdot)$  when using the exact Hessian matrix,  $\mathbf{H} \equiv \nabla^2 f$ , under classical global second-order assumptions. Then, employing the known properties, we can translate it to an arbitrary Hessian approximation.

**Example 1** (Hölder Hessian). Assume that  $f$  has Hölder continuous Hessian of degree  $\nu \in [0, 1]$ :  $\|\nabla^2 f(\mathbf{x}) - \nabla^2 f(\mathbf{y})\| \leq L_{2,\nu} \|\mathbf{x} - \mathbf{y}\|^\nu$ , for all  $\mathbf{x}, \mathbf{y} \in \mathbb{R}^n$ . Then,

$$\gamma(\mathbf{x}, \mathbf{g}) \geq \left( \frac{1+\nu}{L_{2,\nu}} \|\mathbf{g}\|_* \right)^{\frac{1}{1+\nu}}, \quad \mathbf{x}, \mathbf{g} \in \mathbb{R}^n. \quad (7)$$

The most interesting are extreme cases:  $\nu = 0$  (functions with bounded variation of the Hessian) and  $\nu = 1$  (functions with Lipschitz Hessian) that gives, correspondingly:

$$\gamma(\mathbf{x}) \equiv \gamma(\mathbf{x}, \nabla f(\mathbf{x})) \geq \frac{\|\nabla f(\mathbf{x})\|_*}{L_{2,0}} \quad \text{and} \quad \gamma(\mathbf{x}) \equiv \gamma(\mathbf{x}, \nabla f(\mathbf{x})) \geq \sqrt{\frac{2\|\nabla f(\mathbf{x})\|_*}{L_{2,1}}}.$$

The following problem class was initially attributed to the third-order tensor methods (Birgin et al., 2017; Cartis et al., 2019; Nesterov, 2021a; Agafonov et al., 2024). Later on, as it was shown in (Nesterov, 2021b; Grapiglia & Nesterov, 2021; Doikov et al., 2024a), it appears to be appropriate for second-order optimization.

**Example 2** (Hölder Third Derivative). Assume that  $f$  is convex and its third derivative is Hölder of degree  $\nu \in [0, 1]$ :  $\|\nabla^3 f(\mathbf{x}) - \nabla^3 f(\mathbf{y})\| \leq L_{3,\nu} \|\mathbf{x} - \mathbf{y}\|^\nu$ , for all  $\mathbf{x}, \mathbf{y} \in \mathbb{R}^n$ . Then,

$$\gamma(\mathbf{x}, \mathbf{g}) \geq \left( \frac{1+\nu}{2^{1+\nu} L_{3,\nu}} \|\mathbf{g}\|_* \right)^{\frac{1}{2+\nu}}, \quad \mathbf{x}, \mathbf{g} \in \mathbb{R}^n.$$

**Example 3** (Quasi-Self-Concordance). Assume that  $f$  is Quasi-Self-Concordant with parameter  $M \geq 0$ :  $\langle \nabla^3 f(\mathbf{x}) \mathbf{h}, \mathbf{h}, \mathbf{u} \rangle \leq M \|\mathbf{h}\|_{\mathbf{x}}^2 \|\mathbf{u}\|$ , for all  $\mathbf{x}, \mathbf{h}, \mathbf{u} \in \mathbb{R}^n$ . Then,

$$\gamma(\mathbf{x}) \geq \frac{1}{M}.$$

<sup>2</sup>Missing proofs are provided in the appendix.

270 The following examples of  $(L_0, L_1)$ -smooth functions are popular in the context of studying smooth-  
 271 ness properties of neural networks, gradient clipping, and trust-region methods (Zhang et al., 2019;  
 272 Koloskova et al., 2023; Xie et al., 2024).

274 **Example 4**  $((L_0, L_1)$ -smooth functions (Zhang et al., 2019)). Assume that  $\|\nabla^2 f(\mathbf{x})\| \leq L_0 +$   
 275  $L_1 \|\nabla f(\mathbf{x})\|_*$ , for all  $\mathbf{x} \in \mathbb{R}^n$ . Then,

$$\gamma(\mathbf{x}, \mathbf{g}) \geq \frac{\|\mathbf{g}\|_*}{L_0 + L_1 \|\nabla f(\mathbf{x})\|_*} \cdot \left(1 + \exp\left(\frac{\|\mathbf{g}\|_*}{\|\nabla f(\mathbf{x})\|_*}\right)\right)^{-1}, \quad \mathbf{x}, \mathbf{g} \in \mathbb{R}^n.$$

279 **Example 5** (Second-order  $(M_0, M_1)$ -smooth functions (Xie et al., 2024)). Assume that  
 280  $\|\nabla^2 f(\mathbf{x}) - \nabla^2 f(\mathbf{y})\| \leq (M_0 + M_1 \|\nabla f(\mathbf{x})\|_*) \|\mathbf{x} - \mathbf{y}\|$ , for all  $\mathbf{x}, \mathbf{y} \in \mathbb{R}^n$ . Then,

$$\gamma(\mathbf{x}, \mathbf{g}) \geq \left(\frac{2\|\mathbf{g}\|_*}{L_0 + L_1 \|\nabla f(\mathbf{x})\|_*}\right)^{1/2}, \quad \mathbf{x}, \mathbf{g} \in \mathbb{R}^n.$$

284 In practice, the objective function can belong to several of problem classes simultaneously, and  
 285 optimal parameters can vary with  $\mathbf{x}$ . Therefore, it is important that the definition of  $\gamma(\cdot)$  is *local*, just  
 286 adjusting universally to the best of these cases. This allows the method to achieve the fastest rate.

### 287 3 ALGORITHM

288 The method is very simple.

---

#### 290 **Algorithm 1** Gradient-Regularized Newton with Approximate Hessians

---

291 **Initialization:**  $\mathbf{x}_0 \in \mathbb{R}^n$ .

292 1: **for**  $k \geq 0$  **do**  
 293 2:     Choose  $\mathbf{H}(\mathbf{x}_k) \succeq \mathbf{0}$  and  $\gamma_k > 0$ . ▷ In practice, use adaptive search for  $\gamma_k$  (Alg. 3).  
 294 3:     Perform update:  $\mathbf{x}_{k+1} \leftarrow \mathbf{x}_k - \left(\mathbf{H}(\mathbf{x}_k) + \frac{\|\nabla f(\mathbf{x}_k)\|_* \mathbf{B}}{\gamma_k}\right)^{-1} \nabla f(\mathbf{x}_k)$ .  
 295 4: **end for**

296 In this algorithm,  $\mathbf{H}(\mathbf{x}_k) = \mathbf{H}(\mathbf{x}_k)^\top \succeq \mathbf{0}$  could be the Hessian or its approximation, and  $\gamma_k > 0$  is a  
 297 second-order step-size. Our theory suggests to set  $\boxed{\gamma_k = \gamma(\mathbf{x}_k)}$  which takes into account both the  
 298 right problem class and the level of Hessian approximation. We can also use an adaptive search to  
 299 choose the parameter  $\gamma_k$  automatically, that we describe in Appendix D.

300 For simplicity of presentation, we assume that at each iteration  $k \geq 0$  we solve the linear system  
 301 exactly, which can be done easily in case the matrix  $\mathbf{H}(\mathbf{x}_k)$  has a simple structure, e.g. a low-rank  
 302 decomposition. We present several practical examples in Section 5. In general, using a linear system  
 303 solver such as the conjugate gradient method, it will require only to compute matrix-vector products  
 304 of the form  $\mathbf{H}(\mathbf{x}_k) \mathbf{h}$ , for an arbitrary  $\mathbf{h} \in \mathbb{R}^n$ . Such linear solver will typically have a linear rate  
 305 of convergence due to strong convexity of the objective, and therefore it will require only a few  
 306 matrix-vector products each iteration.

307 Using the first power of gradient norm as a normalizing constant is very natural due to several reasons:

- 310 • This ensures:  $\|\mathbf{x}_{k+1} - \mathbf{x}_k\| \leq \gamma_k$ , so the steps are normalized to be bounded in the Euclidean  
 311 ball of a fixed radius  $\gamma_k$ , as in trust-region methods (Conn et al., 2000).
- 312 • When  $\mathbf{H} \equiv \nabla^2 f$ , the first power of the gradient norm ensures *local quadratic convergence*,  
 313 as for classical Newton's method, and we are interested to choose  $\gamma_k$  as large as possible  
 314 (locally, being close to a solution, we admit  $\gamma_k := +\infty$ , no regularization).
- 315 • When  $\mathbf{H} \equiv \mathbf{0}$ , we obtain the *normalized gradient method* with a fixed preconditioning  $\mathbf{B}$ :

$$\mathbf{x}_{k+1} = \mathbf{x}_k - \frac{\gamma_k}{\|\nabla f(\mathbf{x}_k)\|_*} \mathbf{B}^{-1} \nabla f(\mathbf{x}_k)$$

316 317 In this case, our theory recovers the standard rates of the first-order smooth optimization.

318 **Global Progress.** With Definition 1, we prove the progress for each iteration of Algorithm 1:

319 **Lemma 1.** Let  $0 \leq \gamma_k \leq \gamma(\mathbf{x}_k)$ . Then

$$320 f(\mathbf{x}_k) - f(\mathbf{x}_{k+1}) \geq \frac{\gamma_k}{8} \cdot \frac{\|\nabla f(\mathbf{x}_{k+1})\|_*^2}{\|\nabla f(\mathbf{x}_k)\|_*^2}. \quad (8)$$

Inequality (8) does not depend on the structure of  $\gamma(\mathbf{x}_k)$ , showing that Algorithm 1 converges for an arbitrary well-defined  $\gamma_k$ . It is also important that this method converges for *any problem class* and *for any Hessian approximation*, as we did not specify them yet. Notably, for a specific problem class and for a specific  $\mathbf{H}$ , we can lower bound  $\gamma(\cdot)$  globally as in the previous section, which yields state-of-the-art global convergence rates. Let us present a direct consequence of (8), which is a convergence for our algorithm in a general non-convex case.

**Theorem 1** (Non-Convex Functions). *Let  $K \geq 1$  be a fixed number of iterations and let (8) hold for every step. Assume that  $\min_{1 \leq i \leq K} \|\nabla f(\mathbf{x}_i)\|_* \geq \varepsilon$  and let  $\gamma_* := \min_{1 \leq i \leq K} \gamma_i > 0$ . Then,*

$$K \leq \frac{8F_0}{\gamma_* \varepsilon} + \log \frac{\|\nabla f(\mathbf{x}_0)\|_*}{\varepsilon}, \quad \text{where } F_0 := f(\mathbf{x}_0) - f^*. \quad (9)$$

Note that up to now we did not say anything about smoothness assumptions on our objective, thus the result (9) is very general. Let us assume that  $\mathbf{H}(\mathbf{x}_k) \equiv \nabla^2 f(\mathbf{x}_k) \succeq \mathbf{0}$ , and that the Hessian is Hölder continuous of degree  $\nu \in [0, 1]$ , which according to (7) ensures that  $\gamma_* \geq [(1 + \nu)\varepsilon L_{2,\nu}^{-1}]^{1/(1+\nu)}$ . Plugging this bound immediately provides us with the complexity of  $O(1/\varepsilon^{(2+\nu)/(1+\nu)})$  iterations to find a point such that  $\|\nabla f(\bar{\mathbf{x}})\|_* \leq \varepsilon$ . For  $\nu = 1$ , it gives  $O(1/\varepsilon^{3/2})$ , which corresponds to the rate of the cubically regularized Newton method (Nesterov & Polyak, 2006), and for every  $0 < \nu \leq 1$ , this complexity is strictly better than  $O(1/\varepsilon^2)$  of the gradient descent (Nesterov, 2018). In the next sections we show the advanced convergence rates for our methods, under structural assumption on  $\gamma(\cdot)$ , that will recover state-of-the-art rates in all particular cases and allow for inexact Hessians.

## 4 GLOBAL CONVERGENCE THEORY

**Structural Assumption on  $\gamma(\mathbf{x})$ .** Let us assume that the Gradient-Normalized Smoothness  $\gamma(\cdot)$  from Definition 1 admits the following structural lower bound, which is the harmonic mean of monomials of the gradient norm.

For all  $i$ , there exist fixed degrees  $0 \leq \alpha_i \leq 1$  and nonnegative coefficients  $\{M_{1-\alpha}\}_{0 \leq \alpha \leq 1}$ , such that:

$$\gamma(\mathbf{x}) \geq \pi(\|\nabla f(\mathbf{x})\|_*) := \left( \sum_{i=1}^d \frac{M_{1-\alpha_i}}{\|\nabla f(\mathbf{x})\|_*^{\alpha_i}} \right)^{-1} \geq \frac{1}{d} \min_{1 \leq i \leq d} \frac{\|\nabla f(\mathbf{x})\|_*^{\alpha_i}}{M_{1-\alpha_i}}. \quad (10)$$

Here, the coefficients  $\{M_{1-\alpha}\}_{0 \leq \alpha \leq 1}$  serve as the main complexity parameters. Note that all our Examples from Section 2 satisfy this assumption. In Examples 1, 2, 3,  $\pi(\|\nabla f(\mathbf{x})\|_*) = \|\nabla f(\mathbf{x})\|_*^\alpha \cdot M_{1-\alpha}^{-1}$ , for  $\alpha \in [0, 1]$ , is a simple monomial, and the structure in (10) is preserved under all basic operations with functions, such as summation. In what follows, we show that the lowest of the degrees of  $\pi(\cdot)$  characterizes the class of smoothness, while additional exponents contribute to inexact Hessian (see basic properties in Section 2 and examples in Section 5). Defining the coefficients of  $\pi(\|\nabla f(\mathbf{x})\|_*)$  from the set of  $\{M_{1-\alpha}^{-1} : 0 \leq \alpha \leq 1\}$ , where  $M_{1-\alpha}$  corresponds to the smoothness constant of some problem class, we automatically set the state-of-the-art convergence rates for many partial (see Table 1).

**Corollary 1** (Non-Convex Functions). *Let us choose  $\gamma_k = \gamma(\mathbf{x}_k)$  in Algorithm 1, or by performing an adaptive search. Under assumption (10), we can bound  $\gamma_* \geq \pi(\varepsilon)$ . Therefore, to ensure  $\min_{1 \leq i \leq K} \|\nabla f(\mathbf{x}_i)\|_* \leq \varepsilon$  it is enough to perform a number of iterations of*

$$K = \lceil 8dF_0 \cdot \max_{1 \leq i \leq d} \frac{M_{1-\alpha_i}}{\varepsilon^{1+\alpha_i}} + \log \frac{\|\nabla f(\mathbf{x}_0)\|_*}{\varepsilon} \rceil.$$

**Convex Minimization.** Let us define  $\alpha := \min_{1 \leq i \leq d} \alpha_i$  and introduce the following complexity

$$\mathcal{C}(\varepsilon) := \frac{d}{\alpha} \max_{1 \leq i \leq d} \left( \frac{M_{1-\alpha_i} D^{\alpha_i+1}}{\varepsilon^{\alpha_i-\alpha}} \right) \left( \frac{1}{\varepsilon^\alpha} - \frac{1}{F_0^\alpha} \right) \quad \text{for } \alpha > 0, \quad (11)$$

and for  $\alpha \rightarrow 0$ , we have the limit  $\mathcal{C}(\varepsilon) := d \max_{1 \leq i \leq d} \left( \frac{M_{1-\alpha_i} D^{\alpha_i+1}}{\varepsilon^{\alpha_i-\alpha}} \right) \log \left( \frac{F_0}{\varepsilon} \right)$ . For the particular cases  $\mathbf{H} \equiv \nabla^2 f$  and  $\mathbf{H} \equiv \mathbf{0}$ , thus performing the full Newton method or performing the gradient descent, we denote the corresponding complexity by  $\mathcal{C}_{\text{NEWTON}}(\varepsilon)$  and by  $\mathcal{C}_{\text{GD}}(\varepsilon)$ . Note that our

378 theory covers these two important cases as well. We show that complexity  $\mathcal{C}(\varepsilon)$  is the number of  
 379 iteration required by Algorithm 1 to find the global solution, reflecting dynamics of Algorithm 1 and  
 380 its ability to adapt to the right problem class. We denote by  $D := \{\sup \|\mathbf{x} - \mathbf{x}^*\| : f(\mathbf{x}) \leq f(\mathbf{x}_0)\}$   
 381 the diameter of the initial sublevel set, which we assume to be bounded. We establish the main result.  
 382

383 **Theorem 2** (Convex Functions). *Let us choose  $\gamma_k = \gamma(\mathbf{x}_k)$  in Algorithm 1, or by using an  
 384 adaptive search. Let  $f$  be convex. Then, for any  $\varepsilon > 0$ , to ensure  $f(\mathbf{x}_K) - f^* \leq \varepsilon$ , it is enough  
 385 to perform a number of iterations of*

$$386 \quad K = \lceil \mathcal{C}(\varepsilon) + 2 \log \frac{\|\nabla f(\mathbf{x}_0)\|_* D}{\varepsilon} \rceil. \\ 387$$

388 We can extend this result for more general classes of *gradient-dominated* functions, that include  
 389 strongly convex objectives and functions satisfying PL-condition, as well as improved rates for the  
 390 gradient norm minimization, which we include in Appendix F.

391 **Recovering Rates for Particular Problem Classes with  $\gamma(\mathbf{x})$ .** To highlight the power of our  
 392 result, let us consider a simple monomial  $\gamma(\mathbf{x}) \geq \pi(\|\nabla f(\mathbf{x})\|_*) = \|\nabla f(\mathbf{x})\|_*^\alpha M_{1-\alpha}^{-1}$ , for some  
 393  $0 \leq \alpha \leq 1$  and  $M_{1-\alpha} > 0$ . For simplicity, we always assume  $K \geq 2 \log \frac{\|\nabla f(\mathbf{x}_0)\|_* D}{\varepsilon}$ . Then, in  
 394 view of Theorem 2 and (11), we have the complexity of  $O(1/\varepsilon^\alpha)$ , for  $\alpha > 0$ , that corresponds  
 395 to the convergence rate inherent to problem classes from Examples 1, 2, 3. In case  $\alpha = 0$ , the  
 396 complexity  $K = \tilde{O}(M_1 D)$  yields the rate of the Newton method with the Gradient Regularization on  
 397 Quasi-Self-Concordant functions (Doikov, 2023). As we see, Theorem 2 allows us to obtain a variety  
 398 of convergence rates by plugging an appropriate global lower bound for  $\gamma(\mathbf{x}_k)$ . In Appendix G we  
 399 show how the lower bound  $\pi(\|\nabla f(\mathbf{x})\|)$  varies with the problem class. Corollary 7, shows how  
 400 state-of-the-art rates for different problem classes are unified by our choice of  $\gamma(\mathbf{x}_k)$  in Algorithm 1.  
 401

## 402 5 EFFECTIVE HESSIAN APPROXIMATIONS

404 **Our theory automatically covers a setup with inexact Hessian.** From Corollary 7 we see what  
 405 happens to the rate when  $\gamma(\mathbf{x})$  is lower bounded by a simple monomial. However, the case where  
 406  $\pi(\|\nabla f(\mathbf{x})\|_*)$  is not a monomial is also interpretable with our theory. Corresponding convergence  
 407 rate aligns with that of a second-order method with approximate Hessian, where the approximation  
 408 error is bounded by some polynomial of  $\|\nabla f(\mathbf{x})\|_*$ . Theorem 2 already covers this case with the  
 409 complexity of (11) for  $\gamma(\mathbf{x})$  being bounded as in (10). However, some important practical cases of  
 410 Hessian approximations can be described with a much simpler condition

$$411 \quad \|\nabla^2 f(\mathbf{x}) - \mathbf{H}(\mathbf{x})\|_* \leq \mathbf{C}_1 + \mathbf{C}_2 \|\nabla f(\mathbf{x})\|_*^{1-\beta}, \quad 0 \leq \beta \leq 1. \quad (12) \\ 412$$

413 We provide examples of such  $\mathbf{H}(\mathbf{x})$  that are particularly useful for machine learning applications.  
 414 See extended examples in Appendix H.

416 **Example 6** (Separable Optimization). *Let  $f(\mathbf{x}) = \sum_{i=1}^n f_i(\mathbf{x})$ , where  $f_i(\mathbf{x}) := \ell(\langle \mathbf{a}_i, \mathbf{x} \rangle - b_i)$ ,  
 417 for a convex nonnegative loss function. Consider logistic regression,  $\ell(t) := \log(1 + \exp(t))$ . Set  
 418  $\mathbf{B} := \sum_{i=1}^n \mathbf{a}_i \mathbf{a}_i^\top$ . Then, for the following Hessian approximation*

$$419 \quad \mathbf{H}(\mathbf{x}) := \sum_{i=1}^n \nabla f_i(\mathbf{x}) \nabla f_i(\mathbf{x})^\top = \sum_{i=1}^n (\ell'(\langle \mathbf{a}_i, \mathbf{x} \rangle - b_i))^2 \mathbf{a}_i \mathbf{a}_i^\top \succeq \mathbf{0}, \\ 420$$

422 we have  $\|\nabla^2 f(\mathbf{x}) - \mathbf{H}(\mathbf{x})\| \leq f(\mathbf{x}) \leq D \|\nabla f(\mathbf{x})\| + f^*$ , for  $\mathbf{x} \in \mathcal{F}_0$ .

424 **Example 7** (Nonlinear Equations). *Let  $\mathbf{u} : \mathbb{R}^n \rightarrow \mathbb{R}^d$  be a nonlinear operator, and set  $f(\mathbf{x}) :=$   
 425  $\frac{1}{p} \|\mathbf{u}(\mathbf{x})\|^p \equiv \frac{1}{p} \langle \mathbf{G}\mathbf{u}(\mathbf{x}), \mathbf{u}(\mathbf{x}) \rangle^{\frac{p}{2}}$ , for some  $\mathbf{G} = \mathbf{G}^\top \succ \mathbf{0}$  and  $p \geq 2$ . For this objective, we use:*

$$427 \quad \mathbf{H}(\mathbf{x}) := \|\mathbf{u}(\mathbf{x})\|^{p-2} \nabla \mathbf{u}(\mathbf{x})^\top \mathbf{G} \nabla \mathbf{u}(\mathbf{x}) + \frac{p-2}{\|\mathbf{u}(\mathbf{x})\|^p} \nabla f(\mathbf{x}) \nabla f(\mathbf{x})^\top \succeq \mathbf{0}. \quad (13) \\ 428$$

429 Assuming  $\nabla \mathbf{u}(\mathbf{x}) \mathbf{B}^{-1} \nabla \mathbf{u}(\mathbf{x})^\top \succeq \mu \mathbf{G}^{-1}$  and  $\|\nabla^2 \mathbf{u}(\mathbf{x})\| \leq \xi_1$ , for some  $\mu, \xi_1 > 0$ , we have:

$$430 \quad \|\nabla^2 f(\mathbf{x}) - \mathbf{H}(\mathbf{x})\| \leq \xi_1 \|\mathbf{u}(\mathbf{x})\|^{p-1} \leq \frac{\xi_1}{\sqrt{\mu}} \|\nabla f(\mathbf{x})\|_*. \quad (14) \\ 431$$

432

**Example 8** (Soft Maximum). *In applications with multiclass classification, graph problems, and matrix games, we use  $f(\mathbf{x}) := s(\mathbf{u}(\mathbf{x}))$ , where  $\mathbf{u} : \mathbb{R}^n \rightarrow \mathbb{R}^d$  is an operator (e.g. a linear or nonlinear model), and  $s(\mathbf{y}) := \log \sum_{i=1}^d e^{y_i}$  is the LogSumExp loss. Note that  $s(\cdot)$  is Quasi-Self-Concordant (Ex. 3), and  $[\nabla s(\mathbf{y})]_i = \frac{e^{y_i}}{\sum_{j=1}^d e^{y_j}}$  is softmax. For this objective, we can use the following approximation of the Hessian in our algorithm:*

433

$$\mathbf{H}(\mathbf{x}) := \nabla \mathbf{u}(\mathbf{x})^\top \nabla^2 s(\mathbf{u}(\mathbf{x})) \nabla \mathbf{u}(\mathbf{x}) \succeq \mathbf{0}.$$

434

*Assuming that  $\nabla \mathbf{u}(\mathbf{x}) \mathbf{B}^{-1} \nabla \mathbf{u}(\mathbf{x})^\top \succeq \mu \mathbf{I}$  and  $\|\nabla^2 \mathbf{u}(\mathbf{x})\| \leq \xi_1$ , for some  $\mu, \xi_1 > 0$ , we have:*

435

$$\|\nabla^2 f(\mathbf{x}) - \mathbf{H}(\mathbf{x})\| \leq \xi_1 \|\nabla s(\mathbf{u}(\mathbf{x}))\| \leq \frac{\xi_1}{\sqrt{\mu}} \|\nabla f(\mathbf{x})\|_*.$$

436

437

438

439

440

441

442

443

444

**Connection between Gradient-Normalized Smoothness and the Hessian bound 12.** According to the “Hessian inexactness” property of  $\gamma(\cdot)$ , assuming 12, the Gradient Normalized Smoothness is bounded as:  $\gamma(\mathbf{x}) \geq (\gamma_1(\mathbf{x})^{-1} + \frac{\mathbf{C}_1}{\|\nabla f(\mathbf{x})\|} + \frac{\mathbf{C}_2}{\|\nabla f(\mathbf{x})\|^\beta})^{-1}$ , where  $\gamma_1(\mathbf{x})$  is the Gradient Normalized Smoothness for the exact Hessian. In other words, if we know the lower bound  $\pi(\cdot)$  for the exact Hessian (e.g. any of the problem classes above), then  $\pi(\cdot)$  for the method with inexact Hessian can be computed in a form that satisfies the structural assumption 10. And we immediately obtain the complexity result for the method with inexact Hessian (Corollaries 2 and 3). We see that the total complexity of the method becomes the sum of the complexity for the exact case plus two additional terms that depend on  $\mathbf{C}_1, \mathbf{C}_2$ , and the degree of approximation  $\beta$ . Fig. 1 shows the interaction of the minimal degree of the monomial in  $\pi(\cdot)$  and  $\beta$  from Equation (12). And Corollary 2 finalizes Table 1.

445

446

447

448

449

450

451

452

453

454

455

456

**Corollary 2** (Inexact Hessian: Convex Functions). *Assume that condition (12) holds. Then, for any  $\varepsilon > 0$ , to ensure  $f(\mathbf{x}_K) - f^* \leq \varepsilon$ , it is enough to perform a number of iterations of*

457

458

$$K = \tilde{O}\left(\mathcal{C}_{\text{NEWTON}}(\varepsilon) + \frac{\mathbf{C}_1 D^2}{\varepsilon} + \frac{\mathbf{C}_2 D^{1+\beta}}{\varepsilon^\beta}\right), \quad \text{where } \tilde{O}(\cdot) \text{ hides logarithmic factors.}$$

459

460

461

462

463

464

465

466

467

**Corollary 3** (Inexact Hessian: Non-Convex Functions). *Assume that condition (12) holds. Therefore, to ensure  $\min_{1 \leq i \leq K} \|\nabla f(\mathbf{x}_i)\|_* \leq \varepsilon$  it is enough to perform a number of iterations of*

$$K = \lceil 8F_0 \cdot \left( d \max_{1 \leq i \leq d} \frac{M_{1-\alpha_i}}{\varepsilon^{1+\alpha_i}} + \frac{\mathbf{C}_1}{\varepsilon^2} + \frac{\mathbf{C}_2}{\varepsilon^{1+\beta}} \right) + \log \frac{\|\nabla f(\mathbf{x}_0)\|_*}{\varepsilon} \rceil.$$

468

469

470

Let us present illustrative numerical experiments that validate our theoretical findings. Extra experiments are in Appendix B, and the code is available at: grad-norm-smooth-1D57.

471

472

473

474

475

476

477

**Exact Hessian.** In Figure 3 (a), we show convergence of Algorithm 1 with exact Hessian on the Softmax problem (LogSumExp) with linear models. We compare our adaptive search rule  $\gamma_k = \gamma(\mathbf{x}_k)$  (see Lemma 1) with the strategies from Doikov et al. (2024a). We see that our theory predicts the best value of  $\gamma_k$ , which also serves an upper bound on empirical values of other adaptive search procedures (b). In (c), we compare our method with the gradient descent on the problem from Example 7. Our adaptive search denoted by “Func. Search”. As a Hessian approximation for LogSumExp, we use Equation (19).

478

479

480

481

482

483

484

485

**Inexact Hessian.** Our theory is compatible with different Hessian approximations we present in Table 2. In Appendix H we prove the bounds of  $\|\nabla f(\mathbf{x}) - \mathbf{H}(\mathbf{x})\|_*$  for these approximations. Notably, condition 12 does not necessarily hold for all approximations considered; however, Theorem 2 allows us to derive the right convergence rate. We extensively evaluate our methods on both convex and non-convex problems, including extensions of the Rosenbrock function Rosenbrock (1960)—known as the benchmarking problem for optimization algorithms—and we are the first to experimentally study (smooth) Chebyshev polynomials Gürbüzbalaban & Overton (2012); Cartis et al. (2013) with inexact Hessians. In Appendix B we also examine adaptive search, convergence, wall-clock time, and the numerical stability of our method with inexact Hessian on all problems from Table 2.

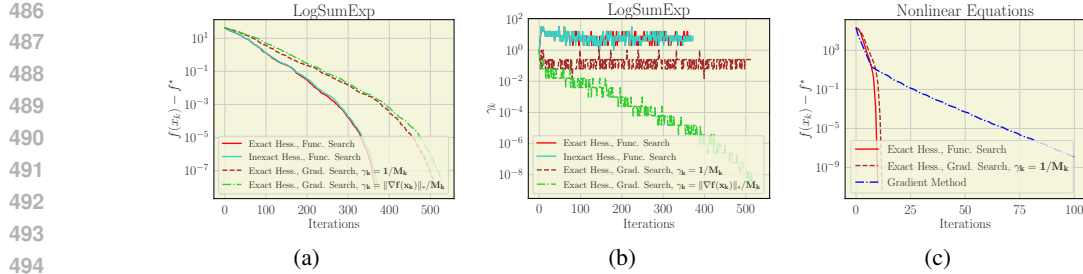


**Figure 3: Convergence of our methods.** We see that the second-order methods show outstanding performance, confirming our choice of the step-size  $\gamma_k$ .

**Table 2: Hessian approximations aligned with our theory, evaluated on convex and non-convex problems.** Importantly, when  $\mathbf{u}(\mathbf{x})$  is a linear operator, the ‘‘Inexact Hessian’’ turns out to be the full Hessian. Thus, we use the ‘‘Fisher Term of  $\mathbf{H}$ .’’ in that case.

Problem	Naming	Approximation
LogSumExp 15	Weighted Gauss-Newton 19	$\frac{1}{\mu} \mathbf{A}^\top \text{Diag}(\text{softmax}(\mathbf{A}, \mathbf{x})) \mathbf{A}$
Equations with linear operator	Fisher Term of $\mathbf{H}$ 21	$\frac{p-2}{\ \mathbf{u}(\mathbf{x})\ ^p} \nabla f(\mathbf{x}) \nabla f(\mathbf{x})^\top$
Nonlinear Equations & Rosenbrock 23	Inexact Hessian (Example 7)	$\ \mathbf{u}(\mathbf{x})\ ^{p-2} \nabla \mathbf{u}(\mathbf{x})^\top \mathbf{G} \nabla \mathbf{u}(\mathbf{x}) + \frac{p-2}{\ \mathbf{u}(\mathbf{x})\ ^p} \nabla f(\mathbf{x}) \nabla f(\mathbf{x})^\top$
Nonlinear Equations & Chebyshev polynomials 24	Inexact Hessian (Example 7)	$\ \mathbf{u}(\mathbf{x})\ ^{p-2} \nabla \mathbf{u}(\mathbf{x})^\top \mathbf{G} \nabla \mathbf{u}(\mathbf{x}) + \frac{p-2}{\ \mathbf{u}(\mathbf{x})\ ^p} \nabla f(\mathbf{x}) \nabla f(\mathbf{x})^\top$

## 7 DISCUSSION

Let us discuss the results we obtained in our paper in the context of some machine learning applications. We demonstrated that the notion of Gradient-Normalized Smoothness,  $\gamma(\mathbf{x})$ , allows us to treat the level of smoothness of the objective and the Hessian approximation error in a unified manner, leading to fast global convergence rates for both convex and non-convex problems, and recovering various smoothness assumptions such as functions with Hölder continuous Hessian or Quasi-Self-Concordant objectives. It is interesting to note that, in the case where the Hessian approximation satisfies the bound (12) with  $\beta = 0$  and  $\mathbf{C}_1 \approx 0$ , the convergence rate of the method with an inexact Hessian is the same as that one of the full Newton method.

An instructive example is the logistic regression problem with the Fisher approximation of the Hessian (Example 6). Using our theory, we are able to establish the *global linear rate* of convergence in the case where the data is well-separable ( $f^* \approx 0$ ), complementing previously known results for gradient descent methods (Axiotis & Sviridenko, 2023) and for Newton-type methods (Karimireddy et al., 2018; Carmon et al., 2020; Doikov, 2023). Moreover, our theory extends beyond this setting to soft maximum problems and the case of non-linear models.

Another interesting situation involves problems with the power loss function,  $f(\mathbf{x}) = \frac{1}{p} \|\mathbf{x}\|^p$ . As we show in Section G, this objective belongs to both the class of generalized self-concordant functions and the class of uniformly convex functions. These advanced properties ensure a *global linear rate* of Newton’s method for all  $p \geq 2$ , thus demonstrating that an automatic renormalization of the problem occurs within our algorithms.

While in this work we discuss only basic versions of the method, it is known in Convex Optimization that algorithms can be *accelerated*, achieving optimal convergence rates (Nesterov, 2018). Developing accelerated versions of our methods that automatically adapt to the problem’s smoothness, as in (Carmon et al., 2022), while simultaneously adjusting to the potential inexactness in the Hessian, is an interesting direction that we leave for future research.

It is also interesting to compare our results with several recently proposed general problem classes and algorithms, such as gradient methods for *anisotropic smoothness* (Laude & Patrinos, 2025),  $\ell$ -smoothness (Li et al., 2023; Tyurin, 2024), and recent advances on global convergence rates for the damped Newton method (Hanzely et al., 2024). We leave these comparisons for further investigation.

540 REFERENCES  
541

542 Artem Agafonov, Dmitry Kamzolov, Pavel Dvurechensky, Alexander Gasnikov, and Martin Takáč.  
543 Inexact tensor methods and their application to stochastic convex optimization. *Optimization  
544 Methods and Software*, 39(1):42–83, 2024.

545 Michael Arbel, Romain Menegaux, and Pierre Wolinski. Rethinking Gauss-Newton for learning  
546 over-parameterized models. *Advances in neural information processing systems*, 36:33379–33402,  
547 2023.

548 Kyriakos Axiotis and Maxim Sviridenko. Gradient descent converges linearly for logistic regression  
549 on separable data. In *International Conference on Machine Learning*, pp. 1302–1319. PMLR,  
550 2023.

551 Francis Bach. Self-concordant analysis for logistic regression. 2010.

552 Heinz H Bauschke, Jérôme Bolte, and Marc Teboulle. A descent lemma beyond Lipschitz gradient  
553 continuity: first-order methods revisited and applications. *Mathematics of Operations Research*,  
554 42(2):330–348, 2017.

555 Ernesto G Birgin, JL Gardenghi, José Mario Martínez, Sandra Augusta Santos, and Ph L Toint. Worst-  
556 case evaluation complexity for unconstrained nonlinear optimization using high-order regularized  
557 models. *Mathematical Programming*, 163:359–368, 2017.

558 Yair Carmon, Arun Jambulapati, Qijia Jiang, Yujia Jin, Yin Tat Lee, Aaron Sidford, and Kevin Tian.  
559 Acceleration with a ball optimization oracle. *Advances in Neural Information Processing Systems*,  
560 33:19052–19063, 2020.

561 Yair Carmon, Danielle Hausler, Arun Jambulapati, Yujia Jin, and Aaron Sidford. Optimal and  
562 adaptive Monteiro-Svaiter acceleration. *Advances in Neural Information Processing Systems*, 35:  
563 20338–20350, 2022.

564 Coralia Cartis and Katya Scheinberg. Global convergence rate analysis of unconstrained optimization  
565 methods based on probabilistic models. *Mathematical Programming*, 169:337–375, 2018.

566 Coralia Cartis, Nicholas IM Gould, and Philippe L Toint. Adaptive cubic regularisation methods for  
567 unconstrained optimization. Part I: motivation, convergence and numerical results. *Mathematical  
568 Programming*, 127(2):245–295, 2011a.

569 Coralia Cartis, Nicholas IM Gould, and Philippe L Toint. Adaptive cubic regularisation methods  
570 for unconstrained optimization. Part II: worst-case function-and derivative-evaluation complexity.  
571 *Mathematical programming*, 130(2):295–319, 2011b.

572 Coralia Cartis, Nicholas IM Gould, and Philippe L Toint. On the oracle complexity of first-order and  
573 derivative-free algorithms for smooth nonconvex minimization. *SIAM Journal on Optimization*, 22  
574 (1):66–86, 2012.

575 Coralia Cartis, Nicholas I.M. Gould, and Philippe L. Toint. A note about the complexity of minimizing  
576 Nesterov’s smooth Chebyshev-Rosenbrock function. *Optimization Methods and Software*, 28(3):  
577 451 – 457, 2013. doi: 10.1080/10556788.2012.722632. URL <https://www.scopus.com/inward/record.uri?eid=2-s2.0-84878316454&doi=10.1080%2f10556788.2012.722632&partnerID=40&md5=26dee5f35df2b5761c54d444002564f5>.  
578 Cited by: 1; All Open Access, Green Open Access.

579 Coralia Cartis, Nicholas IM Gould, and Philippe L Toint. Universal regularization methods: varying  
580 the power, the smoothness and the accuracy. *SIAM Journal on Optimization*, 29(1):595–615, 2019.

581 Chih-Chung Chang and Chih-Jen Lin. Libsvm: A library for support vector machines. *ACM Trans.  
582 Intell. Syst. Technol.*, 2(3), May 2011. ISSN 2157-6904. doi: 10.1145/1961189.1961199. URL  
583 <https://doi.org/10.1145/1961189.1961199>.

584 El Mahdi Chayti, Nikita Doikov, and Martin Jaggi. Unified convergence theory of stochastic and  
585 variance-reduced cubic Newton methods. *arXiv preprint arXiv:2302.11962*, 2023.

594 Andrew R Conn, Nicholas IM Gould, and Philippe L Toint. *Trust region methods*. SIAM, 2000.  
 595

596 John E Dennis, Jr and Jorge J Moré. Quasi-Newton methods, motivation and theory. *SIAM review*,  
 597 19(1):46–89, 1977.

598 Nikita Doikov. Minimizing quasi-self-concordant functions by gradient regularization of Newton  
 599 method. *arXiv preprint arXiv:2308.14742*, 2023.

600

601 Nikita Doikov and Geovani Nunes Grapiglia. First and zeroth-order implementations of the regular-  
 602 ized Newton method with lazy approximated hessians. *Journal of Scientific Computing*, 103(1):32,  
 603 2025.

604 Nikita Doikov and Yurii Nesterov. Minimizing uniformly convex functions by cubic regularization of  
 605 Newton method. *Journal of Optimization Theory and Applications*, 189(1):317–339, 2021.

606

607 Nikita Doikov and Yurii Nesterov. Gradient regularization of Newton method with Bregman distances.  
 608 *Mathematical Programming*, pp. 1–25, 2023.

609

610 Nikita Doikov and Yurii Nesterov. Gradient regularization of Newton method with Bregman distances.  
 611 *Mathematical programming*, 204(1):1–25, 2024.

612

613 Nikita Doikov and Anton Rodomanov. Polynomial preconditioning for gradient methods, 2023. URL  
<https://arxiv.org/abs/2301.13194>.

614

615 Nikita Doikov, Konstantin Mishchenko, and Yurii Nesterov. Super-universal regularized Newton  
 616 method. *SIAM Journal on Optimization*, 34(1):27–56, 2024a.

617

618 Nikita Doikov, Sebastian U Stich, and Martin Jaggi. Spectral preconditioning for gradient methods  
 619 on graded non-convex functions. In *ICML*, 2024b.

620

621 Ilyas Fatkhullin, Jalal Etesami, Niao He, and Negar Kiyavash. Sharp analysis of stochastic optimiza-  
 622 tion under global Kurdyka-Łojasiewicz inequality. *Advances in Neural Information Processing  
 623 Systems*, 35:15836–15848, 2022.

624

625 Curtis Fox, Aaron Mishkin, Sharan Vaswani, and Mark Schmidt. Glocal smoothness: Line search  
 626 can really help! *arXiv preprint arXiv:2506.12648*, 2025.

627

628 Elias Frantar, Eldar Kurtic, and Dan Alistarh. M-fac: Efficient matrix-free approximations of  
 629 second-order information. *Advances in Neural Information Processing Systems*, 34:14873–14886,  
 630 2021.

631

632 Terunari Fuji, Pierre-Louis Poirion, and Akiko Takeda. Randomized subspace regularized Newton  
 633 method for unconstrained non-convex optimization. *arXiv preprint arXiv:2209.04170*, 2022.

634

635 Eduard Gorbunov, Nazarii Tupitsa, Sayantan Choudhury, Alen Aliev, Peter Richtárik, Samuel Horváth,  
 636 and Martin Takáč. Methods for convex  $(l_0, l_1)$ -smooth optimization: Clipping, acceleration, and  
 637 adaptivity. *arXiv preprint arXiv:2409.14989*, 2024.

638

639 Robert Gower, Dmitry Kovalev, Felix Lieder, and Peter Richtárik. Rsn: randomized subspace Newton.  
 640 *Advances in Neural Information Processing Systems*, 32, 2019.

641

642 Geovani Nunes Grapiglia and Yurii Nesterov. On inexact solution of auxiliary problems in tensor  
 643 methods for convex optimization. *Optimization Methods and Software*, 36(1):145–170, 2021.

644

645 Geovani Nunes Grapiglia, Max LN Gonçalves, and GN Silva. A cubic regularization of newton’s  
 646 method with finite difference hessian approximations. *Numerical Algorithms*, pp. 1–24, 2022.

647

648 Serge Gratton, Sadok Jerad, and Philippe L Toint. A fast Newton method under local lipschitz  
 649 smoothness. *arXiv preprint arXiv:2505.04807*, 2025.

650

651 Andreas Griewank. The modification of Newton’s method for unconstrained optimization by bounding  
 652 cubic terms. Technical report, Technical report NA/12, 1981.

653

654 Mert Gürbüzbalaban and Michael L Overton. On Nesterov’s nonsmooth Chebyshev–Rosenbrock  
 655 functions. *Nonlinear Analysis: Theory, Methods & Applications*, 75(3):1282–1289, 2012.

648 Mert Gürbüzbalaban and Michael L. Overton. On Nesterov’s nonsmooth Chebyshev–Rosenbrock  
 649 functions. *Nonlinear Analysis: Theory, Methods & Applications*, 75(3):1282–1289, 2012.  
 650 ISSN 0362-546X. doi: <https://doi.org/10.1016/j.na.2011.07.062>. URL <https://www.sciencedirect.com/science/article/pii/S0362546X1100544X>. Variational  
 651 Analysis and Its Applications.

652 Slavomír Hanzely. Sketch-and-project meets Newton method: Global  $O(1/k^2)$  convergence with  
 653 low-rank updates. In *The 28th International Conference on Artificial Intelligence and Statistics*,  
 654 2025.

655 Slavomír Hanzely, Dmitry Kamzolov, Dmitry Pasechnyuk, Alexander Gasnikov, Peter Richtárik, and  
 656 Martin Takáč. A damped newton method achieves global  $O(1/k^2)$  and local quadratic convergence  
 657 rate. *Advances in Neural Information Processing Systems*, 35:25320–25334, 2022.

658 Slavomír Hanzely, Farshed Abdukhakimov, and Martin Takáč. Newton method revisited: Global  
 659 convergence rates up to  $O(k^{-3})$  for stepsize schedules and linesearch procedures. *arXiv preprint*  
 660 *arXiv:2405.18926*, 2024.

661 Florian Jarre. On Nesterov’s smooth Chebyshev–Rosenbrock function. *Optimization Methods &*  
 662 *Software*, iFirst, 12 2011. doi: 10.1080/10556788.2011.638924.

663 Yuntian Jiang, Chang He, Chuwen Zhang, Dongdong Ge, Bo Jiang, and Yinyu Ye. Beyond non-  
 664 convexity: A universal trust-region method with new analyses. *arXiv e-prints*, pp. arXiv–2311,  
 665 2023.

666 Qiujiang Jin and Aryan Mokhtari. Non-asymptotic superlinear convergence of standard quasi-Newton  
 667 methods. *Mathematical Programming*, 200(1):425–473, 2023.

668 Qiujiang Jin, Ruichen Jiang, and Aryan Mokhtari. Non-asymptotic global convergence analysis of  
 669 BFGS with the Armijo-Wolfe line search. *arXiv preprint arXiv:2404.16731*, 2024.

670 Nocedal Jorge and J Wright Stephen. *Numerical optimization*. Springer, 2006.

671 Alireza Kabgani and Masoud Ahookhosh. Moreau envelope and proximal-point methods under the  
 672 lens of high-order regularization, 2025. URL <https://arxiv.org/abs/2503.04577>.

673 Dmitry Kamzolov, Klea Ziu, Artem Agafonov, and Martin Takáč. Cubic regularization is the key!  
 674 the first accelerated quasi-Newton method with a global convergence rate of  $O(k^{-2})$  for convex  
 675 functions. *arXiv preprint arXiv:2302.04987*, 2023.

676 Sai Praneeth Karimireddy, Sebastian U Stich, and Martin Jaggi. Global linear convergence of New-  
 677 ton’s method without strong-convexity or Lipschitz gradients. *arXiv preprint arXiv:1806.00413*,  
 678 2018.

679 Anastasia Koloskova, Hadrien Hendrikx, and Sebastian U Stich. Revisiting gradient clipping:  
 680 Stochastic bias and tight convergence guarantees. In *International Conference on Machine  
 681 Learning*, pp. 17343–17363. PMLR, 2023.

682 Frederik Kunstner, Philipp Hennig, and Lukas Balles. Limitations of the empirical fisher approx-  
 683 imation for natural gradient descent. *Advances in neural information processing systems*, 32,  
 684 2019.

685 Emanuel Laude and Panagiotis Patrinos. Anisotropic proximal gradient. *Mathematical Programming*,  
 686 pp. 1–45, 2025.

687 Haochuan Li, Jian Qian, Yi Tian, Alexander Rakhlin, and Ali Jadbabaie. Convex and non-convex  
 688 optimization under generalized smoothness. *Advances in Neural Information Processing Systems*,  
 689 36:40238–40271, 2023.

690 Haihao Lu, Robert M Freund, and Yurii Nesterov. Relatively smooth convex optimization by  
 691 first-order methods, and applications. *SIAM Journal on Optimization*, 28(1):333–354, 2018.

692 Cong Ma, Xingyu Xu, Tian Tong, and Yuejie Chi. Provably accelerating ill-conditioned low-  
 693 rank estimation via scaled gradient descent, even with overparameterization. *arXiv preprint*  
 694 *arXiv:2310.06159*, 2023.

702 James Martens. New insights and perspectives on the natural gradient method. *Journal of Machine*  
 703 *Learning Research*, 21(146):1–76, 2020.  
 704

705 A Woodbury Max. Inverting modified matrices. In *Memorandum Rept. 42, Statistical Research*  
 706 *Group*, pp. 4. Princeton Univ., 1950.  
 707

708 Konstantin Mishchenko. Regularized Newton method with global  $\mathcal{O}(1/k^2)$  convergence. *SIAM*  
 709 *Journal on Optimization*, 33(3):1440–1462, 2023.  
 710

711 Aaron Mishkin, Ahmed Khaled, Yuanhao Wang, Aaron Defazio, and Robert M. Gower. Directional  
 712 smoothness and gradient methods: Convergence and adaptivity. *Advances in Neural Information*  
 713 *Processing Systems*, 2025. URL <https://arxiv.org/abs/2403.04081>.  
 714

715 Arkadi Nemirovski and David Yudin. Problem complexity and method efficiency in optimization.  
 716 1983.  
 717

718 Yurii Nesterov. Modified Gauss–Newton scheme with worst case guarantees for global performance.  
 719 *Optimisation methods and software*, 22(3):469–483, 2007.  
 720

721 Yurii Nesterov. Universal gradient methods for convex optimization problems. *Mathematical*  
 722 *Programming*, 152(1):381–404, 2015.  
 723

724 Yurii Nesterov. *Lectures on convex optimization*, volume 137. Springer, 2018.  
 725

726 Yurii Nesterov. Implementable tensor methods in unconstrained convex optimization. *Mathematical*  
 727 *Programming*, 186:157–183, 2021a.  
 728

729 Yurii Nesterov. Superfast second-order methods for unconstrained convex optimization. *Journal of*  
 730 *Optimization Theory and Applications*, 191:1–30, 2021b.  
 731

732 Yurii Nesterov. Primal subgradient methods with predefined step sizes. *Journal of Optimization*  
 733 *Theory and Applications*, pp. 1–33, 2024.  
 734

735 Yurii Nesterov and Arkadi Nemirovski. *Interior-point polynomial algorithms in convex programming*.  
 736 SIAM, 1994.  
 737

738 Yurii Nesterov and Boris T Polyak. Cubic regularization of newton method and its global performance.  
 739 *Mathematical programming*, 108(1):177–205, 2006.  
 740

741 Boris T Polyak. Newton’s method and its use in optimization. *European Journal of Operational*  
 742 *Research*, 181(3):1086–1096, 2007.  
 743

744 Roman A Polyak. Regularized Newton method for unconstrained convex optimization. *Mathematical*  
 745 *programming*, 120:125–145, 2009.  
 746

747 Anton Rodomanov. *Quasi-Newton methods with provable efficiency guarantees*. PhD thesis, PhD  
 748 thesis, UCL-Université Catholique de Louvain, 2022.  
 749

750 Anton Rodomanov. Global complexity analysis of BFGS. *arXiv preprint arXiv:2404.15051*, 2024.  
 751

752 Anton Rodomanov and Yurii Nesterov. New results on superlinear convergence of classical quasi-  
 753 Newton methods. *Journal of optimization theory and applications*, 188:744–769, 2021.  
 754

755 H. H. Rosenbrock. An automatic method for finding the greatest or least value of a function. *The*  
 756 *Computer Journal*, 3(3):175–184, 01 1960. ISSN 0010-4620. doi: 10.1093/comjnl/3.3.175. URL  
 757 <https://doi.org/10.1093/comjnl/3.3.175>.  
 758

759 Damien Scieur. Adaptive quasi-Newton and Anderson acceleration framework with explicit global  
 760 (accelerated) convergence rates. In *International Conference on Artificial Intelligence and Statistics*,  
 761 pp. 883–891. PMLR, 2024.  
 762

763 Tianxiao Sun and Quoc Tran-Dinh. Generalized self-concordant functions: A recipe for newton-type  
 764 methods, 2018. URL <https://arxiv.org/abs/1703.04599>.  
 765

756 Alexander Tyurin. Toward a unified theory of gradient descent under generalized smoothness. *arXiv*  
 757 *preprint arXiv:2412.11773*, 2024.  
 758

759 Kenji Ueda and Nobuo Yamashita. A regularized Newton method without line search for uncon-  
 760 strained optimization. *Technical Report*, 2009.

761 Daniil Vankov, Anton Rodomanov, Angelia Nedich, Lalitha Sankar, and Sebastian U Stich. Optimiz-  
 762 ing  $(l_0, l_1)$ -smooth functions by gradient methods. *arXiv preprint arXiv:2410.10800*, 2024.  
 763

764 Chenghan Xie, Chenxi Li, Chuwen Zhang, Qi Deng, Dongdong Ge, and Yinyu Ye. Trust region  
 765 methods for nonconvex stochastic optimization beyond Lipschitz smoothness. In *Proceedings of*  
 766 *the AAAI Conference on Artificial Intelligence*, volume 38, pp. 16049–16057, 2024.

767 Gavin Zhang, Salar Fattah, and Richard Y Zhang. Preconditioned gradient descent for overpara-  
 768 meterized nonconvex Burer–Monteiro factorization with global optimality certification. *Journal of*  
 769 *Machine Learning Research*, 24(163):1–55, 2023.  
 770

771 Jingzhao Zhang, Tianxing He, Suvrit Sra, and Ali Jadbabaie. Why gradient clipping accelerates  
 772 training: A theoretical justification for adaptivity. *arXiv preprint arXiv:1905.11881*, 2019.  
 773

774 Jim Zhao, Aurelien Lucchi, and Nikita Doikov. Cubic regularized subspace Newton for non-convex  
 775 optimization. In *The 28th International Conference on Artificial Intelligence and Statistics*, 2025.  
 776

## 777 CONTENTS

779	<b>1</b>	<b>Introduction</b>	<b>1</b>
780			
781	<b>2</b>	<b>Gradient-Normalized Smoothness</b>	<b>4</b>
782			
783	<b>3</b>	<b>Algorithm</b>	<b>6</b>
784			
785	<b>4</b>	<b>Global Convergence Theory</b>	<b>7</b>
786			
787	<b>5</b>	<b>Effective Hessian Approximations</b>	<b>8</b>
788			
789	<b>6</b>	<b>Experiments</b>	<b>9</b>
790			
791	<b>7</b>	<b>Discussion</b>	<b>10</b>
792			
793	<b>A</b>	<b>Extended Related Work</b>	<b>17</b>
794			
795	<b>B</b>	<b>Experiments</b>	<b>18</b>
796			
797	B.1	Comparison of Adaptive Search Approaches . . . . .	19
798	B.2	Inexact Hessian: LogSumExp . . . . .	19
799	B.3	Nonlinear Equations: Studying the Degree of Smoothness . . . . .	23
800	B.4	Non-Convex Objectives . . . . .	26
801	B.5	Comparison with Adaptive and Universal Methods . . . . .	30
802			
803	<b>C</b>	<b>Composite Optimization Problems</b>	<b>31</b>
804			
805	C.1	Composite Newton Step with Hessian Approximation . . . . .	31
806	C.2	The Algorithm for Composite Optimization . . . . .	33
807			
808			
809			

---

810	<b>D The Choice of the Regularization Parameter</b>	<b>34</b>
811	D.1 The Constant Rule . . . . .	34
812	D.2 The Method with Adaptive Search . . . . .	35
813		
814		
815	<b>E Convergence for Non-Convex Functions</b>	<b>37</b>
816	E.1 Convergence for Inexact Hölder Hessian . . . . .	38
817		
818		
819	<b>F Improved Rates for Gradient-Dominated Functions</b>	<b>38</b>
820		
821	<b>G Applications</b>	<b>41</b>
822	G.1 Functions with Hölder Hessian . . . . .	42
823	G.2 Convex Functions with Hölder Third Derivative . . . . .	42
824	G.3 Quasi-Self-Concordant Functions . . . . .	43
825	G.4 Generalized Self-Concordant Functions . . . . .	44
826	G.5 $(L_0, L_1)$ -Smooth Functions . . . . .	46
827	G.6 Second-Order $(M_0, M_1)$ -Smooth Functions . . . . .	47
828		
829		
830		
831		
832	<b>H Bounds on Effective Hessian Approximations</b>	<b>48</b>
833	H.1 Soft Maximum . . . . .	48
834	H.2 Nonlinear Equations . . . . .	50
835	H.3 Separable Optimization . . . . .	52
836	H.4 Recovering Complexities for Practical Approximations . . . . .	53
837		
838		
839		
840		
841		
842		
843		
844		
845		
846		
847		
848		
849		
850		
851		
852		
853		
854		
855		
856		
857		
858		
859		
860		
861		
862		
863		

864 **A EXTENDED RELATED WORK**  
865866 **Connections and differences with other methods with gradient regularization.**  
867

868 We propose Algorithm 1 with the only one hyperparameter—second-order step-size  $\gamma_k$ . Importantly,  
869 this step-size has an immediate natural interpretation of the radius of the ball within which we can rely  
870 on our approximate model, similarly in spirit to trust-region methods (Conn et al., 2000). However,  
871 instead of directly adding the ball constraints into minimization of the model, we apply the gradient  
872 regularization technique, considered in (Polyak, 2009; Ueda & Yamashita, 2009; Mishchenko, 2023;  
873 Doikov & Nesterov, 2024). This technique simplifies every step of the method, requiring to solve  
874 only one linear system per iteration. As compared to these previous works, we do not require to  
875 use an exact Hessian. We show that the inexactness condition on the matrix aligns well with the  
876 smoothness condition of the problem class, and our method works in a universal manner among the  
877 widest possible range of smoothness conditions.

878 In (Doikov et al., 2024a), it was shown that the Newton method with gradient regularization and  
879 adaptive search automatically adjusts to the problem classes with Hölder second or third derivative,  
880 and in (Doikov, 2023), the global linear rate of convergence on Quasi-Self-Concordant functions  
881 was proven for a similar method. In contrast to these works, we prove universal global rates for a  
882 method with inexact Hessian, both unifying analysis from (Doikov et al., 2024a; Doikov, 2023) and  
883 extending it beyond to the *generalized Self-Concordant functions* (Sun & Tran-Dinh, 2018). To the  
884 best of our knowledge, our global rates for generalized self-concordant functions are new.

885 An interesting insight from our analysis is that for different smoothness classes of the objective, we  
886 can allow different degrees of Hessian inexactness. Moreover, for popular choices of the Hessian  
887 approximations, such as the Fisher or Gauss-Newton approximations, the resulting methods perform  
888 *as well as for the method with the exact Hessian*. Using such approximations ultimately allows us to  
889 extend the gradient regularization technique for non-convex problems.

890 For the choice of the second-order step-size  $\gamma_k$ , we consider three possible strategies:

- 891 • The theoretical choice  $\gamma_k = \gamma(\mathbf{x}_k, F'(\mathbf{x}_k))$ , which is the best *local* value at  $\mathbf{x}_k$  following  
892 our Definition 1.
- 893 • The constant choice,  $\gamma_k \equiv \gamma_*$  for a certain value of  $\gamma_* > 0$  (see Section D.1). Our value of  
894  $\gamma_*$  is defined for a wide range of classes. However, despite seemingly too conservative, this  
895 rule recovers all state-of-the-art rates for the Newton method with gradient regularization,  
896 including those from (Doikov et al., 2024a; Doikov, 2023). To the best of our knowledge,  
897 this constant choice is new.
- 898 • Adaptive search to ensure the progress from Lemma 1. We discuss this strategy deeply  
899 in Appendix D.2. Importantly, our Algorithm 1 with adaptive search is equivalent to the  
900 Super-Universal Newton Method from (Doikov et al., 2024a). However, we use a different  
901 stopping condition in the adaptive search: we follow the condition based on the function  
902 value, while Doikov et al. (2024a) ensures a different inequality (17). Thus, our stopping  
903 condition is also suitable for *non-convex problems*.

904 From the theoretical perspective, equipped with the notion of Gradient-Normalized Smoothness, we  
905 cover the complexity results of the Super-Universal method, and extend the analysis to the Quasi-  
906 Self-Concordant functions (Doikov, 2023) and furthermore, to the generalized Self-Concordant functions  
907 (Sun & Tran-Dinh, 2018). Thus, even for the exact Hessians, we cover all results from (Doikov  
908 et al., 2024a; Doikov, 2023), and enhance them with the undiscovered rates for the generalized  
909 Self-Concordant class. Our framework also covers recently popular for the first-order methods ( $L_0$ ,  
910  $L_1$ )-functions (Zhang et al., 2019), and beyond. The breadth of rates for second-order methods  
911 covered by our framework (see Table 1) is unmatched in the existing literature.

912 **First state-of-the-art rates for inexact Hessians.**

913 The main power of our framework is the ability to *automatically* obtain the best rates for inexact  
914 Hessians. Moreover, thanks to Gradient-Normalized Smoothness and the structural assumption (10),  
915 we derive these results for convex (Theorem 2) and non-convex (Corollary 1) objectives *for free*. We  
916 additionally use condition (12) that connects the error coming from the Hessian inexactness with the  
917 gradient norm. We find such a condition very appealing for some practical Hessian approximations  
918 on fundamental problems such as logistic regression and softmax. Condition (12) allows us to write

918 complexity results with inexact Hessian in a compact and feasible manner. Combining both  $\gamma_k$  and  
 919 Eq. (12), we study the interplay between the smoothness class and the Hessian approximation—  
 920 Figure 1—also a new result.

921 **Discussions of other types of smoothness.**

923 Since we are introducing a new notion for characterizing smoothness of the objective, we should  
 924 mention previously established relative (Lu et al., 2018) and anisotropic (Laude & Patrinos, 2025)  
 925 smoothness. While being theoretically appealing, these concepts are designed specifically for the  
 926 first-order methods. Indeed, given a function that is anisotropic smooth or relative smooth (w.r.t. some  
 927 reference function), and adding a quadratic function to this, will generally change the smoothness  
 928 parameter of the objective. However, our Definition 1 is insensitive to such perturbations because  
 929 of the second-order formulation. We also would like to highlight a very recently proposed, for the  
 930 first-order, methods Glocal (Fox et al., 2025) and directional (Mishkin et al., 2025) smoothness. While  
 931 we define Gradient-Normalized smoothness independently of the problem class in the way to use the  
 932 local information to judge on the global behaviour of the method, the authors of Glocal smoothness  
 933 are inspired by a similar plot. With their framework, it occurs that near the solution the curvature  
 934 is much milder and line search or adaptive step-sizes can take advantage of that by increasing the  
 935 steps, yielding faster progress in that region. Glocal smoothness allows a fair comparison between  
 936 complexity results of many gradient-based methods, and the authors obtain better iteration-complexity  
 937 bounds compared to using global smoothness only. The authors also claim that Gradient Method  
 938 with line search can beat the accelerated gradient. These studies are worth further investigation.

939 **B EXPERIMENTS**

941 In this section, we explore two main aspects:

942 • how our adaptive search approach aligns with theoretical findings and with the previously established  
 943 adaptive search variant (Doikov et al., 2024a) (see Appendix B.1 for experimental details); and  
 944  
 945 • the convergence behavior of Algorithm 1 for inexact and true Hessians<sup>3</sup> (see Appendices B.2, B.3,  
 946 B.4).

947 We open-source our code at: <https://anonymous.4open.science/r/grad-norm-smooth-1D57>.

948 **Setup.** We consider two well-adopted problems: LogSumExp and Nonlinear Equations. We use a  
 949 very simple setup for both. We define the LogSumExp problem as:

$$951 \quad f(\mathbf{x}) = \mu \log \sum_{i=1}^d \exp \left( \frac{\langle \mathbf{a}_i, \mathbf{x} \rangle - b_i}{\mu} \right), \quad (15)$$

953 here  $\mathbf{a}_i$  denotes the  $i$ -th row of the design matrix  $\mathbf{A}$ , and  $\mu$  is a smoothing parameter varied across  
 954 experiments (see Figure 6). The Nonlinear Equations problem is:

$$955 \quad f(\mathbf{x}) = \frac{1}{p} \|\mathbf{u}(\mathbf{x})\|^p,$$

957 where the choice of the operator  $\mathbf{u}(\mathbf{x})$  ranges from the linear model (Appendix B.3), to non-convex  
 958 problems — Rosenbrock function, Chebyshev polynomials (Appendix B.4).

959 For the basic examples in the main part and in Appendix B.3 that can be run on real datasets, we utilize  
 960 the linear operator  $\mathbf{u}(\mathbf{x}) = \mathbf{A}\mathbf{x} - \mathbf{b}$ . The design matrix  $\mathbf{A}$  and the vector of labels  $\mathbf{b}$  may represent a  
 961 real or synthetic dataset. If we randomly generate both  $\mathbf{A}$  and  $\mathbf{b}$ , we do this by sampling their entries  
 962 independently from a uniform distribution  $U[-1, 1]$ . In all experiments, our method is run with an  
 963 adaptive search procedure (see Appendix D), which ensures the inequality (8) and thus selects the  
 964 best value of  $\gamma_k$ . Furthermore, the values of  $\gamma_k$  obtained through this adaptive scheme also serve as  
 965 upper bounds for the empirical values obtained by the alternative adaptive search strategy studied  
 966 in (Doikov et al., 2024a). In particular, we see that Algorithm 1 with inexact Hessians performs  
 967 similarly to the method with true Hessian on the LogSumExp problem, which also highlights the  
 968 power of our theoretical result: Indeed, the functions we consider in our experiments correspond to  
 969 Examples 7 and 8, and in both cases, this aligns with the  $\mathbf{C}_1 = 0$  scenario in Table 1.

970 <sup>3</sup>We emphasize that there is no need for an extensive comparison between Algorithm 1 and variants of the  
 971 Newton Method with alternative adaptive search procedures, as the practical improvement primarily lies in  
 obtaining a better constant within the adaptive scheme, while the overall convergence pattern remains unchanged.

972 We use the following naming throughout the experiments:  
 973

- 974 **Exact Hess., Func. Search or Exact Newton:** stands for the partial case of Algorithm 1  
 975 using our adaptive search procedure (16), and  $\mathbf{H}(\mathbf{x}) \equiv \nabla^2 f(\mathbf{x})$ .
- 976 **Inexact Hess., Func. Search or Weighted Gauss-Newton:** refers to the variant of Algo-  
 977 rithm 1 with Hessian approximation of the form (13) or (19), combined with our adaptive  
 978 search (16).
- 979 **Exact Hess., Grad. Search,  $\gamma_k = \frac{1}{M_k}$ :** denotes the Gradient-Regularized Newton Method  
 980 with adaptive search as in (Doikov et al., 2024a), using  $\gamma_k := \frac{1}{M_k}$  and  $M_k$  is chosen to  
 981 satisfy the condition (17).
- 982 **Exact Hess., Grad. Search,  $\gamma_k = \frac{\|\nabla f(\mathbf{x}_k)\|_*}{M_k}$ :** denotes the Gradient-Regularized Newton  
 983 Method with adaptive search as in (Doikov et al., 2024a), using  $\gamma_k := \frac{\|\nabla f(\mathbf{x}_k)\|_*}{M_k}$  and  $M_k$  is  
 984 chosen to satisfy the condition (17).
- 985 **Gradient Method:** is a partial case of Algorithm 1 where  $\mathbf{H}(\mathbf{x}) \equiv \mathbf{0}$  and  $\mathbf{B} \equiv \mathbf{I}$ , using our  
 986 adaptive search strategy (16).
- 987 **Gauss-Newton:** the Gradient Method with a preconditioning matrix  $\mathbf{B} \equiv \mathbf{A}^\top \mathbf{A}$ , also  
 988 combined with our adaptive search (16).

991 To demonstrate that our theoretical findings are reflected in practice, we validate the effects observed  
 992 in (Fig. 3 (a, b, c)) on additional standard classification problems from `libsvm` (Chang & Lin, 2011).

993 We elaborate further on the connection between our theory and experiments in the following sections.  
 994

## 995 B.1 COMPARISON OF ADAPTIVE SEARCH APPROACHES

997 First, we compare two different adaptive search procedures. Our approach, that is described in  
 998 Appendix D, and uses a condition based on the function value:

$$1000 f(\mathbf{x}_k) - f(\mathbf{x}_{k+1}) \geq \frac{\gamma_k}{8} \frac{\|\nabla f(\mathbf{x}_{k+1})\|_*^2}{\|\nabla f(\mathbf{x}_k)\|_*}. \quad (16)$$

1001 And the adaptive search strategy from (Doikov et al., 2024a), where the sequence  $M_k$  is selected in  
 1002 order to ensure the following condition

$$1004 \langle \nabla f(\mathbf{x}_{k+1}), \mathbf{x}_k - \mathbf{x}_{k+1} \rangle \geq \frac{\|\nabla f(\mathbf{x}_{k+1})\|_*^2}{4M_k \|\nabla f(\mathbf{x}_k)\|_*^l}, \quad \text{where } l \in \left[\frac{2}{3}, 1\right]. \quad (17)$$

1006 Importantly, our theory covers this adaptive search scheme as a special case. Specifically, by selecting  
 1007  $\gamma_k$  as a simple monomial  $\pi(\|\nabla f(\mathbf{x})\|_*) = \frac{1}{M_k} \|\nabla f(\mathbf{x})\|_*^{1-\alpha}$ , we recover the behavior of the method  
 1008 from (Doikov et al., 2024a). This connection is formally established in Section 4.

1009 From our experiments, we observe a nice property of  $\gamma_k$ : it tends to remain nearly constant throughout  
 1010 the iterations of our method (1). Moreover, our value of  $\gamma_k$  is typically larger than the one obtained  
 1011 by the alternative adaptive search procedure proposed in (Doikov et al., 2024a). For representing  
 1012 (Fig. 3 (a)), we use a randomly generated matrix  $\mathbf{A} \in \mathbb{R}^{1000 \times 500}$  and set a large factor  $\mu = 1$ ,  
 1013 which simplifies the problem and yields a more numerically stable and smooth approximation of the  
 1014 maximum function. By varying both  $\mu$  and the data size, we present in Figures 4 and 5 a comparison  
 1015 of convergence behavior and the Gradient-Normalized Smoothness values measured throughout  
 1016 training. These results further support our theoretical findings by illustrating how  $\gamma_k$ , computed via  
 1017 our adaptive search procedure, either increases over time or remains a sufficiently large constant. In  
 1018 both cases, it provides an upper bound for the corresponding  $\gamma_k$  values observed under other variants  
 1019 of the Newton Method and the Gradient Method (i.e., when  $\mathbf{H}(\mathbf{x}) \equiv \mathbf{0}$ ).

## 1020 B.2 INEXACT HESSIAN: LOGSUMEXP

1022 We see that our theory correctly predicts the behavior of the Gradient-Normalized Smoothness  
 1023 across various practical problems. Now, let us focus on the performance of our Algorithm 1 with  
 1024 inexact Hessian. Our goal is to show that our method with inexact Hessian achieves the rate of the  
 1025 full Newton Method and, thus, significantly outperforms the Gradient Method. It is known, that  
 preconditioning the gradient descent direction with an informative matrix substantially improves the

1026 convergence of first-order methods. For instance, one may consider using a method with the inverse  
 1027 curvature matrix  $\mathbf{B}^{-1}$  or a family of polynomials (Doikov & Rodomanov, 2023) as preconditioner  
 1028 in  $\mathbf{x}_{k+1} = \mathbf{x}_k - \gamma_k \mathbf{B}^{-1} \frac{\nabla f(\mathbf{x}_k)}{\|\nabla f(\mathbf{x}_k)\|_*}$ , instead of the standard Gradient Method that does not take into  
 1029 account the physics of the problem and uses  $\mathbf{B} \equiv \mathbf{I}$ . Building on this insight, we outline the method  
 1030 we call the *Gauss-Newton* as our algorithm with  
 1031

$$\mathbf{H}(\mathbf{x}) := \mathbf{A}^\top \mathbf{A}. \quad (18)$$

1032 Note that the Newton Method with matrix (18) corresponds to the classical Gauss-Newton method for  
 1033 linear models, where the Jacobian is simply  $\mathbf{A}$ . In Figures 6 and 7, we show that the Gauss-Newton  
 1034 algorithm significantly outperforms the plain Gradient Method with  $\mathbf{B} := \mathbf{I}$ .  
 1035

1036 However, our theory suggests that Algorithm 1 with Hessian approximation that satisfies condition  
 1037 (2) with  $\mathbf{C}_1 \approx 0$  should achieve the same convergence rate as the full Newton and outperform both  
 1038 the Gradient and Gauss-Newton methods on the LogSumExp problem. For that, we consider the  
 1039 following approximation that we call the *Weighted Gauss-Newton*:  
 1040

$$1042 \mathbf{H}(\mathbf{x}) := \frac{1}{\mu} \mathbf{A}^\top \text{Diag}(\text{smax}(\mathbf{A}, \mathbf{x})) \mathbf{A}, \quad [\text{smax}(\mathbf{A}, \mathbf{x})]_k := \frac{\exp[\frac{1}{\mu}(\langle \mathbf{a}_k, \mathbf{x} \rangle - b_k)]}{\sum_{j=1}^d \exp[\frac{1}{\mu}(\langle \mathbf{a}_j, \mathbf{x} \rangle - b_j)]}. \quad (19)$$

1043 In other words, Equation (19) corresponds to Equation (18) with entries of  $\mathbf{A}$ , weighted by  $\text{smax}(\cdot) \in$   
 1044  $\mathbb{R}^d$ . Since the Hessian of the LogSumExp objective (15) is given by  
 1045

$$1046 \nabla^2 f(\mathbf{x}) = \frac{1}{\mu} \mathbf{A}^\top \left( \text{Diag}(\text{smax}(\mathbf{A}, \mathbf{x})) - \text{smax}(\mathbf{A}, \mathbf{x}) \text{smax}(\mathbf{A}, \mathbf{x})^\top \right) \mathbf{A} \\ 1047 = \mathbf{H}(\mathbf{x}) - \frac{1}{\mu} \mathbf{A}^\top \left( \text{smax}(\mathbf{A}, \mathbf{x}) \text{smax}(\mathbf{A}, \mathbf{x})^\top \right) \mathbf{A} = \mathbf{H}(\mathbf{x}) - \frac{1}{\mu} \nabla f(\mathbf{x}) \nabla f(\mathbf{x})^\top,$$

1048 we see that with such approximation  $\mathbf{H}(\mathbf{x})$  we can perfectly match the condition (2) (refer to  
 1049 Appendix H for more details). This is one of the main examples of approximations that are covered  
 1050 by our analysis.  
 1051

1052 We show that the Newton Method with Hessian approximation (19) and with  $\gamma$  selected by an adaptive  
 1053 search (Algorithm 3), performs comparably to the Newton Method with the exact Hessian and the  
 1054 same adaptive search procedure, see Figure 6. Moreover, as our theory suggests, the LogSumExp  
 1055 objective corresponds to the case  $\mathbf{C}_1 = 0$  with  $\mathbf{C}_2 > 0$  being some constant (see Example 8). Thus,  
 1056 according to the results in Table 1, which are also visualized in Figure 1, it places us in the regime  
 1057 where the smoothness of the objective dominates the Hessian inexactness, i.e., we should observe the  
 1058 rate of the full Newton Method for our Algorithm 1 with approximation (19). We actually see this  
 1059 behavior in further examples as well.  
 1060

1061  
 1062  
 1063  
 1064  
 1065  
 1066  
 1067  
 1068  
 1069  
 1070  
 1071  
 1072  
 1073  
 1074  
 1075  
 1076  
 1077  
 1078  
 1079

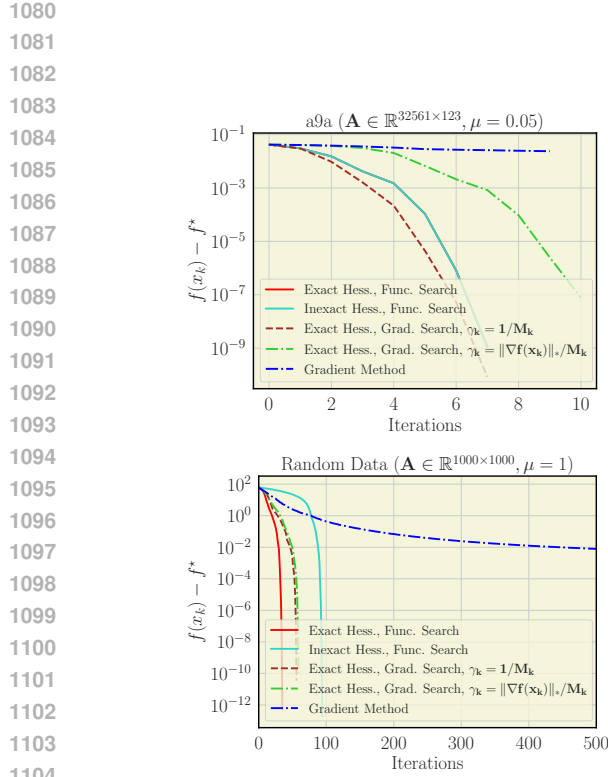


**Figure 4: LogSumExp objective. Convergence (left) and the Gradient-Normalized Smoothness (right).** An interesting effect we observe in the figure is that, e.g., on the a9a dataset, ever since Algorithm 1 exhibits a sharper convergence on the log-scaled plot, its corresponding  $\gamma_k$  values start increasing more rapidly than those produced by other adaptive search procedures. Additionally, for a9a, we observe an almost perfect match between the exact Hessian and its approximation, likely due to the simplicity of the problem (the Newton Method need only 8 iterations to converge). Notably, we also observe a predictable, rapid decrease in  $\gamma_k$  for the Gradient Method on a relatively hard problem ( $\sim 30$  iterations of the Newton Method to converge).

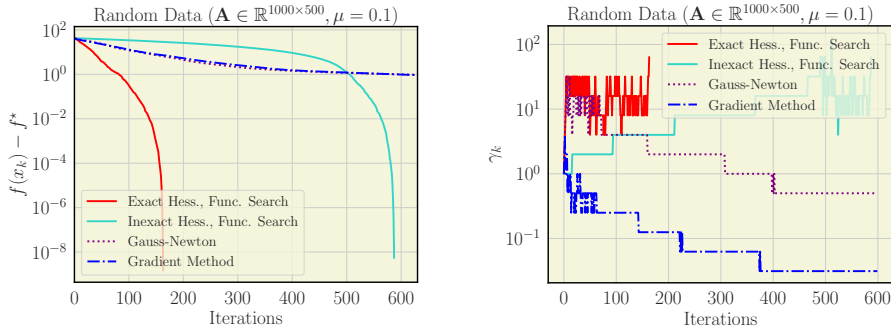


**Figure 5: LogSumExp objective. Convergence (left) and the Gradient-Normalized Smoothness (right).** In the left figure, we may observe almost identical performance of Gradient Method and Gauss-Newton on a sufficiently hard task ( $\sim 150$  iterations of Newton Method to converge). However, we see that the empirical values of Gradient-Normalized Smoothness for Gauss-Newton decrease significantly more slowly than those for Gradient Method. For our future experiments, this indicates a particular power of Gradient Method with Gauss-Newton preconditioner that adapts better to the physics of the problem.

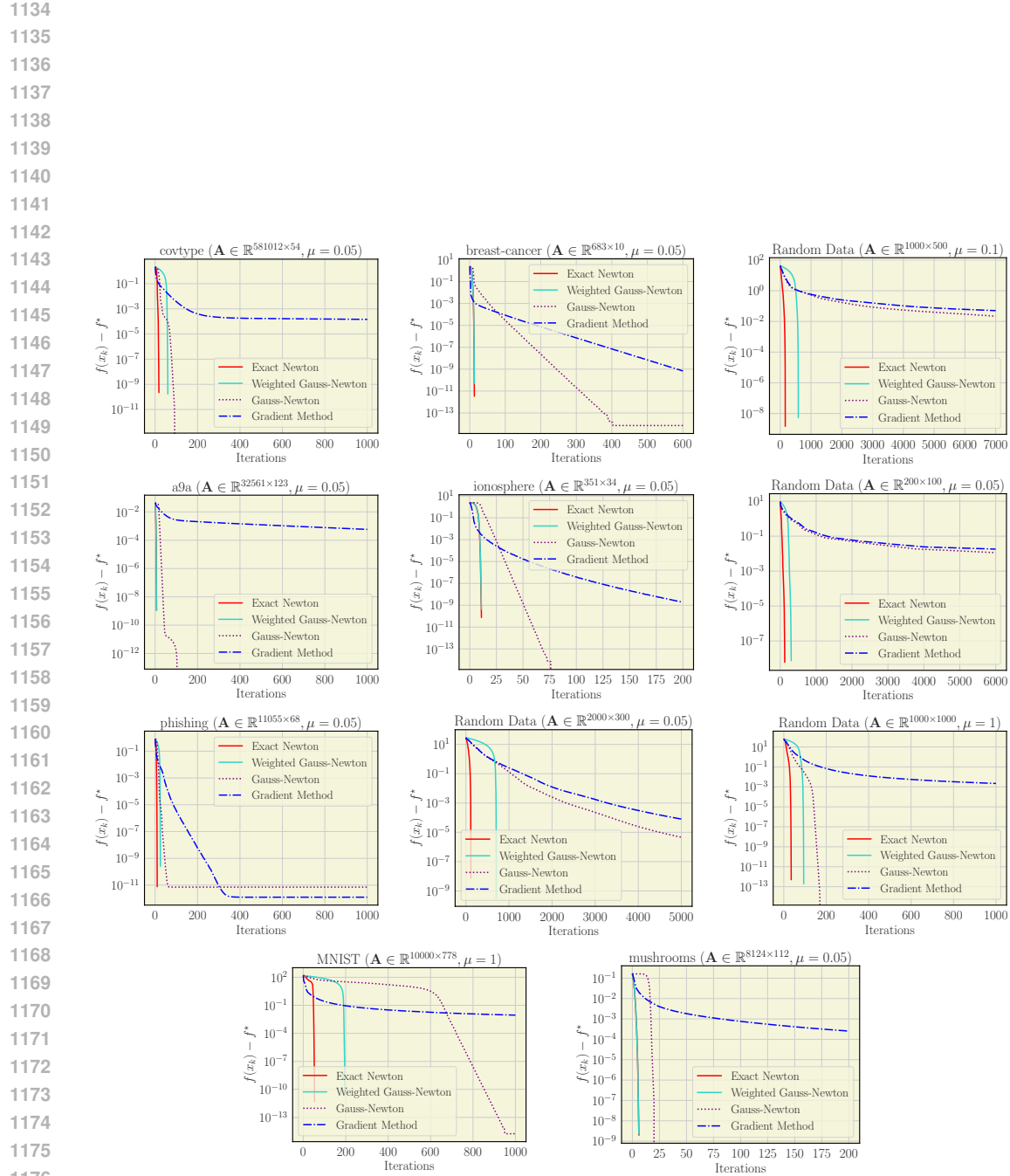


**Figure 6: LogSumExp objective. Our method with approximation noticeably outperforms both Gradient Method and its Gauss-Newton preconditioned variant.** According to our theoretical results, this problem falls into a regime where the convergence rate matches that of the full Newton method. Indeed, we observe consistent convergence behavior between the Exact and Inexact variants of our method across a wide range of examples.

1188

## B.3 NONLINEAR EQUATIONS: STUDYING THE DEGREE OF SMOOTHNESS

1189

Let us consider a setup with the Nonlinear Equations objective defined in Example 7:

1190

$$f(\mathbf{x}) := \frac{1}{p} \|\mathbf{u}(\mathbf{x})\|^p \equiv \frac{1}{p} \langle \mathbf{G}\mathbf{u}(\mathbf{x}), \mathbf{u}(\mathbf{x}) \rangle^{\frac{p}{2}}, \quad \mathbf{G} = \mathbf{G}^T \succ 0, \quad p \geq 2.$$

1191

**The Exact Case.** First, we study the case of the linear operator  $\mathbf{u}(\cdot)$ . We elaborate the nonlinear case in Appendix B.4. Here, the Hessian approximation  $\mathbf{H}(\mathbf{x})$  suggested by our theory is equal to the true Hessian if the operator  $\mathbf{u}(\mathbf{x})$  is linear. Indeed, from Example 7 and taking into account that  $\mathbf{u}(\mathbf{x}) = \mathbf{A}\mathbf{x} - \mathbf{b}$  and  $\nabla^2\mathbf{u}(\mathbf{x}) = \mathbf{0}$ , we have

1192

1193

1194

1195

1196

1197

1198

$$\nabla^2 f(\mathbf{x}) = \|\mathbf{u}(\mathbf{x})\|^{p-2} \mathbf{A}^T \mathbf{G} \mathbf{A} + \frac{p-2}{\|\mathbf{u}(\mathbf{x})\|^p} \nabla f(\mathbf{x}) \nabla f(\mathbf{x})^\top \equiv \mathbf{H}(\mathbf{x}). \quad (20)$$

1199

1200

1201

1202

1203

1204

1205

1206

Thus, we demonstrate the comparison of the exact Newton Method with the Gradient Method and the Gauss-Newton. Importantly, if  $p = 2$ ,  $\mathbf{H}(\mathbf{x})$  appears to be the scaled Gauss-Newton matrix, while for any  $p > 2$  we also have an additional rank-one term. As increasing  $p$  complicates our problem, in this experiment we vary the power  $p$ , starting with a simple quadratic problem,  $p = 2$ , and extending up to  $p = 5$ . Our results show that, for all values  $p$  considered, the Gradient Method preconditioned with the curvature matrix  $\mathbf{B} \equiv \mathbf{A}^T \mathbf{A}$  performs comparably to, or even outperforms, the variant of our algorithm that uses the full Hessian  $\nabla^2 f(\mathbf{x}) \equiv \mathbf{H}(\mathbf{x})$ . This observation highlights a significant consequence of our theoretical analysis, particularly in relation to Example 7.

1207

1208

1209

1210

1211

1212

1213

1214

1215

1216

**Towards Inexact Hessians for Linear Operators.** Nevertheless the Hessian approximation  $\mathbf{H}(\mathbf{x})$  suggested in Example 7 is equivalent to the exact Hessian when the operator  $\mathbf{u}(\cdot)$  is linear, one still can treat this matrix as a sum of two: a rank-one term  $\frac{p-2}{\|\mathbf{u}(\mathbf{x})\|^p} \nabla f(\mathbf{x}) \nabla f(\mathbf{x})^\top$ , and the summand with Jacobians  $\|\mathbf{u}(\mathbf{x})\|^{p-2} \mathbf{A}^T \mathbf{B} \mathbf{A}$ . The latter term can be viewed as the Gauss-Newton preconditioner scaled by  $\|\mathbf{u}(\mathbf{x})\|^{p-2}$ , while the last term corresponds to the Fisher approximation up to a multiplicative factor  $\frac{p-2}{\|\mathbf{u}(\mathbf{x})\|^p}$ . Hence, we can consider those chunks of the Hessian  $\mathbf{H}(\mathbf{x})$  from Example 7 as a potential approximations. While usage of the scaled Gauss-Newton term of  $\mathbf{H}(\mathbf{x})$  resembles the Gauss-Newton method from our previous experiments, the Fisher term of  $\mathbf{H}(\mathbf{x})$  arouses interest. Therefore, in this part of our experimental validations, we consider the Exact Newton Method, Gradient Method and the following algorithm

1217

1218

$$\mathbf{x}_{k+1} = \mathbf{x}_k - \left( \frac{p-2}{\|\mathbf{u}(\mathbf{x})\|^p} \nabla f(\mathbf{x}_k) \nabla f(\mathbf{x}_k)^\top + \frac{\|\nabla f(\mathbf{x}_k)\|_*}{\gamma_k} \mathbf{A}^T \mathbf{A} \right)^{-1} \nabla f(\mathbf{x}_k). \quad (21)$$

1219

1220

I.e., the derived update corresponds to the Gauss-Newton method with rank-one correction. In experiments, we call this method — **Fisher Term of H**.

1221

1222

1223

1224

1225

1226

1227

1228

1229

We run the comparison of methods on the same the Nonlinear Equations problem on MNIST and a small, randomly generated dataset. Note, that for the random dataset, we chose exactly the same runs of the Exact Newton and the Gradient Method as in Figure 7. Results for this experiment are in Figures 8 and 9. Importantly, our version of Algorithm 1 with Fisher approximation not only achieves the comparable convergence as the Exact Newton, but also a way more faster in terms of the wall-clock time. In Figure 8, we show that our method with the Fisher-type approximation consistently outperforms the Gradient Method and, in some cases, even the Exact Newton Method, while having almost as cheap per-iteration cost as the Gradient Method, especially if the problem is a small dimensional.

1230

1231

1232

1233

1234

We pose that, in practice, the most time-consuming part of computations for Algorithm 1 with approximation from (21) are in the inverting of the  $\mathbf{A}^T \mathbf{A}$ , however the overall computational time can be significantly accelerated via the usage of the Woodbury-Sherman-Morrison formula (Max, 1950) to exactly compute the invert in Equation (21). We do this in practice and achieve almost the same speed on small-scale problems, while having an insignificant slowdown on large-scale ones.

1235

1236

1237

1238

1239

1240

1241

Besides the results in Figure 8, we also investigate the behavior of our method with Fisher-like approximation on the Nonlinear Equations problem varying the power  $p$ . Throughout those experiments with modifications of  $p$ , we observe a consistent improvement of our method with approximation over the Gradient Method and the comparable performance of it compared to the Exact Newton Method. We summarize our experimental observations in Figure 9. This result suggests that one of the approximations suggested by our theory (see Appendix H) not only resembles the converge of the full Newton, but also is very cheap in per-iteration costs (compared to the Gradient Method), which makes it a powerful tool for such a problems and verifies our theoretical findings.

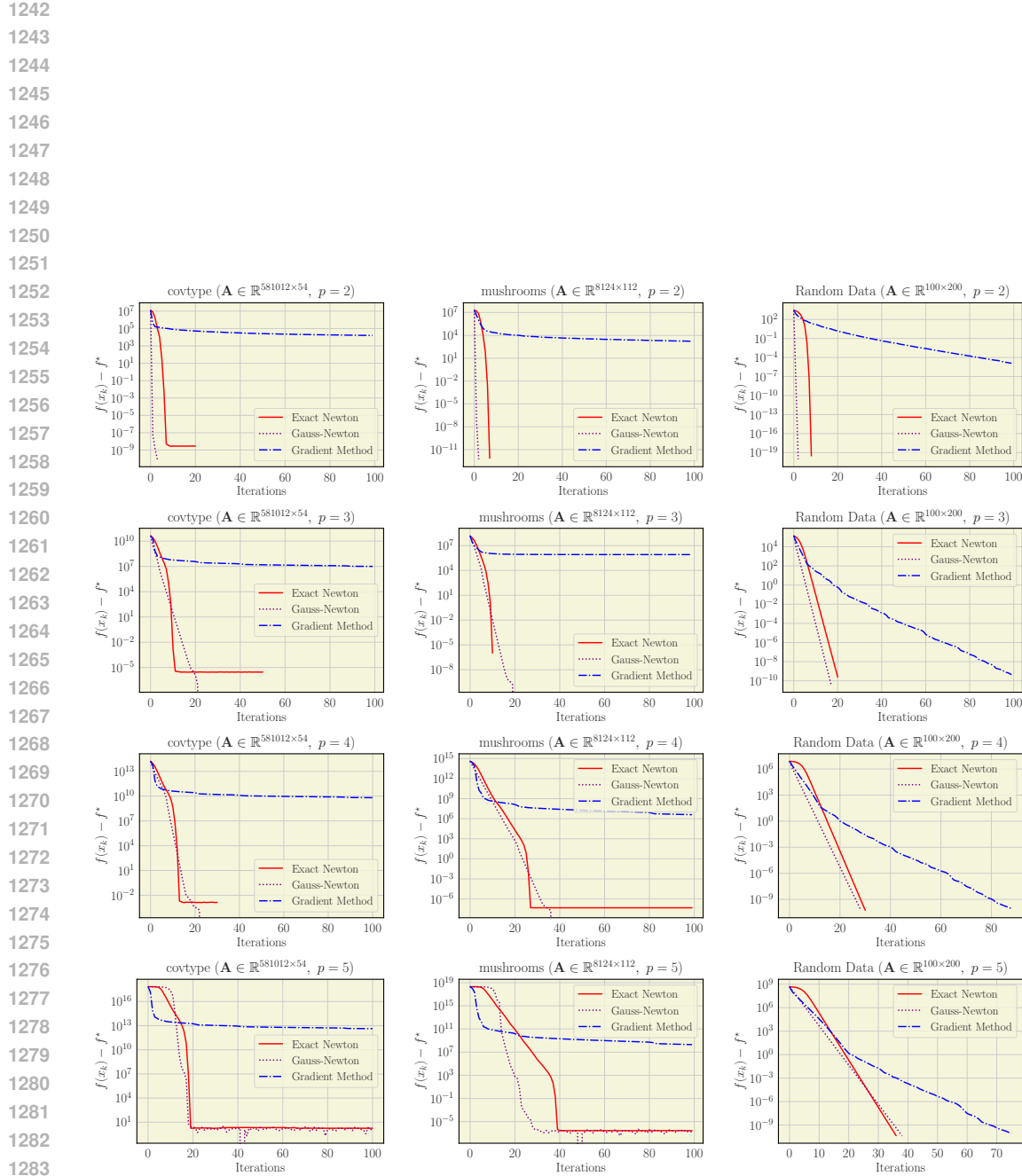


**Figure 7: Objective with Linear Operator.** In this setting, our method is identical when using either the exact or inexact Hessian given by (20). Notably, the Gauss-Newton preconditioning enables the Gradient Method to achieve performance comparable to the Newton Method. In contrast, the Gradient Method with our adaptive search exhibits significantly slower convergence for large values of  $p$ .

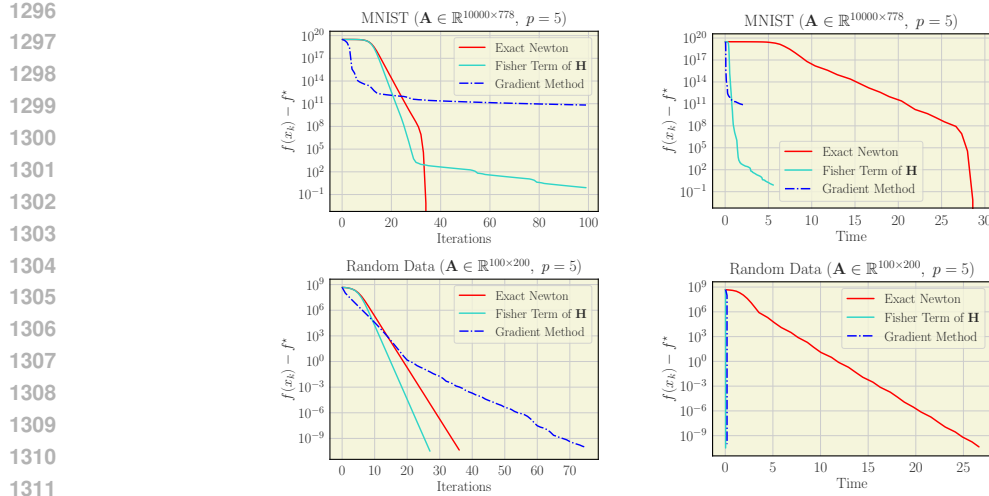


**Figure 8: Objective with Linear Operator. Our method with the inexact Hessian of a Fisher-type form (21) performs comparably to the Exact Newton Method.** In this experiment, we compare method (21) with the Exact Newton Method with the Hessian of (20) and the Gradient Method. We utilize objective from Example 7 with large values of  $p = 2$ , which complicates the problem. As our theory suggests, one can consider instead of the full Hessian (20) only its rank-one Fisher term  $\frac{p-2}{\|\mathbf{u}(\mathbf{x})\|^p} \nabla f(\mathbf{x}) \nabla f(\mathbf{x})^\top$ . If additionally we set  $\mathbf{B} := \mathbf{A}^\top \mathbf{A}$  in Algorithm 1 with the approximation above, then we get a matrix that is can be inverted fast with by the Woodbury-Sherman-Morrison formula. Moreover, it appears that such a method performs relatively similar to the Exact Newton. Indeed, in all cases with large  $p$ , both exact and inexact algorithm significantly outperform the Gradient Method, as well as for the moderate powers  $p$  in Figure 9. At the same time, Algorithm 1 with the Fisher-type approximation works much faster than the Exact Newton in the wall-clock time comparisons. Interestingly, that we also can observe how the difference in the wall-clock time performance for the Inexact Newton and the Gradient Method increases with dimensionality of the problem (MNIST versus small synthetic dataset). We see that this difference diminishes when the problem is small-dimensional, since the inversion in (21) happens much faster.

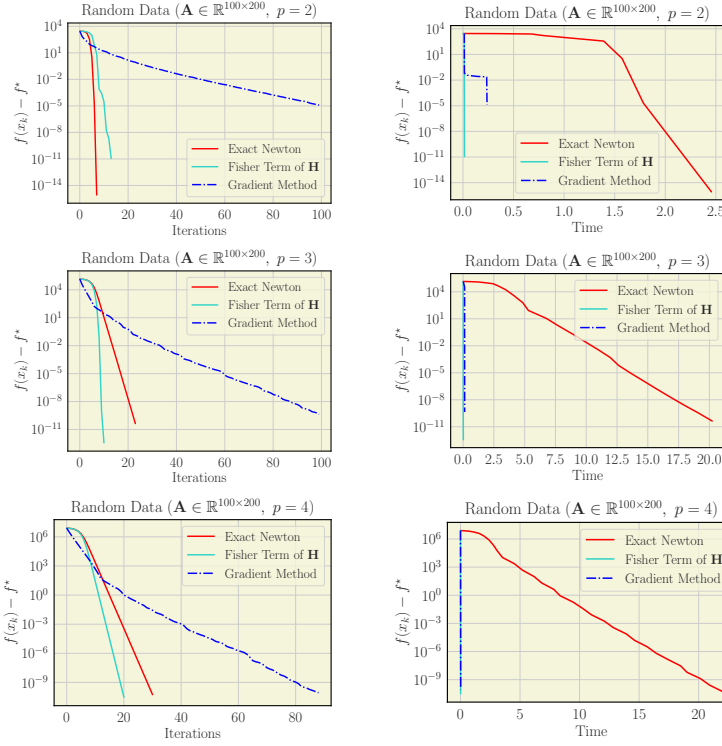


**Figure 9: Objective with Linear Operator. Our method with the inexact Hessian of a Fisher-type form (21) performs comparably to the Exact Newton Method.** In this experiment, we show that problem in Example 7 with linear operator  $\mathbf{u}(\mathbf{x}) = \mathbf{A}\mathbf{x} - \mathbf{b}$  can also be considered via the inexact Hessians perspective. Indeed, the update rule for the Exact Newton Method with (20), in this case, resembles a combination of the Gauss-Newton term and the rank-one Fisher update. However, if one would use the matrix  $\mathbf{B} := \mathbf{A}^\top \mathbf{A}$  in Algorithm 1, then it is possible to get rid of the Gauss-Newton term and use only rank-one correction as in (21). Thus, the most computationally expensive part in the algorithm is inversion of  $\mathbf{A}^\top \mathbf{A}$ . But, with the Woodbury-Sherman-Morrison formula this inversion becomes a particularly cheap operation and can be done relatively fast. As we see, our algorithm with the inexact Hessian not only remains the convergence of the Exact Newton in this case, but also works almost as fast as the Gradient Method in the wall-clock time comparison.

1350 B.4 NON-CONVEX OBJECTIVES  
1351

1352 Let us also delve into numerical experiments on non-convex functions. In this part, we consider a  
1353 simple yet widespread problem of the optimization of the Rosenbrock function (Rosenbrock, 1960).  
1354 And the the Nonlinear Equations problem with the operator being from a family of Chebyshev  
1355 polynomials. The latter example is particularly novel for the experiments and, to the best of our  
1356 knowledge, has been investigated in practice in the non-smooth case in (Kabgani & Ahookhosh, 2025;  
1357 Gürbüzbalaban & Overton, 2012) (a so-called Chebyshev oscillator problem), and in the smooth case  
1358 in (Cartis et al., 2013). We extend all prior experimental results on these objectives to the Nonlinear  
1359 Equations problem with different powers  $p$  and usage of the inexact Hessian.

1360 **Two-Dimensional Rosenbrock Function.** We utilize a non-convex smooth objective of the following  
1361 form

$$1362 f(\mathbf{x}) = (1 - x_1)^2 + 100 (x_2 - x_1^2)^2, \quad \text{where } \mathbf{x} := (x_1, x_2)^\top \in \mathbb{R}^2. \quad (22)$$

1363 Note that (22) can be seen as a smooth variant of the Nesterov-Chebyshev-Rosenbrock function  
1364 (Gürbüzbalaban & Overton, 2012). In scientific computing, this function is used as a benchmarking  
1365 problem for optimization algorithms. It has a unique global minimizer  $(1, 1)$ , where  $f^* = 0$ . This  
1366 global minimum is inside a parabolic-shaped valley (Figure 12) that is easy to find, but, for the  
1367 Gradient Method, it takes thousands of iterations to approach the vicinity of the solution (Figure 10).

1368 **Nonlinear Equations with the Rosenbrock Function.** To follow our theoretical justifications, we  
1369 not only investigate the convergence of Algorithm 1 on the plain Rosenbrock function, but also  
1370 introduce a new objective that relates to our previous finding and to Example 7. We formalize it as

$$1372 f(\mathbf{x}) = \frac{1}{p} \|\mathbf{u}(\mathbf{x})\|^p, \quad \text{where } \mathbf{u}(\mathbf{x}) := (1 - x_1, 10(x_2 - x_1^2))^\top. \quad (23)$$

1373 We call such an operator  $\mathbf{u}(\mathbf{x})$  — vector of the Rosenbrock residuals and refer to the problem of  
1374 minimizing (23) as **Nonlinear Equations & Rosenbrock**. For the case  $p = 2$ , the objective (23)  
1375 resembles (22) up to a constant factor  $\frac{1}{2}$ , thus both problems have the same optimum and are similar  
1376 (see Figure 10). However, reformulation (23) allows us to introduce the notion of Hessian inexactness  
1377 that we cover in our theoretical analysis. Thus, using our approximation from Example 7, we can  
1378 approach problem (23) with Algorithm 1 using an inexact Hessian. As theory suggests, our method  
1379 should achieve the same convergence rate as the full Newton, which we observe in Figure 10 (b) and  
1380 in Figure 11 when varying the power  $p$ , making the problem harder for the Gradient Method.

1381 Furthermore, we see that the Gradient Method and our algorithm with exact and inexact Hessian  
1382 follow the same optimization direction through this narrow parabolic-shaped valley of the Rosenbrock  
1383 function — Figure 12. However, our method accelerates much when finds a sweet spot in this valley.

1384 As an advantage of using the Hessian approximation in this setup, we pose the fact that the Newton  
1385 Method with an exact Hessian fails to converge given some inappropriate starting point which can  
1386 actually be close to the optimum — Figure 13. Which happens due to the inability to invert the  
1387 regularized Hessian of the objective at the beginning of the run. At the same time, Algorithm 1 with  
1388 an inexact Hessian succeeds for any starting points we have tried.

1389 **Inexact Hessian and the Chebyshev Polynomials.** We illustrate our theoretical finding on a new,  
1390 particularly interesting problem — Nonlinear Equations with Chebyshev polynomials. We formulate  
1391 our objective as follows

$$1393 f(\mathbf{x}) = \frac{1}{p} \|\mathbf{u}(\mathbf{x})\|^p; \quad \text{where } \mathbf{u}(\mathbf{x}) = (u_1(\mathbf{x}), \dots, u_d(\mathbf{x}))^\top, \quad \text{such that} \\ 1394 \\ 1395 u_1(\mathbf{x}) = \frac{1}{2}(1 - x_1), \quad u_i(\mathbf{x}) = x_i - p_2(x_{i-1}), \quad p_2(\tau) = 2\tau^2 - 1.$$

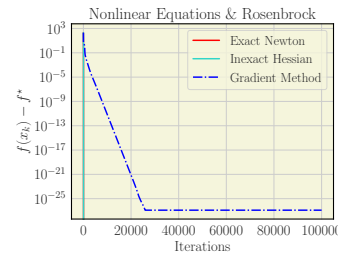
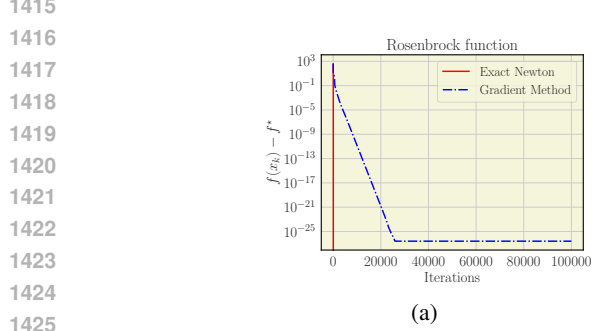
1396 Where  $p_2$  is the Chebyshev polynomial of degree two. Clearly, for the case  $p = 2$ , our objective (24)  
1397 resembles the smooth Nesterov-Chebyshev-Rosenbrock function studied in (Jarre, 2011; Cartis et al.,  
1398 2013) up to a constant factor  $\frac{1}{2}$ . Indeed,

$$1400 \|\mathbf{u}(\mathbf{x})\|^2 = \frac{1}{4} (1 - x_1)^2 + \sum_{i=1}^{d-1} (x_{i+1} - 2x_i^2 + 1)^2.$$

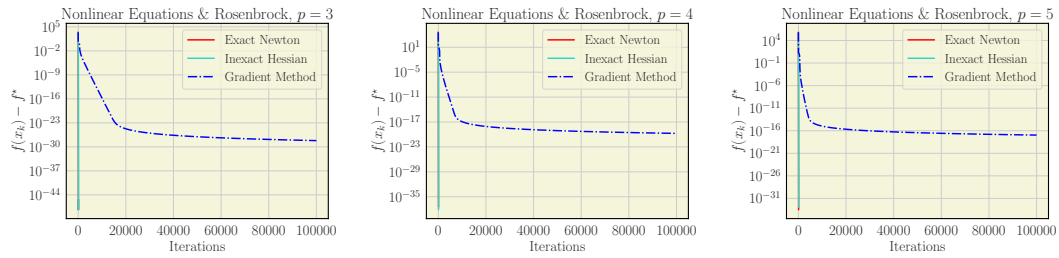
1403 As for the plain Rosenbrock function (22) and our adaptation of it to the Nonlinear Equations problem  
(23), the only stationary point  $(1, \dots, 1)$  of the Nesterov-Chebyshev-Rosenbrock objective is the

1404 global minimizer. Although this function is very difficult for numerical methods in both its smooth  
 1405 (Jarre, 2011) and non-smooth (Gürbüzbalaban & Overton, 2012) variants.  
 1406

1407 In our experiments, we extend the Nesterov-Chebyshev-Rosenbrock function to (24). Thus, we are  
 1408 able to use the approximation of Example 7 in our method. We demonstrate the convergence of  
 1409 the full Newton, Algorithm 1 with the inexact Hessian and the Gradient Method. And show how it  
 1410 depends on the effects that come from the increase in the dimensionality of the vector function  $u(\cdot)$   
 1411 and the increase of power  $p$  in our objective (24). We notice that our method with approximation  
 1412 performs remarkably well in all settings we have tried, as depicted in Figures 14 and 15. In particular,  
 1413 both exact and inexact variants of Algorithm 1 perform significantly better than the Gradient Method  
 1414 when  $p$  is small enough (Figure 14), but when increasing  $p$  (Figure 15), we observe that the Gradient  
 1415 Method also starts to perform better.



1427 **Figure 10: Optimization of the Rosenbrock function (a), and the Nonlinear Equation problem for  $p = 2$  with Rosenbrock residuals (b),**  
 1428 looks quite similar. For the second problem we can use the Hessian approximation suggested by our theory (see Example 7). With such an  
 1429 approximation our method is in the regime where it has the same convergence as the Newton Method with the full Hessian. However, by using  
 1430 an inexact Hessian, we obtain a more numerically stable algorithm with respect to the choice of the starting iterate, as depicted in Figure 13.



1438 **Figure 11: Varying the power  $p$  in the Nonlinear Equations problem (23)** we complicate the convergence for the Gradient Method. However,  
 1439 our method with an approximation and the Newton Method works quite similarly even for different values of  $p$ . Here, "Inexact Hessian" stands  
 1440 for the approximation suggested by our theory in Example 7.

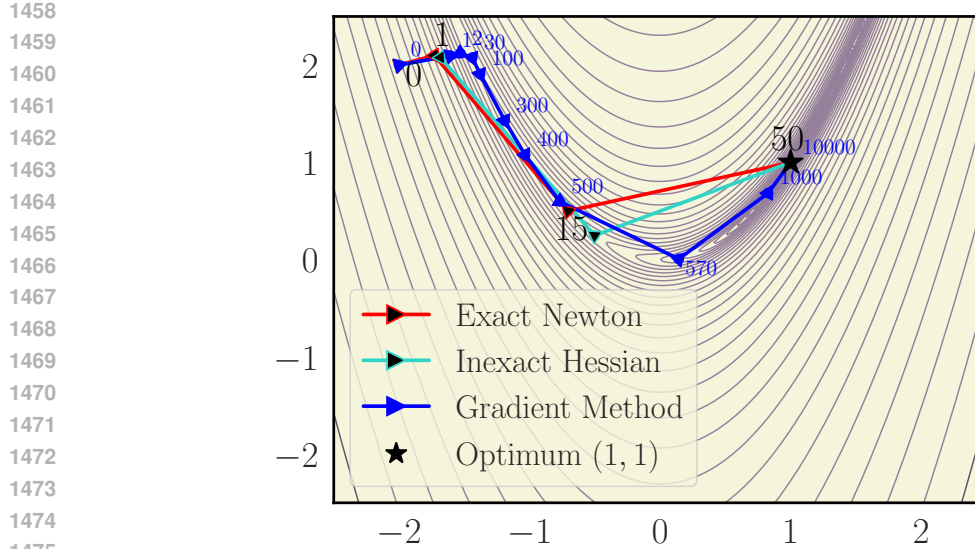


**Figure 12: Contour plot of the Nonlinear Equations problem with the Rosenbrock residuals in the two-dimensional case.** In a similar way that the authors of (Kabgani & Ahookhosh, 2025; Gürbüzbalaban & Overton, 2012) do for the problems they consider, we plot the level contours for the objective  $f(\mathbf{x}) = \frac{1}{2} \|\mathbf{u}(\mathbf{x})\|^2$  with operator  $\mathbf{u}(\mathbf{x}) := (1 - x_1, 10(x_2 - x_1^2))^\top$  being a vector-function of two Rosenbrock residuals as in Equation (23). The contour we obtain for this objective also similar to that of the *non-smooth* variant of the Nesterov-Chebyshev-Rosenbrock function from (Gürbüzbalaban & Overton, 2012). However, our objective (23) remains a *non-convex smooth* function, thus, serves as a good example complementing our theory. Points connected by line segments show the iterates generated by Algorithm 1 with exact Hessian, Algorithm 1 with approximation described in Example 7, and the Gradient Method. The markers for Exact and Inexact methods are of the same color because the optimization trajectory of both algorithms is quite similar and their consecutive iterates lie relatively close to each other. For all methods we utilize our adaptive search procedure (see Equation (16) and Appendix D). The comparison run of exactly those methods in terms of the functional residual is depicted in Figure 10 (b) and the starting point is  $(-2, 2)$ . In our contour plot, we see that all three methods, when initialized outside the parabolic valley of the objective, firstly tend to find this valley as soon as possible, and then follow down to the global minimizer  $(1, 1)$ . However, both Exact and Inexact methods move significantly faster once they found the valley. Indeed, we see that the first iterate returned by the Gradient Method is closer to the valley, but then, 15-th iterate of Algorithm 1 variations is ahead of 500-th iterate of the Gradient Method.

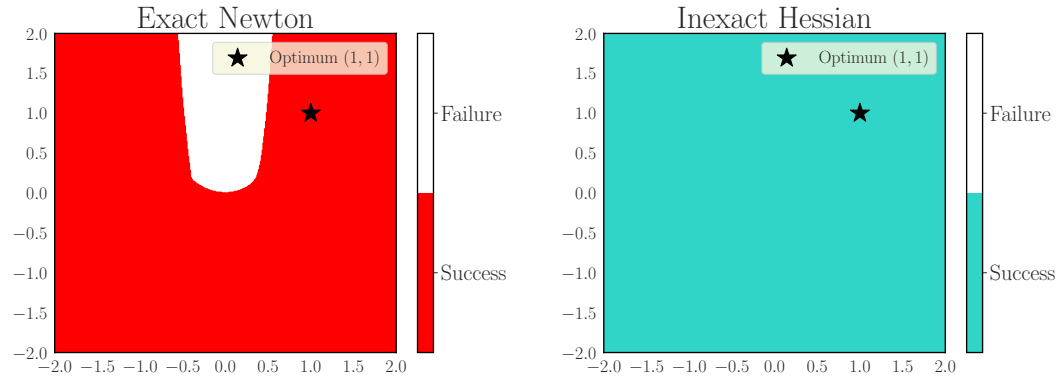


**Figure 13: Region of Starting Points Where Method Fails to Converge.** In this experiment, we consider Algorithm 1 with an exact Hessian and the same method with approximation described in Example 7. We employ our adaptive search procedure (see Equation (16) and Appendix D), and run both methods on the Nonlinear Equations problems with the Rosenbrock residuals in the two-dimensional case. We chose the starting point  $\mathbf{x}_0$  from a grid in the range  $(-2, 2)$  for both its coordinates. Interestingly, the method with the full Hessian fails to converge given certain starting points that are relatively close to the global minimizer. This happens due to the ill-conditioning issues with the exact Hessian matrix during the inversion. Fixing those issues with another choice of regularization or update rule means changing the algorithm, therefore we did not perform those changes. However, our algorithm with inexact Hessian works remarkably well without for any starting iterate given from the range we considered. Therefore, our experimental validations suggests that Algorithm 1 with inexact Hessian not only performs similarly to the full Newton if the approximation is in accordance with our theory, but also serves as more numerically stable method.

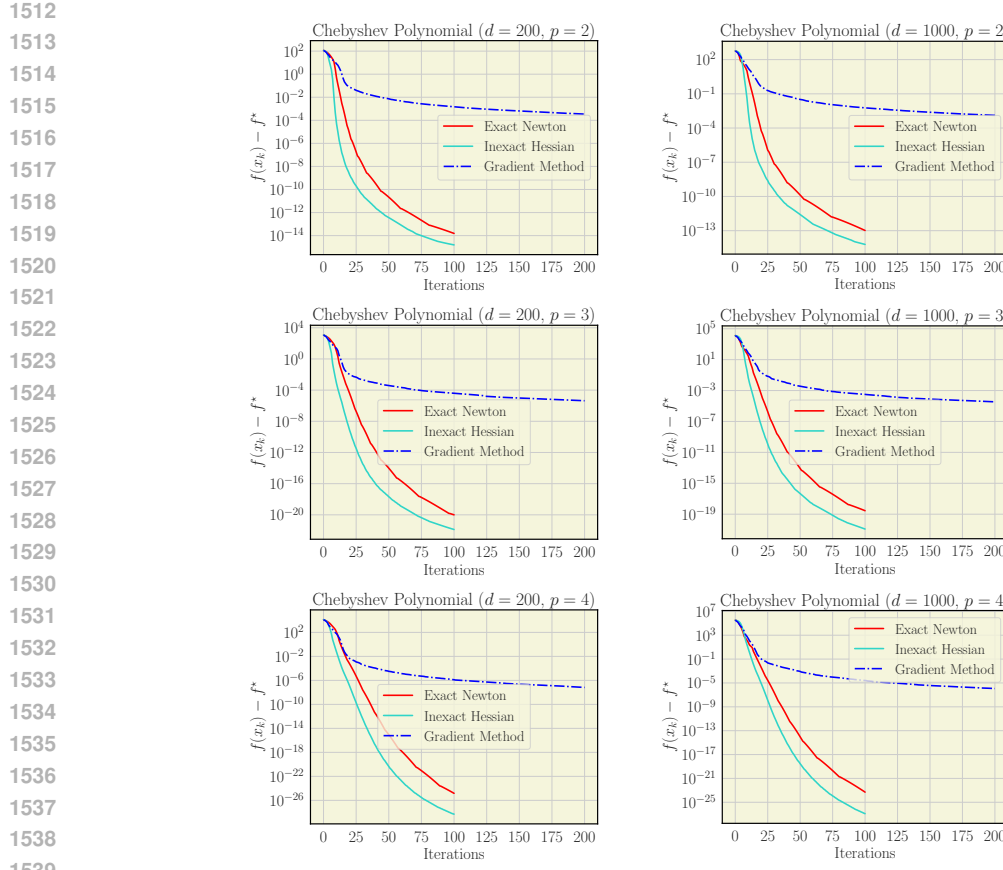


**Figure 14: Algorithm 1 with the inexact Hessian noticeably outperforms both the full Newton and the Gradient Method on the Nonlinear Equations problem with the Chebyshev polynomial objective.** For this experiment, we utilize the objective (24), where  $d$  stands for the dimension of the vector-function  $\mathbf{u}(\cdot)$ . Importantly,  $\|\mathbf{u}(\mathbf{x})\|^2$  correspond to the smooth variant of the Nesterov-Chebyshev-Rosenbrock function which is known as a hard problem for numerical methods. Throughout this experiment, we vary both  $p$  and  $d$  to complicate the optimization of our objective. Noticeably, in all these cases Algorithm 1 with approximation outperforms the full Newton.

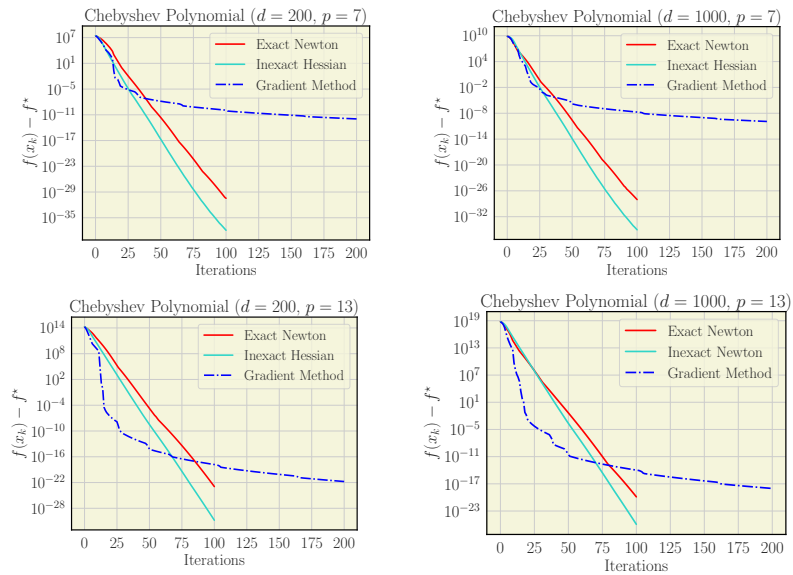


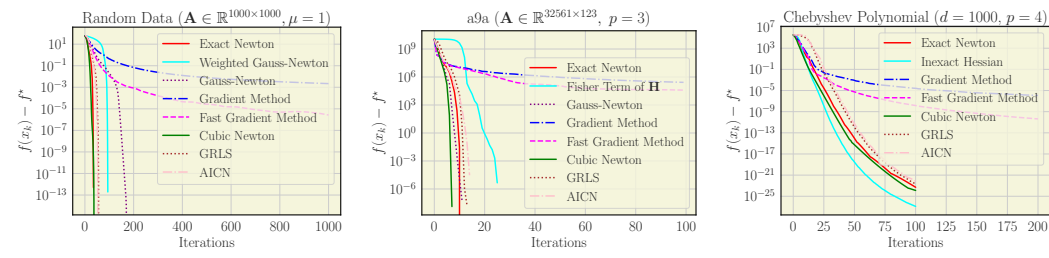
**Figure 15: When increasing the power  $p$ , we see that the gap between Algorithm 1 and the Gradient Method narrows.** We run three methods on objective (24) and, in the same way as in Figure 14, we increase both  $p$  and the dimension of  $\mathbf{u}(\cdot)$ . Clearly, we observe a dynamics that the gain of Algorithm 1 with and without approximation becomes less significant when the  $p$  is large.

1566  
1567

## B.5 COMPARISON WITH ADAPTIVE AND UNIVERSAL METHODS

1568  
1569  
1570  
1571  
1572  
1573  
1574  
1575  
1576  
1577  
1578  
1579  
1580  
1581

In this section, we elaborate more on comparisons of our framework with other adaptive and universal methods. We experimentally study the Cubic Newton method (Nesterov & Polyak, 2006) and two more algorithms, namely—Affine-Invariant Cubic Newton AICN (Hanzely et al., 2022) and Gradient-Regulated Line Search (GRLS) (Hanzely et al., 2024). Both AICN and GRLS are instances of the Damped Newton method, but with different adaptive rules for the step-size selection. While for the Exact Newton method with gradient regularization and its version with the inexact Hessian, we use the adaptive search for parameter  $\gamma(\cdot)$ , which controls the regularization term in line 3 of Algorithm 1. We also compare their performance with the Fast Gradient Method (Nesterov, 2018) to observe the advantage from using (an approximate) second-order information. As problems for this comparison visualized in Figure 16, we choose: LogSumExp (a), Nonlinear Equations (b) on the a9a dataset, and Chebyshev polynomials (c). Their descriptions match those from prior sections. Subsequently, we employ the Weighted Gauss-Newton approximation (Eq. 19) for LogSumExp, Fisher Term of  $\mathbf{H}$  (Eq. 21) for Nonlinear Equations, and the approximation from Example 7 for Chebyshev polynomials.

1582  
1583  
1584  
1585  
1586  
1587  
1588  
15891590  
1591

(a) LogSumExp &amp; approx. 19. (b) Nonlinear Equations &amp; approx. 21. (c) Chebyshev &amp; approx. from Example 7.

1592  
1593  
1594  
1595  
1596  
1597  
1598  
1599  
1600  
1601  
1602  
1603  
1604  
1605  
1606  
1607  
1608  
1609  
1610  
1611  
1612  
1613  
1614  
1615  
1616  
1617  
1618  
1619

**Figure 16: Comparison with Cubic Newton and versions of the Damped Newton method with adaptive step-size.** In all figures, we demonstrate a clear improvement of second-order methods and Algorithm 1 with inexact Hessians and adaptive search over first-order methods on both convex ((a,b)) and non-convex (c) objectives, for important problems, corresponding to Examples 8 and 7. Runs in (a), follow the recipe from Appendix B.2, where we used the Weighted Gauss-Newton approximation (Eq. 19), theoretical bounds for this kind of approximation are proven in Example 11. The only difference with a setup from the prior section, is that we study more methods here: Cubic Newton, accelerated gradient method, and two versions of the Damped Newton with adaptive step-sizes—GRLS and AICN. In (b), we replicate our experiments from Appendix B.3, utilizing the Fisher Term of  $\mathbf{H}$  approximation (Eq. 21). The main difference here, except for the methods, is a new a9a dataset that is not presented in Figures 7, 8, 9. See proofs for the bounds on the approximation in Example 12. Finally, in (c), we show results for the non-convex smooth Chebyshev polynomials problem, studied in Appendix B.4. When the operator is nonlinear,  $\mathbf{H}(\mathbf{z})$  from Example 7 does not resemble the full Hessian and we can explicitly use this equation. For this case, extended bounds are also proven in Example 12.

1620 C COMPOSITE OPTIMIZATION PROBLEMS  
16211622 Let us consider a more general formulation of the Composite Optimization Problem (Nesterov, 2018):  
1623

1624 
$$\min_{\mathbf{x} \in Q} \{F(\mathbf{x}) := f(\mathbf{x}) + \psi(\mathbf{x})\}, \quad (25)$$
  
1625

1626 where  $f : Q \rightarrow \mathbb{R}$  is a differentiable function, which can be non-convex, and  $\psi : Q \rightarrow \mathbb{R}$  is a *simple*  
1627 closed convex function with  $Q := \text{dom } \psi$ . This setup covers optimization problems with simple  
1628 constraints, in which case  $\psi$  is  $\{0, +\infty\}$ -indicator of a given closed convex set  $Q \subset \mathbb{R}^n$ .  
16291630 We denote  $F^* := \inf_{\mathbf{x} \in Q} F(\mathbf{x}) > -\infty$  which we assume to be bounded.  
16311632 C.1 COMPOSITE NEWTON STEP WITH HESSIAN APPROXIMATION  
16331634 In case of the presence of the composite component  $\psi$ , we have to modify our method accordingly.  
1635 Now, begin at point  $\mathbf{x} \in Q$  and for a certain vector  $F'(\mathbf{x}) := \nabla f(\mathbf{x}) + \psi'(\mathbf{x})$ , where  $\psi'(\mathbf{x}) \in \partial\psi(\mathbf{x})$ ,  
1636 we compute the next iterate  $\mathbf{x}^+$  as the solution to the following subproblem:  
1637

1638 
$$\mathbf{x}^+ = \arg \min_{\mathbf{y} \in Q} \left\{ \langle \nabla f(\mathbf{x}), \mathbf{y} - \mathbf{x} \rangle + \frac{1}{2} \langle \mathbf{H}(\mathbf{x})(\mathbf{y} - \mathbf{x}), \mathbf{y} - \mathbf{x} \rangle + \frac{\|F'(\mathbf{x})\|_*}{2\gamma} \|\mathbf{y} - \mathbf{x}\|^2 + \psi(\mathbf{y}) \right\}, \quad (26)$$
  
1639

1640 where  $\mathbf{H}(\mathbf{x}) = \mathbf{H}(\mathbf{x})^\top \succeq \mathbf{0}$  is a positive semidefinite approximation of the Hessian of the smooth  
1641 part, and  $\gamma > 0$  is our step-size parameter. Note that the subproblem in (26) is strongly convex, and  
1642 in case  $\psi \equiv 0$  it corresponds to one iteration of Algorithm 1.  
16431644 In general, the solution to (26) satisfies the following optimality condition (Nesterov, 2018):  
1645

1646 
$$\langle F'(\mathbf{x}) + \left( \mathbf{H}(\mathbf{x}) + \frac{\|F'(\mathbf{x})\|_*}{\gamma} \mathbf{B} \right) (\mathbf{x}^+ - \mathbf{x}), \mathbf{x}^+ - \mathbf{x} \rangle + \psi(\mathbf{y}) \geq \psi(\mathbf{x}^+), \quad \forall \mathbf{y} \in Q, \quad (27)$$
  
1647

1648 or, in other words, the vector  
1649

1650 
$$\psi'(\mathbf{x}^+) := -\nabla f(\mathbf{x}) - \mathbf{H}(\mathbf{x})(\mathbf{x}^+ - \mathbf{x}) - \frac{\|F'(\mathbf{x})\|_*}{\gamma} \mathbf{B}(\mathbf{x}^+ - \mathbf{x}) \quad (28)$$
  
1651

1652 belongs to the subdifferential of  $\psi$  at new point:  $\psi'(\mathbf{x}^+) \in \partial\psi(\mathbf{x}^+)$ .  
16531654 Let us derive useful inequalities for one step of the composite method. Note that for any stationary  
1655 point  $\mathbf{x}^*$  to problem (25), setting  $\mathbf{x} := \mathbf{x}^*$  we have  $\mathbf{x}^+ = \mathbf{x}^*$ , as it satisfies the optimality  
1656 condition (27). Therefore, without loss of generality we can always assume that  $\mathbf{x} \neq \mathbf{x}^*$ .  
16571658 **Lemma 2.** Let  $\psi'(\mathbf{x}) \in \partial\psi(\mathbf{x})$  be an arbitrary subgradient and denote  $F'(\mathbf{x}) := \nabla f(\mathbf{x}) +$   
1659  $\psi'(\mathbf{x}) \neq \mathbf{0}$ . Then, for any  $\gamma > 0$ , it holds

1660 
$$\langle F'(\mathbf{x}), \mathbf{x} - \mathbf{x}^+ \rangle > 0, \quad (29)$$
  
1661

1662 
$$\|\mathbf{x}^+ - \mathbf{x}\| \leq \gamma, \quad (30)$$
  
1663

1664 and  
1665

1666 
$$\begin{aligned} \|\mathbf{x}^+ - \mathbf{x}\|_x^2 &:= \langle \nabla^2 f(\mathbf{x})(\mathbf{x}^+ - \mathbf{x}), \mathbf{x}^+ - \mathbf{x} \rangle \leq \langle F'(\mathbf{x}), \mathbf{x} - \mathbf{x}^+ \rangle \\ &+ \|\mathbf{x}^+ - \mathbf{x}\| \cdot \left( \|\nabla^2 f(\mathbf{x}) - \mathbf{H}(\mathbf{x})\|_* (\mathbf{x}^+ - \mathbf{x}) - \frac{\|F'(\mathbf{x})\|_* \|\mathbf{x}^+ - \mathbf{x}\|}{\gamma} \right). \end{aligned} \quad (31)$$
  
1667

1668 *Proof.* Indeed, multiplying (28) by  $\mathbf{x}^+ - \mathbf{x}$  and using convexity of  $\psi$ , we have  
1669

1670 
$$\begin{aligned} \langle \mathbf{H}(\mathbf{x})(\mathbf{x}^+ - \mathbf{x}), \mathbf{x}^+ - \mathbf{x} \rangle + \frac{\|F'(\mathbf{x})\|_*}{\gamma} \|\mathbf{x}^+ - \mathbf{x}\|^2 &= \langle \nabla f(\mathbf{x}) + \psi'(\mathbf{x}^+), \mathbf{x} - \mathbf{x}^+ \rangle \\ &\leq \langle F'(\mathbf{x}), \mathbf{x} - \mathbf{x}^+ \rangle. \end{aligned}$$
  
1671

1672 Therefore, taking into account that  $\mathbf{H}(\mathbf{x}) \succeq \mathbf{0}$ , we conclude that  
1673

1674 
$$0 < \frac{\|F'(\mathbf{x})\|_*}{\gamma} \|\mathbf{x}^+ - \mathbf{x}\|^2 \leq \langle F'(\mathbf{x}), \mathbf{x} - \mathbf{x}^+ \rangle,$$
  
1675

which proves (29). Applying Cauchy-Schwartz inequality also gives (30). Now, to establish (31), we notice that

$$\begin{aligned}
 & \langle \nabla^2 f(\mathbf{x})(\mathbf{x}^+ - \mathbf{x}), \mathbf{x}^+ - \mathbf{x} \rangle \\
 &= \langle \mathbf{H}(\mathbf{x})(\mathbf{x}^+ - \mathbf{x}), \mathbf{x}^+ - \mathbf{x} \rangle + \langle (\nabla^2 f(\mathbf{x}) - \mathbf{H}(\mathbf{x}))(\mathbf{x}^+ - \mathbf{x}), \mathbf{x}^+ - \mathbf{x} \rangle \\
 &\leq \langle F'(\mathbf{x}), \mathbf{x} - \mathbf{x}^+ \rangle - \frac{\|F'(\mathbf{x})\|_*}{\gamma} \|\mathbf{x}^+ - \mathbf{x}\|^2 + \|(\nabla^2 f(\mathbf{x}) - \mathbf{H}(\mathbf{x}))(\mathbf{x}^+ - \mathbf{x})\|_* \|\mathbf{x}^+ - \mathbf{x}\|,
 \end{aligned}$$

which completes the proof.  $\square$

We see that according to our definition (26), we ensure that every step remains bounded (30) by our parameter  $\gamma > 0$ . Let us recall our Definition 1 of the Gradient-Normalized Smoothness from the main part, for any  $\mathbf{x} \in Q$  and  $\mathbf{g} \in \mathbb{R}^n$ :

$$\gamma(\mathbf{x}, \mathbf{g}) := \max \{ \gamma \geq 0 : \|\nabla f(\mathbf{x} + \mathbf{h}) - \nabla f(\mathbf{x}) - \mathbf{H}(\mathbf{x})\mathbf{h}\|_* \leq \frac{\|\mathbf{g}\|_* \|\mathbf{h}\|}{\gamma}, \forall \mathbf{h} \in B_\gamma \cap \mathcal{O}_{\mathbf{x}, \mathbf{g}} \},$$

where  $B_\gamma := \{\mathbf{h} : \|\mathbf{h}\| \leq \gamma\}$  is the Euclidean ball, and  $\mathcal{O}_{\mathbf{x}, \mathbf{g}} := \{\|\mathbf{h}\|_\mathbf{x}^2 + \langle \mathbf{g}, \mathbf{h} \rangle \leq 0\}$  is the local region. Note that this definition measures the local level of smoothness for our differentiable part  $f$ , and it does not take into account the composite component  $\psi$ . However, as we will see, in the composite case we change the direction  $\mathbf{g}$  in our algorithm to define the step-size, by taking the *perturbed gradient*:  $\mathbf{g} := \nabla f(\mathbf{x}) + \psi'(\mathbf{x})$ .

First, let us derive simple consequences of the definition of  $\gamma(\mathbf{x}, \mathbf{g})$ .

**Lemma 3.** *Let  $0 < \gamma \leq \gamma(\mathbf{x}, \mathbf{g})$ . Then, for any  $\mathbf{h} \in B_\gamma \cap \mathcal{O}_{\mathbf{x}, \mathbf{g}}$ , it holds*

$$|f(\mathbf{x} + \mathbf{h}) - f(\mathbf{x}) - \langle \nabla f(\mathbf{x}), \mathbf{h} \rangle - \frac{1}{2} \langle \mathbf{H}(\mathbf{x})\mathbf{h}, \mathbf{h} \rangle| \leq \frac{\|\mathbf{g}\|_* \|\mathbf{h}\|^2}{2\gamma}. \quad (32)$$

*Proof.* Indeed, we have

$$\begin{aligned}
 & |f(\mathbf{x} + \mathbf{h}) - f(\mathbf{x}) - \langle \nabla f(\mathbf{x}), \mathbf{h} \rangle - \frac{1}{2} \langle \mathbf{H}(\mathbf{x})\mathbf{h}, \mathbf{h} \rangle| \\
 &= \left| \int_0^1 \langle \nabla f(\mathbf{x} + \tau\mathbf{h}) - \nabla f(\mathbf{x}) - \tau\mathbf{H}(\mathbf{x})\mathbf{h}, \mathbf{h} \rangle d\tau \right| \\
 &\leq \int_0^1 \|\nabla f(\mathbf{x} + \tau\mathbf{h}) - \nabla f(\mathbf{x}) - \tau\mathbf{H}(\mathbf{x})\mathbf{h}\|_* d\tau \cdot \|\mathbf{h}\| \\
 &\leq \frac{\|\mathbf{g}\|_* \|\mathbf{h}\|^2}{2\gamma},
 \end{aligned}$$

where we used the definition of  $\gamma(\mathbf{x}, \mathbf{g})$  in the last inequality.  $\square$

**Lemma 4.** *Let  $0 < \gamma \leq \gamma(\mathbf{x}, \mathbf{g})$ . Then, for any  $\mathbf{s} \in \mathbb{R}^n$  s.t.  $\|\mathbf{s}\| = 1$  and  $\langle \mathbf{g}, \mathbf{s} \rangle < 0$  we have*

$$\|(\nabla^2 f(\mathbf{x}) - \mathbf{H}(\mathbf{x}))\mathbf{s}\|_* \leq \frac{\|\mathbf{g}\|_*}{\gamma}. \quad (33)$$

*Proof.* Let us take  $\mathbf{h} := \tau\mathbf{s}$ , where  $0 < \tau \leq \gamma \leq \gamma(\mathbf{x}, \mathbf{g})$ . Clearly,  $\mathbf{h} \in B_\gamma$ . Moreover,

$$\|\mathbf{h}\|_\mathbf{x}^2 + \langle \mathbf{g}, \mathbf{h} \rangle = \tau \left( \tau \langle \nabla^2 f(\mathbf{x})\mathbf{s}, \mathbf{s} \rangle + \langle \mathbf{g}, \mathbf{s} \rangle \right) \leq 0,$$

for sufficiently small  $\tau > 0$ . Hence, for sufficiently small  $\tau$ , we have:

$$\left\| \frac{1}{\tau} (\nabla f(\mathbf{x} + \tau\mathbf{s}) - \nabla f(\mathbf{x})) - \mathbf{H}(\mathbf{x})\mathbf{s} \right\|_* \leq \frac{\|\mathbf{g}\|_*}{\gamma}.$$

Taking the limit  $\tau \rightarrow +0$  completes the proof.  $\square$

1728 Note that according to Lemma 2, normalized direction of our method,  $s := \frac{\mathbf{x}^+ - \mathbf{x}}{\|\mathbf{x}^+ - \mathbf{x}\|}$  satisfies  
 1729  $\langle g, s \rangle < 0$  for  $g := F'(\mathbf{x})$  (inequality 29). Therefore, we obtain the following direct result.  
 1730

1731 **Corollary 4.** *Let  $0 < \gamma \leq \gamma(\mathbf{x}, F'(\mathbf{x}))$ . Then, one composite step (26) satisfies*

$$1733 \quad \|\mathbf{x}^+ - \mathbf{x}\|_{\mathbf{x}}^2 \leq \langle F'(\mathbf{x}), \mathbf{x} - \mathbf{x}^+ \rangle. \quad (34)$$

1734 *Thus,*

$$1735 \quad \mathbf{x}^+ - \mathbf{x} \in B_{\gamma} \cap \mathcal{O}_{\mathbf{x}, F'(\mathbf{x})}. \quad (35)$$

1737 Due to inclusion (35), we show the following one step progress for our method. Note that Lemma 1  
 1738 is a simple direct consequence of this result, using  $\psi \equiv 0$ .  
 1739

1740 **Lemma 5.** *Let  $0 < \gamma \leq \gamma(\mathbf{x}, F'(\mathbf{x}))$ . Then,*

$$1741 \quad F(\mathbf{x}) - F(\mathbf{x}^+) \geq \frac{\gamma}{8} \frac{\|F'(\mathbf{x}^+)\|_*^2}{\|F'(\mathbf{x})\|_*^2} \quad (36)$$

1744 *Proof.* Substituting the optimality condition (27) into global bound on the function progress (32),  
 1745 we get

$$1746 \quad \begin{aligned} f(\mathbf{x}^+) &\leq f(\mathbf{x}) - \frac{1}{2} \langle \mathbf{H}(\mathbf{x})(\mathbf{x}^+ - \mathbf{x}), \mathbf{x}^+ - \mathbf{x} \rangle - \frac{\|F'(\mathbf{x})\|_* \|\mathbf{x}^+ - \mathbf{x}\|^2}{2\gamma} + \langle \psi'(\mathbf{x}^+), \mathbf{x} - \mathbf{x}^+ \rangle \\ 1747 &\leq F(\mathbf{x}) - \frac{1}{2} \langle \mathbf{H}(\mathbf{x})(\mathbf{x}^+ - \mathbf{x}), \mathbf{x}^+ - \mathbf{x} \rangle - \frac{\|F'(\mathbf{x})\|_* \|\mathbf{x}^+ - \mathbf{x}\|^2}{2\gamma} - \psi(\mathbf{x}^+), \end{aligned}$$

1750 which gives

$$1751 \quad F(\mathbf{x}) - F(\mathbf{x}^+) \geq \frac{\|F'(\mathbf{x})\|_* \|\mathbf{x}^+ - \mathbf{x}\|^2}{2\gamma}. \quad (37)$$

1753 At the same time,

$$1754 \quad \begin{aligned} \|F'(\mathbf{x}^+) + \frac{\|F'(\mathbf{x})\|_*}{\gamma} \mathbf{B}(\mathbf{x}^+ - \mathbf{x})\|_* &= \|\nabla f(\mathbf{x}^+) - \nabla f(\mathbf{x}) - \mathbf{H}(\mathbf{x}^+ - \mathbf{x})\|_* \\ 1755 &\leq \frac{\|F'(\mathbf{x})\|_* \|\mathbf{x}^+ - \mathbf{x}\|}{\gamma}, \end{aligned}$$

1758 where we used the definition of  $\gamma(\mathbf{x}, F'(\mathbf{x})) \geq \gamma$  in the last inequality. Hence, applying triangle  
 1759 inequality, we obtain:

$$1760 \quad \|F'(\mathbf{x}^+)\|_* \leq \frac{2\|F'(\mathbf{x})\|_* \|\mathbf{x}^+ - \mathbf{x}\|}{\gamma}.$$

1762 Combining this inequality with (37) gives the required bound.  $\square$

## 1764 C.2 THE ALGORITHM FOR COMPOSITE OPTIMIZATION

1765 We are ready to formalize our method for the general composite case, as follows.

---

### 1767 **Algorithm 2** Composite Gradient-Regularized Newton with Approximate Hessians

---

1769 **Initialization:**  $\mathbf{x}_0 \in Q$  and  $\psi'(\mathbf{x}_0) \in \partial\psi(\mathbf{x}_0)$ . Set  $F'(\mathbf{x}_0) \leftarrow \nabla f(\mathbf{x}_0) + \psi'(\mathbf{x}_0)$ .

1770 1: **for**  $k \geq 0$  **do**

1771 2: Choose  $\mathbf{H}(\mathbf{x}_k) \succeq \mathbf{0}$  and  $\gamma_k > 0$ .

1772 3: Compute

$$1773 \quad \mathbf{x}_{k+1} \leftarrow \arg \min_{\mathbf{y} \in Q} \left\{ \langle \nabla f(\mathbf{x}_k), \mathbf{y} - \mathbf{x}_k \rangle + \frac{1}{2} \langle \mathbf{H}(\mathbf{x}_k)(\mathbf{y} - \mathbf{x}_k), \mathbf{y} - \mathbf{x}_k \rangle \right. \\ 1774 \quad \left. + \frac{\|F'(\mathbf{x}_k)\|_*}{2\gamma_k} \|\mathbf{y} - \mathbf{x}_k\|^2 + \psi(\mathbf{y}) \right\}.$$

1777 4: Set  $\psi'(\mathbf{x}_{k+1}) \leftarrow -\nabla f(\mathbf{x}_k) - \mathbf{H}(\mathbf{x}_k)(\mathbf{x}_{k+1} - \mathbf{x}_k) - \frac{\|F'(\mathbf{x}_k)\|_*}{\gamma_k} \mathbf{B}(\mathbf{x}_{k+1} - \mathbf{x}_k)$ .

1779 5: Set  $F'(\mathbf{x}_{k+1}) \leftarrow \nabla f(\mathbf{x}_{k+1}) + \psi'(\mathbf{x}_{k+1})$ .

1780 6: **end for**

---

1781 In the case  $\psi \equiv 0$ , this method is the same as Algorithm 1.

1782 **D THE CHOICE OF THE REGULARIZATION PARAMETER**

1783  
1784 Note that the only parameter of Algorithm 2 is a (second-order) step-size  $\gamma_k > 0$  that describes  
1785 the radius of the ball where the iteration belongs to:  $\|\mathbf{x}_{k+1} - \mathbf{x}_k\| \leq \gamma_k$ , similarly to trust-region  
1786 approach (Conn et al., 2000).

1787 Our theory suggests that the right choice of this parameter is provided by the Gradient-Normalized  
1788 Smoothness (Definition 1), that is, in the general composite case:

1790  
1791 
$$\gamma_k := \gamma(\mathbf{x}_k, F'(\mathbf{x}_k)).$$

1792  
1793 Then, according to Lemma 5, we ensure the following progress of each step:

1794  
1795 
$$F(\mathbf{x}_k) - F(\mathbf{x}_{k+1}) \geq \frac{\gamma_k}{8} \frac{\|F'(\mathbf{x}_{k+1})\|_*^2}{\|F'(\mathbf{x}_k)\|_*}.$$

1796  
1797 Therefore,  $\gamma_k \approx \gamma(\mathbf{x}_k)$  is *the best value* of a step-size that we can use. However, in practice, it can  
1798 be difficult to compute the exact value of the Gradient-Normalized Smoothness. In this section, we  
1799 show two different strategies that can work for a practical implementation of our method.

1800  
1801 The first choice (Section D.1) is the **constant rule** for selecting  $\gamma_k$ :

1802  
1803 
$$\gamma_k \equiv \gamma_*, \quad \forall k \geq 0,$$

1804  
1805 where  $\gamma_* > 0$  is a certain value, fixed once for *all iterations* of the method. Hence, since this is  
1806 just one hyperparameter, one can perform a simple grid search for choosing  $\gamma_*$ , in a similar spirit to  
1807 step-size tuning for the stochastic gradient descent (SGD). However, we noticed in our experiments,  
1808 that the value  $\gamma_* \approx 1$  is always a good guess for second-order methods, which also ensures local  
1809 quadratic convergence of the method with exact Hessian, as for the classical Newton's method.

1810  
1811 The second choice (Section D.2) that we will present is the use of **adaptive search** to estimate  $\gamma_k$   
1812 at each iteration, which is a standard and cheap procedure, which also equips the method with fast  
1813 global rates, without the need to know the exact value of  $\gamma(\mathbf{x})$  or  $\gamma_*$ .

1814  
1815 In this section, for simplicity we focus on convex optimization problems, while our results can be  
1816 generalized to other classes of problems. We consider non-convex optimization in Section E and the  
1817 gradient-dominated objectives in Section F.

1818 **D.1 THE CONSTANT RULE**

1819  
1820 Let us assume that the desired accuracy  $\varepsilon > 0$  is fixed. This assumption is not very restrictive.  
1821 Additionally, it allows to have a *stopping condition* for the method. Then, we denote the following  
1822 set of function suboptimality:

1823  
1824 
$$\mathfrak{F}_\varepsilon := \left\{ \mathbf{x} \in Q : F(\mathbf{x}) - F^* \geq \varepsilon \right\},$$

1825  
1826 and, for a fixed initialization  $\mathbf{x}_0 \in \mathfrak{F}_\varepsilon$ , we denote the sublevel set by

1827  
1828 
$$\mathcal{F}_0 := \left\{ \mathbf{x} \in Q : F(\mathbf{x}) \leq F(\mathbf{x}_0) \right\},$$

1829  
1830 which we assume to be bounded, i.e.,  $D := \text{diam}(\mathcal{F}_0) < +\infty$ . Note that by convexity, we obtain, for  
1831 any subgradient  $F'(\mathbf{x}) \in \partial F(\mathbf{x})$ , with  $\mathbf{x} \in \mathfrak{F}_\varepsilon \cap \mathcal{F}_0$ :

1832  
1833 
$$\|F'(\mathbf{x})\|_* \geq \frac{F(\mathbf{x}) - F^*}{D} \geq \delta := \frac{\varepsilon}{D}.$$

1834  
1835 We are ready to formulate our main result, for the constant selection of  $\gamma_k$  in our algorithm.

1836

**Theorem 3.** Let  $\varepsilon > 0$  be fixed, and assume that there exists  $\gamma_* > 0$  satisfying

1837

$$\gamma_* \leq \inf \left\{ \gamma(\mathbf{x}, F'(\mathbf{x})) : \mathbf{x} \in \mathfrak{F}_\varepsilon \cap \mathcal{F}_0, F'(\mathbf{x}) \in \partial F(\mathbf{x}) \right\}. \quad (40)$$

1838

Consider  $K \geq 1$  iterations of Algorithm 2 with

1839

$$\gamma_k \equiv \gamma_*, \quad (41)$$

1840

and assume that  $\mathbf{x}_k \in \mathfrak{F}_\varepsilon$ , for all  $0 \leq k \leq K$ . Then,

1841

$$K \leq \frac{8D}{\gamma_*} \ln \frac{F(\mathbf{x}_0) - F^*}{\varepsilon} + 2 \ln \frac{\|F'(\mathbf{x}_0)\|_* D}{\varepsilon} \quad (42)$$

1842

1843

*Proof.* Indeed, by Lemma 5, our constant choice of  $\gamma_k$  ensure the following progress of every iteration, denoting  $F_k := F(\mathbf{x}_k) - F^*$  and  $g_k := \|F'(\mathbf{x}_k)\|_*$ :

1844

$$F_k - F_{k+1} \geq \frac{\gamma_*}{8} \frac{g_{k+1}^2}{g_k} = \frac{\gamma_*}{8} \left( \frac{g_{k+1}}{g_k} \right)^2 g_k \stackrel{(39)}{\geq} \frac{\gamma_*}{8D} \left( \frac{g_{k+1}}{g_k} \right)^2 F_k. \quad (43)$$

1845

Then, using concavity of the logarithm, we have

1846

$$\ln \frac{F_k}{F_{k+1}} \geq \frac{F_k - F_{k+1}}{F_k} \stackrel{(43)}{\geq} \frac{\gamma_*}{8D} \left( \frac{g_{k+1}}{g_k} \right)^2. \quad (44)$$

1847

Telescoping this bound for the first  $K$  iterations of the method, and using the inequality between arithmetic and geometric means, we obtain

1848

$$\begin{aligned} \ln \frac{F_0}{\varepsilon} &\geq \ln \frac{F_0}{F_K} \stackrel{(43)}{\geq} \frac{\gamma_* K}{8D} \cdot \frac{1}{K} \sum_{k=0}^{K-1} \left( \frac{g_{k+1}}{g_k} \right)^2 \geq \frac{\gamma_* K}{8D} \cdot \left( \frac{g_K}{g_0} \right)^{\frac{2}{K}} \\ &\stackrel{(39)}{\geq} \frac{\gamma_* K}{8D} \cdot \left( \frac{\varepsilon}{g_0 D} \right)^{\frac{2}{K}} = \frac{\gamma_* K}{8D} \cdot \exp \left[ \frac{2}{K} \ln \frac{\varepsilon}{g_0 D} \right] \geq \frac{\gamma_* K}{8D} \cdot \left[ 1 + \frac{2}{K} \ln \frac{\varepsilon}{g_0 D} \right]. \end{aligned}$$

1849

Rearranging the terms proves the required bound.  $\square$

1850

Note that the result of Theorem 3 is very general, as it does not assume any particular smoothness conditions, except separation from zero of the Gradient-Normalized Smoothness  $\gamma(\cdot)$  on the bounded set  $\mathfrak{F}_\varepsilon \cap \mathcal{F}_0$ :  $\gamma_* > 0$ . Under this condition, we show that our method with a constant rule  $\gamma_k \equiv \gamma_*$  needs

1851

$$K = \tilde{\mathcal{O}}(\gamma_*^{-1} D) \quad (45)$$

1852

iterations to solve the problem, up to logarithmic terms.

1853

Despite the constant rule (41) seems too conservative, it appears that it recovers the correct rates in all particular cases. For example, for the functions with  $L_2$ -Lipschitz Hessian, we have

1854

$$\gamma(\mathbf{x}, F'(\mathbf{x})) \geq \sqrt{\frac{2}{L_2} \|F'(\mathbf{x})\|_*} \stackrel{(39)}{\geq} \sqrt{\frac{2\varepsilon}{L_2 D}} \equiv \gamma_*.$$

1855

Substituting this value of  $\gamma_*$  into (45) gives the complexity of  $\tilde{\mathcal{O}}\left(\sqrt{\frac{L_2 D^3}{\varepsilon}}\right)$ , which matches the complexity of the Cubic Newton Nesterov & Polyak (2006) on convex functions, up to a logarithmic factor.

1856

In Section F, we develop a more refined analysis that covers convex functions as a particular case, and allows us to avoid a logarithmic factor in some particular cases.

1857

## D.2 THE METHOD WITH ADAPTIVE SEARCH

1858

In this section, we provide another practical choice for  $\gamma_k$ , which is to adaptively ensure inequality (38). We present this strategy in the following algorithmic form. This method needs a parameter  $\delta > 0$ , which is a desired accuracy in terms of the gradient norm. It is used for the stopping condition.

1859

This is the same method as Algorithm 2, but with a specific adaptive procedure to choose parameter  $\gamma_k > 0$ . It is clear that the method is well defined, as for a sufficiently large  $t_k \geq 0$  we can ensure

---

**Algorithm 3** Adaptive Method with Approximate Hessians

---

1890   **Initialization:**  $\mathbf{x}_0 \in Q$ ,  $\psi'(\mathbf{x}_0) \in \partial\psi(\mathbf{x}_0)$ ,  $\gamma_0 > 0$ , and  $\delta > 0$ . Set  $F'(\mathbf{x}_0) \leftarrow \nabla f(\mathbf{x}_0) + \psi'(\mathbf{x}_0)$ .

1891   1: **for**  $k \geq 0$  **do**

1892   2:    **If**  $\|F'(\mathbf{x}_k)\|_* \leq \delta$  **then stop and return**  $\mathbf{x}_k$ .

1893   3:    Choose  $\mathbf{H}(\mathbf{x}_k) \succeq 0$ .

1894   4:    Find the smallest integer  $t_k \geq 0$  such that for  $\gamma := 2^{-t_k} \cdot \gamma_k$  and  $\mathbf{T}(\gamma), \mathbf{g}(\gamma)$  computed as

1895    
$$\mathbf{T}(\gamma) \leftarrow \arg \min_{\mathbf{y} \in Q} \left\{ \langle \nabla f(\mathbf{x}_k), \mathbf{y} - \mathbf{x}_k \rangle + \frac{1}{2} \langle \mathbf{H}(\mathbf{x}_k)(\mathbf{y} - \mathbf{x}_k), \mathbf{y} - \mathbf{x}_k \rangle \right.$$

1896    
$$\left. + \frac{\|F'(\mathbf{x}_k)\|_*}{2\gamma} \|\mathbf{y} - \mathbf{x}_k\|^2 + \psi(\mathbf{y}) \right\},$$

1897    and

1898    
$$\mathbf{g}(\gamma) \leftarrow \nabla f(\mathbf{T}(\gamma)) - \nabla f(\mathbf{x}_k) - \mathbf{H}(\mathbf{x}_k)(\mathbf{T}(\gamma) - \mathbf{x}_k) - \frac{\|F'(\mathbf{x}_k)\|_*}{\gamma} \mathbf{B}(\mathbf{T}(\gamma) - \mathbf{x}_k)$$

1899    it holds

1900    
$$F(\mathbf{x}_k) - F(\mathbf{T}(\gamma)) \geq \frac{\gamma}{8} \frac{\|\mathbf{g}(\gamma)\|_*^2}{\|F'(\mathbf{x}_k)\|_*^2} \quad \text{or} \quad \|\mathbf{g}(\gamma)\|_* \leq \delta.$$

1901   5:    Set  $\mathbf{x}_{k+1} \leftarrow \mathbf{T}(2^{-t_k} \cdot \gamma_k)$  and  $F'(\mathbf{x}_{k+1}) \leftarrow \mathbf{g}(2^{-t_k} \cdot \gamma_k)$ .

1902   6:    Set  $\gamma_{k+1} \leftarrow 2^{-t_k+1} \cdot \gamma_k$ .

1903   7: **end for**

---

1910  
1911   that  $2^{-t_k} \cdot \gamma_k \leq \gamma(\mathbf{x}_k, F'(\mathbf{x}_k))$  and therefore the condition of the adaptive search will be satisfied.  
1912   At the same time, the total number  $N_K$  of oracle calls during  $K \geq 0$  iterations is bounded as

1913   
$$N_K := \sum_{k=0}^{K-1} (1 + t_k) = 2K + \sum_{k=0}^{K-1} \log_2 \frac{\gamma_k}{\gamma_{k+1}} = 2K + \log_2 \frac{\gamma_0}{\gamma_{K-1}} \leq 2K + \log_2 \frac{\gamma_0}{\bar{\gamma}_K}, \quad (46)$$

1916   where  $\bar{\gamma}_K := \min_{0 \leq k \leq K-1} \gamma_k$ .

1917   Note also that Algorithm 3 with  $\mathbf{H}(\mathbf{x}_k) \equiv \nabla^2 f(\mathbf{x}_k)$  (exact Hessian) is equivalent to the Super-  
1918   Universal Newton Method from (Doikov et al., 2024a), using a different stopping condition in the  
1919   adaptive search. Even in the exact case, our theory enhances the complexity results from (Doikov  
1920   et al., 2024a) to the broader classes of generalized Self-Concordant functions (Sun & Tran-Dinh,  
1921   2018) and beyond, including problems with  $(L_0, L_1)$ -functions (Zhang et al., 2019).

1922   Moreover, our results allow us to use an arbitrary positive semidefinite approximation  $\mathbf{H}(\mathbf{x}_k) \approx$   
1923    $\nabla^2 f(\mathbf{x}_k)$  of the Hessian in our methods, and all our algorithms are applicable to possibly non-convex  
1924   problems as well, while the method in (Doikov et al., 2024a) works primarily for convex optimization,  
1925   using the exact Hessian.

1926   We establish the following result about this algorithm.

1928   **Theorem 4.** *Let  $\varepsilon > 0$  be fixed, and assume that there exists  $\gamma_* > 0$  satisfying*

1930   
$$\gamma_* \leq \inf \left\{ \gamma(\mathbf{x}, F'(\mathbf{x})) : \mathbf{x} \in \mathfrak{F}_\varepsilon \cap \mathcal{F}_0, F'(\mathbf{x}) \in \partial F(\mathbf{x}) \right\}.$$

1932   *Let  $\delta := \frac{\varepsilon}{D}$ . Assume that Algorithm 3 does not stop for the first  $K \geq 1$  iterations, and that*  
1933    *$\mathbf{x}_k \in \mathfrak{F}_\varepsilon$  for all  $0 \leq k \leq K$ . Then,*

1934   
$$K \leq \frac{16D}{\min\{\gamma_0, \gamma_*\}} \ln \frac{F(\mathbf{x}_0) - F^*}{\varepsilon} + 2 \ln \frac{\|F'(\mathbf{x}_0)\|_* D}{\varepsilon} \quad (47)$$

1936   *and the total number of oracle calls during these iterations is bounded as*

1938   
$$N_K \leq 2K + \log_2 \frac{\gamma_0}{\gamma_*}.$$

1940  
1941   *Proof.* First, we note that the method is well-defined. Indeed, by our assumption, there exists a global  
1942   value of  $\gamma_*$  such that the first stopping condition of the adaptive search will be satisfied at least for  
1943    $t_k \geq 0$  such that  $2^{-t_k} \cdot \gamma_k \leq \gamma_*$ , unless  $\|F'(\mathbf{x}_k)\|_* \leq \delta$ . The last inequality implies that we solved  
the problem with the desired accuracy and we stop the algorithm.

1944

Therefore, by induction we have the following lower bound on values of our step-sizes:

1945

$$\gamma_k \geq \min\{\gamma_0, \gamma_*\}, \quad 0 \leq k \leq K. \quad (48)$$

1946

Hence, for every iteration  $k \geq 0$  of the method, we ensure

1948

1949

$$F(\mathbf{x}_k) - F(\mathbf{x}_{k+1}) \geq \frac{\gamma_{k+1}}{16} \frac{\|F'(\mathbf{x}_{k+1})\|_*^2}{\|F'(\mathbf{x}_k)\|_*} \stackrel{(48)}{\geq} \frac{\min\{\gamma_*, \gamma_0\}}{16} \frac{\|F'(\mathbf{x}_{k+1})\|_*^2}{\|F'(\mathbf{x}_k)\|_*}.$$

1950

1951

Now, repeating the reasoning from the proof of Theorem 3 we establish (47), and using (46) we immediately obtain the bound on the total number of oracle calls,  $\square$

1952

1953

## E CONVERGENCE FOR NON-CONVEX FUNCTIONS

1954

1955

First, let us formulate Theorem 1 for more general composite optimization problems (25). Then, Theorem 1 is a direct consequence of this result for  $\psi \equiv 0$ .

1956

1957

**Theorem 5.** *Let  $K \geq 1$  be a fixed number of iterations of Algorithm 2 and let (5) hold for every step. Assume that  $\min_{1 \leq i \leq K} \|F'(\mathbf{x}_i)\|_* \geq \varepsilon$  and let  $\gamma_* = \min_{1 \leq i \leq K} \gamma_i > 0$ . Then,*

1961

1962

$$K \leq \frac{8F_0}{\gamma_* \varepsilon} + \log \frac{\|F'(\mathbf{x}_0)\|_*}{\varepsilon}, \quad \text{where } F_0 := F(\mathbf{x}_0) - F^*. \quad (49)$$

1963

*Proof.* According to (5), we have for every iteration of the method,

1964

1965

$$F(\mathbf{x}_k) - F(\mathbf{x}_{k+1}) \geq \frac{\gamma_k}{8} \frac{\|F'(\mathbf{x}_{k+1})\|_*^2}{\|F'(\mathbf{x}_k)\|_*} \geq \frac{\gamma_* \varepsilon}{8} \frac{\|F'(\mathbf{x}_{k+1})\|_*}{\|F'(\mathbf{x}_k)\|_*}.$$

1966

Telescoping this bound and using the inequality between arithmetic and geometric means, we get

1967

1968

$$\begin{aligned} F(\mathbf{x}_0) - F^* &\geq F(\mathbf{x}_0) - F(\mathbf{x}_k) \geq \frac{k\gamma_* \varepsilon}{8} \frac{1}{k} \sum_{i=1}^k \frac{\|F'(\mathbf{x}_i)\|_*}{\|F'(\mathbf{x}_{i-1})\|_*} \geq \frac{k\gamma_* \varepsilon}{8} \left[ \frac{\|F'(\mathbf{x}_k)\|_*}{\|F'(\mathbf{x}_0)\|_*} \right]^{1/k} \\ &\geq \frac{k\gamma_* \varepsilon}{8} \left[ \frac{\varepsilon}{\|F'(\mathbf{x}_0)\|_*} \right]^{1/k} = \frac{k\gamma_* \varepsilon}{8} \exp \left[ \frac{1}{k} \log \frac{\varepsilon}{\|F'(\mathbf{x}_0)\|_*} \right] \\ &\geq \frac{k\gamma_* \varepsilon}{8} \left[ 1 + \frac{1}{k} \log \frac{\varepsilon}{\|F'(\mathbf{x}_0)\|_*} \right]. \end{aligned}$$

1975

Rearranging the terms proves the required complexity bound.  $\square$

1976

We see that this result is very general: we did not specify anything about the problem class our function belongs to. Theorem 5 shows that for general composite objectives, with possibly non-convex smooth part, our method will have a global convergence to a stationary point. To quantify the convergence rate further, we need to impose some structural assumption on the Gradient-Normalized Smoothness  $\gamma(\cdot)$  of the function. Following our assumption 10 from the main part, let us assume that  $\gamma(\cdot)$  is lower bounded by the harmonic mean of monomials of (sub)gradient norms:

1977

1978

1979

1980

1981

1982

1983

1984

1985

1986

$$\gamma(\mathbf{x}, F'(\mathbf{x})) \geq \pi(\|F'(\mathbf{x})\|_*) := \left( \sum_{i=1}^d \frac{M_{1-\alpha_i}}{\|F'(\mathbf{x})\|_*^{\alpha_i}} \right)^{-1} \geq \frac{1}{d} \min_{1 \leq i \leq d} \frac{\|F'(\mathbf{x})\|_*^{\alpha_i}}{M_{1-\alpha_i}}, \quad (50)$$

1987

1988

1989

1990

1991

where for all  $i$ ,  $0 \leq \alpha_i \leq 1$  are fixed degrees and  $\{M_{1-\alpha}\}_{0 \leq \alpha \leq 1}$  are non-negative coefficients describing the complexity of the problem. Note that this assumption holds for all particular examples of problem classes that we consider (see Section 2). Substituting this bound into Theorem 5, we immediately obtain the following corollary.

1992

1993

1994

1995

1996

1997

**Corollary 5.** *Let us choose  $\gamma_k = \gamma(\mathbf{x}_k)$  in Algorithm 2, or by performing an adaptive search. Under assumptions of Theorem 5, we can bound  $\gamma_* \geq \pi(\varepsilon)$ . Therefore, to ensure  $\min_{1 \leq i \leq K} \|F'(\mathbf{x}_i)\|_* \leq \varepsilon$  it is enough to perform a number of iterations of*

$$K = \left[ 8dF_0 \cdot \max_{1 \leq i \leq d} \frac{M_{1-\alpha_i}}{\varepsilon^{1+\alpha_i}} + \log \frac{\|F'(\mathbf{x}_0)\|_*}{\varepsilon} \right].$$

1998  
1999

## E.1 CONVERGENCE FOR INEXACT HÖLDER HESSIAN

2000  
2001  
2002  
2003

Let us consider a particular important consequence of our result. For simplicity, we set  $\psi \equiv 0$  (unconstrained minimization). We assume that the Hessian of  $f$  is Hölder continuous of a certain degree  $0 \leq \nu \leq 1$  (Example 1). Then, according to 7, the Gradient-Normalized Smoothness  $\gamma_{\text{NEWTON}}(\cdot)$  using the *exact Hessian*, is bounded by

2004  
2005  
2006

$$\gamma_{\text{NEWTON}}(\mathbf{x}) \geq \left( \frac{1+\nu}{L_{2,\nu}} \|\nabla f(\mathbf{x})\|_* \right)^{\frac{1}{1+\nu}}. \quad (51)$$

2007  
2008

At the same time, in our method we use *inexact Hessian matrix*, with the following general guarantee (see Section 5):

2009  
2010  
2011  
2012

$$\|\nabla^2 f(\mathbf{x}) - \mathbf{H}(\mathbf{x})\|_* \leq \mathbf{C}_1 + \mathbf{C}_2 \|\nabla f(\mathbf{x})\|_*^{1-\beta}, \quad (52)$$

for a certain  $0 \leq \beta \leq 1$ . Then, according to the basic properties, we can lower bound the Gradient-Normalized Smoothness  $\gamma(\cdot)$  for our problem and with inexact Hessian, as follows:

2013  
2014

$$\gamma(\mathbf{x}) \geq \left[ \gamma_{\text{NEWTON}}(\mathbf{x})^{-1} + \frac{\mathbf{C}_1}{\|\nabla f(\mathbf{x})\|_*} + \frac{\mathbf{C}_2}{\|\nabla f(\mathbf{x})\|_*^\beta} \right]^{-1}. \quad (53)$$

2015  
2016

Therefore, substituting our condition 51, we obtain the following lower bound for the Gradient-Normalized Smoothness, that matches the structure of (50):

2017  
2018  
2019

$$\gamma(\mathbf{x}) \geq \left[ \left( \frac{L_{2,\nu}}{(1+\nu)\|\nabla f(\mathbf{x})\|_*} \right)^{\frac{1}{1+\nu}} + \frac{\mathbf{C}_1}{\|\nabla f(\mathbf{x})\|_*} + \frac{\mathbf{C}_2}{\|\nabla f(\mathbf{x})\|_*^\beta} \right]^{-1}.$$

2020  
2021  
2022  
2023  
2024

Therefore, our theory immediately provides us with the following complexity result.

**Corollary 6.** *Let us choose  $\gamma_k = \gamma(\mathbf{x}_k)$  in Algorithm 2, or by performing an adaptive search, using an inexact Hessian that satisfies (52). Then, to ensure  $\min_{1 \leq i \leq K} \|\nabla f(\mathbf{x}_i)\|_* \leq \varepsilon$  it is enough to perform a number of iterations of*

$$K = O \left( F_0 \cdot \left[ \left( \frac{L_{2,\nu}}{\varepsilon^{2+\nu}} \right)^{\frac{1}{1+\nu}} + \frac{\mathbf{C}_1}{\varepsilon^2} + \frac{\mathbf{C}_2}{\varepsilon^{1+\beta}} \right] + \log \frac{\|\nabla f(\mathbf{x}_0)\|_*}{\varepsilon} \right).$$

2025  
2026  
2027  
2028

For example, for  $\nu = 1$  (Lipschitz continuous Hessian), we obtain the complexity of

2029  
2030

$$F_0 \cdot O \left( \frac{\sqrt{L_{2,1}}}{\varepsilon^{3/2}} + \frac{\mathbf{C}_1}{\varepsilon^2} + \frac{\mathbf{C}_2}{\varepsilon^{1+\beta}} \right),$$

2031  
2032  
2033  
2034  
2035  
2036  
2037

up to an additive logarithmic term. Note that the first term corresponds to the state-of-the-art rate of the Cubically regularized Newton method (Nesterov & Polyak, 2006; Cartis et al., 2011a). We see that when  $\mathbf{C}_1 \approx 0$  and  $\beta \leq 1/2$ , which corresponds to our examples, Algorithm 1 with inexact Hessian has the same complexity as the exact Newton method. In the following section, we show how to improve these complexity bounds further, under additional assumptions on our objective, such as convexity.

2038  
2039

## F IMPROVED RATES FOR GRADIENT-DOMINATED FUNCTIONS

2040  
2041  
2042  
2043

In this section, let us assume additionally that the objective function  $F$  satisfies the following inequality, for a certain  $0 \leq c \leq 1$  and constant  $D_c > 0$  (see (Nesterov & Polyak, 2006; Fatkhullin et al., 2022; Doikov et al., 2024a)):

2044  
2045

$$\|F'(\mathbf{x}_k)\|_*^{1+c} D_c \geq F_k := F(\mathbf{x}_k) - F^*, \quad k \geq 0. \quad (54)$$

2046  
2047  
2048

Let us denote by  $\mathcal{F}_0$  the initial level set of the function

$$\mathcal{F}_0 := \left\{ \mathbf{x} \in Q : F(\mathbf{x}) \leq F(\mathbf{x}_0) \right\}.$$

2049  
2050

Note that due to Lemma 5, all iterations of our method belong to this set:  $\{\mathbf{x}_k\}_{k \geq 0} \subset \mathcal{F}_0$ . Then, we denote by  $D_0$  the diameter of this set, which we assume to be bounded:

2051

$$D_0 := \sup_{\mathbf{x}, \mathbf{y} \in \mathcal{F}_0} \|\mathbf{x} - \mathbf{y}\| < +\infty.$$

2052 • **Convex Functions.** Assume that  $F$  is convex. Then,

$$2054 F(\mathbf{x}_k) - F^* \leq \langle F'(\mathbf{x}_k), \mathbf{x}_k - \mathbf{x}^* \rangle \leq \|F'(\mathbf{x}_k)\|_* \|\mathbf{x}_k - \mathbf{x}^*\| \leq \|F'(\mathbf{x}_k)\|_* D_0. \\ 2055$$

2056 Therefore, inequality (54) is satisfied with  $c := 0$ .

2057 • **Uniformly Convex Functions.** Assume that  $F$  satisfies the following inequality, for a  
2058 certain  $p \geq 2$  and  $\sigma_p > 0$  (see (Nesterov, 2018)):

$$2060 F(\mathbf{y}) \geq F(\mathbf{x}) + \langle F'(\mathbf{x}), \mathbf{y} - \mathbf{x} \rangle + \frac{\sigma_p}{p} \|\mathbf{y} - \mathbf{x}\|^p. \quad (55) \\ 2061$$

2062 Then (54) is satisfied with

$$2064 c := \frac{1}{p-1} \quad \text{and} \quad D_c := \frac{p-1}{p} \left( \frac{1}{\sigma_p} \right)^{\frac{1}{p-1}}. \\ 2065$$

2066 • **Strongly Convex Functions** correspond to the previous case, when  $p = 2$ .

2068 We are ready to establish improved global convergence rates for our method under condition (54) of  
2069 gradient-dominance. Then, Theorem 2 from the main part is a direct consequence of this result for  
2070  $\psi \equiv 0$  and  $c = 0$  (Convex Unconstrained Minimization).

2071 **Theorem 6.** *Let us choose  $\gamma_k = \gamma(\mathbf{x}_k)$  in Algorithm 2 or by performing an adaptive search. Let  
2072 the Gradient-Normalized Smoothness  $\gamma(\cdot)$  satisfies our structural assumption (50), and denote  
2073  $\alpha := \min_{1 \leq i \leq d} \alpha_i$ . Assume that  $F$  is gradient-dominated (54) of degree*

$$2074 c \leq \alpha. \quad (56) \\ 2075$$

2076 Then, for  $\varepsilon > 0$ , to ensure  $F(\mathbf{x}_K) - F^* \leq \varepsilon$ , it is enough to perform a number of iterations of

$$2078 K = \left\lceil \mathcal{C}(\varepsilon) + 2 \log \frac{\|F'(\mathbf{x}_0)\|_* D_0}{\varepsilon} \right\rceil, \\ 2079$$

2080 where

$$2081 \mathcal{C}(\varepsilon) := \frac{8d}{\eta} \max_{1 \leq i \leq d} \left( M_{1-\alpha_i} \left[ \frac{D_c^{1+\alpha_i}}{\varepsilon^{\alpha_i-\alpha}} \right]^{\frac{1}{1+c}} \right) \left( \frac{1}{\varepsilon^\eta} - \frac{1}{F_0^\eta} \right), \quad \text{for } \eta := \frac{\alpha-c}{1+c} > 0, \\ 2083$$

2084 and, for  $\eta = 0$ , we have the limit:

$$2085 \mathcal{C}(\varepsilon) := 8d \max_{1 \leq i \leq d} \left( M_{1-\alpha_i} \left[ \frac{D_c^{1+\alpha_i}}{\varepsilon^{\alpha_i-\alpha}} \right]^{\frac{1}{1+c}} \right) \log \frac{F_0}{\varepsilon}. \quad (57) \\ 2087$$

2088  
2089 *Proof.* Let us fix some  $k \geq 0$  and assume that  $F_k := F(\mathbf{x}_k) - F^* \geq \varepsilon$ . Let  $g_k := \|F'(\mathbf{x}_k)\|_*$ . By  
2090 assumption (50), we have

$$2092 g_k \geq \left( \frac{F_k}{D_c} \right)^{\frac{1}{1+c}}. \quad (58) \\ 2093$$

2094 Then, from Lemma 5, we obtain

$$2096 F_k - F_{k+1} \geq \frac{\gamma_k}{8} \left( \frac{g_{k+1}}{g_k} \right)^2 \cdot g_k \stackrel{(50)}{\geq} \frac{1}{8d} \left( \frac{g_{k+1}}{g_k} \right)^2 \cdot \min_{1 \leq i \leq d} \left( \frac{g_k^{1+\alpha_i}}{M_{1-\alpha_i}} \right) \\ 2097 \stackrel{(54)}{\geq} \frac{1}{8d} \left( \frac{g_{k+1}}{g_k} \right)^2 \cdot \min_{1 \leq i \leq d} \left( \frac{1}{M_{1-\alpha_i}} \left[ \frac{F_k}{D_c} \right]^{\frac{1+\alpha_i}{1+c}} \right). \quad (59) \\ 2098$$

2099 Recall that  $\alpha := \min_{1 \leq i \leq d} \alpha_i$ . Denote  $\eta := \frac{\alpha-c}{1+c} \stackrel{(56)}{\geq} 0$ . Applying the Mean Value Theorem for  
2100  $y(x) = x^\eta$  we get

$$2101 b^\eta - a^\eta \geq \frac{\eta}{b^{1-\eta}} (b - a), \quad b \geq a \geq 0. \quad (60) \\ 2102$$

2106 Thus, we have, assuming that  $\eta > 0$ :  
2107

$$\begin{aligned} 2108 \quad \frac{1}{\eta} \left( \frac{1}{F_{k+1}^\eta} - \frac{1}{F_k^\eta} \right) &= \frac{F_k^\eta - F_{k+1}^\eta}{\eta \cdot F_k^\eta F_{k+1}^\eta} \stackrel{(60)}{\geq} \frac{F_k - F_{k+1}}{F_k F_{k+1}^\eta} \\ 2110 &\stackrel{(59)}{\geq} \frac{1}{8d} \left( \frac{g_{k+1}}{g_k} \right)^2 \left( \frac{F_k}{F_{k+1}} \right)^\eta \min_{1 \leq i \leq d} \left( \frac{1}{M_{1-\alpha_i}} \left[ \frac{F_k^{\alpha_i} - \alpha}{D_c^{1+\alpha_i}} \right]^{\frac{1}{1+c}} \right) \\ 2112 &\geq A(\varepsilon) \cdot \left( \frac{g_{k+1}}{g_k} \right)^2 \left( \frac{F_k}{F_{k+1}} \right)^\eta, \\ 2114 \end{aligned}$$

2115 where

$$2116 \quad A(\varepsilon) := \frac{1}{8d} \min_{1 \leq i \leq d} \left( \frac{1}{M_{1-\alpha_i}} \left[ \frac{\varepsilon^{\alpha_i} - \alpha}{D_c^{1+\alpha_i}} \right]^{\frac{1}{1+c}} \right).$$

2118 Telescoping this bound and using the inequality between arithmetic and geometric means, we obtain  
2119

$$\begin{aligned} 2120 \quad \frac{1}{\eta} \left( \frac{1}{F_k^\eta} - \frac{1}{F_0^\eta} \right) &\geq A(\varepsilon) \cdot \sum_{i=1}^{k-1} \left( \frac{g_{i+1}}{g_i} \right)^2 \left( \frac{F_i}{F_{i+1}} \right)^\eta \geq kA(\varepsilon) \cdot \left( \frac{g_k^2 F_k^\eta}{g_0^2 F_0^\eta} \right)^{\frac{1}{k}} \\ 2122 &\geq kA(\varepsilon) \cdot \left( \frac{F_0^\eta \varepsilon^{2-\eta}}{g_0^2 D_0^2} \right)^{\frac{1}{k}} \geq kA(\varepsilon) \cdot \left( \frac{\varepsilon}{g_0 D_0} \right)^{\frac{2}{k}} \\ 2124 &= kA(\varepsilon) \cdot \exp \left( -\frac{2}{k} \log \frac{g_0 D_0}{\varepsilon} \right) \geq kA(\varepsilon) \cdot \left( 1 - \frac{2}{k} \log \frac{g_0 D_0}{\varepsilon} \right). \\ 2126 \end{aligned}$$

2127 Rearranging the terms, we get

$$2128 \quad k \leq \frac{1}{\eta A(\varepsilon)} \left( \frac{1}{\varepsilon^\eta} - \frac{1}{F_0^\eta} \right) + 2 \log \frac{g_0 D_0}{\varepsilon}.$$

2130 Note that for  $\eta = 0$ , we can use the following limit

$$2132 \quad \lim_{\eta \rightarrow 0} \frac{1}{\eta} \left( \frac{1}{a^\eta} - \frac{1}{b^\eta} \right) = \log \frac{a}{b}, \quad a, b > 0.$$

2133 Therefore, in this case, we obtain

$$2135 \quad k \leq \frac{1}{A(\varepsilon)} \log \frac{F_0}{\varepsilon} + 2 \log \frac{g_0 D_0}{\varepsilon},$$

2136 which completes the proof.  $\square$

2138 Let us consider an important particular case of convex functions ( $c = 0$ ), and for specific assumptions on smoothness. In these cases and for the exact Hessian, we have that  $\gamma(\mathbf{x}_k, F'(\mathbf{x}_k)) \geq$   
2139  $\pi(\|F'(\mathbf{x}_k)\|_*) = \|F'(\mathbf{x}_k)\|_*^\alpha M_{1-\alpha}^{-1}$ , thus  $\pi(\cdot)$  is a simple monomial of degree  $0 \leq \alpha \leq 1$ .  
2140

2142 **Corollary 7 (Convex Function).** Consider exact Newton method:  $\mathbf{H}(\mathbf{x}_k) := \nabla^2 f(\mathbf{x}_k)$ .

2143 • Let the Hessian have bounded variation (Ex. 1,  $\nu = 0$ ), then  $\alpha = 1$ ,  $M_0 = L_{2,0}$  and we get:

$$2144 \quad K = O\left(\frac{M_0 D_0^2}{\varepsilon}\right) = O\left(\frac{L_{2,0} D_0^2}{\varepsilon}\right).$$

2147 • Let the Hessian be Lipschitz continuous (Ex. 1,  $\nu = 1$ ), then  $\alpha = 1/2$ ,  $M_{1/2} = \sqrt{L_{2,1}}$ , and  
2148 our method has the same rate as the Cubic Newton (Nesterov & Polyak, 2006):

$$2149 \quad K = O\left(\frac{M_{1/2} D_0^{3/2}}{\varepsilon^{1/2}}\right) = O\left(\sqrt{\frac{L_{2,1} D_0^3}{\varepsilon}}\right).$$

2151 • Let the third derivative be Lipschitz continuous (Ex. 2,  $\nu = 1$ ), then  $\alpha = 1/3$ ,  $M_{2/3} = L_{3,1}^{1/3}$ ,  
2152 and we obtain the rate as that of the third-order tensor method (Nesterov, 2021a):

$$2154 \quad K = O\left(\frac{M_{2/3} D_0^{4/3}}{\varepsilon^{1/3}}\right) = O\left(\left[\frac{L_{3,1} D_0^4}{\varepsilon}\right]^{1/3}\right).$$

2156 • Let  $f$  be Quasi-Self-Concordant (Ex. 3), then  $\alpha = 0$ , and we obtain the global liner rate (Doikov,  
2157 2023):

$$2158 \quad K = O\left(M_1 D_0 \log \frac{F_0}{\varepsilon}\right).$$

We see that our theory covers all the known state-of-the-art global convergence rates of the Newton method in a unified manner.

Now, assume that we use an inexact Hessian,  $\mathbf{H}(\mathbf{x}_k) \approx \nabla^2 f(\mathbf{x}_k)$ , that satisfies condition (52). Then, the corresponding Gradient-Normalized Smoothness  $\gamma(\cdot)$  will be changed accordingly (53) and Theorem 6 leads us to the following result. We assume  $\psi \equiv 0$  (unconstrained minimization).

**Corollary 8** (Inexact Hessian). *Let us choose  $\gamma_k = \gamma(\mathbf{x}_k)$  in Algorithm 1, or by performing an adaptive search, using an inexact Hessian that satisfies (52). Assume that  $c \leq \beta$ . Then, to ensure  $f(\mathbf{x}_K) - f^* \leq \varepsilon$  it is enough to perform a number of iterations of*

$$K = \tilde{O}\left(C_{\text{NEWTON}}(\varepsilon) + \mathbf{C}_1 \left[\frac{D_c^2}{\varepsilon^{1-c}}\right]^{\frac{1}{1+c}} + \mathbf{C}_2 \left[\frac{D_c^{1+\beta}}{\varepsilon^{\beta-c}}\right]^{\frac{1}{1+c}}\right), \quad (61)$$

where  $C_{\text{NEWTON}}(\varepsilon)$  is the complexity of the method with exact Hessian.

According to (61), we see that a large degree  $c \geq 0$  of gradient dominance helps to accelerate the method. Thus, for  $c := 0$  (convex functions), we obtain

$$K = \tilde{O}\left(C_{\text{NEWTON}}(\varepsilon) + \mathbf{C}_1 \frac{D_0^2}{\varepsilon} + \mathbf{C}_2 \frac{D_0^{1+\beta}}{\varepsilon^\beta}\right).$$

At the same time, for  $c := 1/2$  (e.g., uniformly convex functions of degree 3), we already obtain a complexity of

$$K = \tilde{O}\left(C_{\text{NEWTON}}(\varepsilon) + \mathbf{C}_1 \frac{D_{1/2}^{4/3}}{\varepsilon^{1/3}} + \mathbf{C}_2 \left[\frac{D_{1/2}^{1+\beta}}{\varepsilon^{\beta-1/2}}\right]^{\frac{2}{3}}\right),$$

which is much better in terms of dependence on  $\varepsilon$ , etc. It is important that all these rates correspond to the same algorithm, with a universal step-size selection. Therefore, the method is able to *automatically* adapt to the best degree of smoothness and gradient dominance.

Combining Corollary 8 with Corollary 7, we obtain the following classification of complexities, for Convex Unconstrained Minimization ( $c = 0, \psi \equiv 0$ ), with inexact Hessians.

**Corollary 9** (Inexact Hessian: Convex Functions). *Consider inexact Hessians (52).*

- *Let the Hessian have bounded variation, and  $\alpha = \beta = 1$ . Then,*

$$K = O\left(\frac{(M_0 + \mathbf{C}_2)D_0}{\varepsilon} + \frac{\mathbf{C}_1 D_0^2}{\varepsilon}\right).$$

- *Let the Hessian be Lipschitz continuous, and  $\alpha = \beta = 1/2$ . Then,*

$$K = O\left(\frac{(M_{1/2} + \mathbf{C}_2)D_0^{3/2}}{\varepsilon^{1/2}} + \frac{\mathbf{C}_1 D_0^2}{\varepsilon}\right).$$

- *Let the third derivative be Lipschitz continuous, and  $\alpha = \beta = 1/3$ . Then*

$$K = O\left(\frac{(M_{2/3} + \mathbf{C}_2)D_0^{4/3}}{\varepsilon^{1/3}} + \frac{\mathbf{C}_1 D_0^2}{\varepsilon}\right).$$

- *Let  $f$  be Quasi-Self-Concordant, and  $\alpha = \beta = 0$ . Then*

$$K = O\left(\left[(M_1 + \mathbf{C}_2)D_0 + \frac{\mathbf{C}_1 D_0^2}{\varepsilon}\right] \log \frac{F_0}{\varepsilon}\right).$$

## G APPLICATIONS

In this section, we provide concrete examples of problems that satisfy our assumptions of smoothness and Hessian approximation, and that offer direct, practical applications of our theory.

Let us study the case of the exact Hessian:  $\mathbf{H}(\mathbf{x}) \equiv \nabla^2 f(\mathbf{x})$ , and consider some standard assumptions on the smoothness of our objective. We demonstrate that any such global assumption can be effectively translated into appropriate bounds on our Gradient-Normalized Smoothness  $\gamma(\cdot)$ . As a consequence, by Theorems 5 and 6, we immediately obtain global convergence guarantees for our algorithms.

2214 For simplicity of our presentation, we always assume that  $K \geq 2 \log \frac{\|\nabla f(\mathbf{x}_0)\|_*}{\varepsilon}$  in our complexity  
 2215 bounds, to omit an additive logarithmic term.  
 2216

2217 **G.1 FUNCTIONS WITH HÖLDER HESSIAN**  
 2218

2219 Let us assume that the Hessian of  $f$  is Hölder continuous of degree  $\nu \in [0, 1]$ , with some constant  
 2220  $L_{2,\nu} > 0$ :

$$2221 \quad \|\nabla^2 f(\mathbf{x}) - \nabla^2 f(\mathbf{y})\| \leq L_{2,\nu} \|\mathbf{x} - \mathbf{y}\|^\nu, \quad \mathbf{x}, \mathbf{y} \in \mathbb{R}^n. \quad (62)$$

2222 Therefore, by direct integration, we obtain the following bound, for any  $\mathbf{h} \in \mathbb{R}^n$ :

$$2223 \quad \|\nabla f(\mathbf{x} + \mathbf{h}) - \nabla f(\mathbf{x}) - \nabla^2 f(\mathbf{x})\mathbf{h}\| \leq \frac{L_{2,\nu}}{1+\nu} \|\mathbf{h}\|^{1+\nu}. \quad (63)$$

2225 Now, let us choose  $\gamma := \left(\frac{1+\nu}{L_{2,\nu}} \|\mathbf{g}\|_*\right)^{\frac{1}{1+\nu}}$ , for an arbitrary fixed  $\mathbf{g} \in \mathbb{R}^n$  and consider  $\mathbf{h} \in B_\gamma :=$   
 2226  $\{\mathbf{h} \in \mathbb{R}^n : \|\mathbf{h}\| \leq \gamma\}$ . We have

$$2229 \quad \|\nabla f(\mathbf{x} + \mathbf{h}) - \nabla f(\mathbf{x}) - \nabla^2 f(\mathbf{x})\mathbf{h}\| \stackrel{(63)}{\leq} \frac{L_{2,\nu} \gamma^\nu}{1+\nu} \|\mathbf{h}\| = \frac{\|\mathbf{g}\|_* \|\mathbf{h}\|}{\gamma}, \quad (64)$$

2231 where the last equation holds due to our choice of  $\gamma$ . By our definition  $\gamma(\mathbf{x}, \mathbf{g})$  is the *maximal* such  
 2232 value that (64) holds. Hence, we obtain the following bound.

2233 **Proposition 1.** *Let  $f$  satisfy (62) for some  $\nu \in [0, 1]$  and  $L_{2,\nu} > 0$ . Then,*

$$2235 \quad \gamma_f(\mathbf{x}, \mathbf{g}) \geq \left(\frac{1+\nu}{L_{2,\nu}} \|\mathbf{g}\|_*\right)^{\frac{1}{1+\nu}}.$$

2238 Plugging this estimate into Theorem 5 we obtain the complexity to find  $\|F'(\mathbf{x}_k)\|_* \leq \varepsilon$  of order

$$2239 \quad K = O\left(\frac{F_0 L_{2,\nu}^{1/(1+\nu)}}{\varepsilon^{(2+\nu)/(1+\nu)}}\right)$$

2241 for our algorithms, up to an additive logarithmic terms. For  $\nu = 1$ , this corresponds to the complexity  
 2242 of the Cubic Newton method (Nesterov & Polyak, 2006), and for  $\nu = 0$ , this is the same rate as  
 2243 for the Gradient Descent on general non-convex problems (Nesterov, 2018). At the same time, for  
 2244 convex problems (Theorem 6,  $c = 0$ ), we get the complexity to find global solution in terms of the  
 2245 functional residual,  $F(\mathbf{x}_K) - F^* \leq \varepsilon$  of order

$$2247 \quad K = O\left(\left[\frac{L_{2,\nu} D_0^{2+\nu}}{\varepsilon}\right]^{\frac{1}{1+\nu}}\right).$$

2249 **G.2 CONVEX FUNCTIONS WITH HÖLDER THIRD DERIVATIVE**  
 2250

2251 Now, we assume that function  $f$  is convex and its third derivative is Hölder continuous of degree  
 2252  $\nu \in [0, 1]$ , with constant  $L_{3,\nu} > 0$ :

$$2253 \quad \|\nabla^3 f(\mathbf{y}) - \nabla^3 f(\mathbf{x})\| \leq L_{3,\nu} \|\mathbf{x} - \mathbf{y}\|^\nu, \quad \mathbf{x}, \mathbf{y} \in \mathbb{R}^n. \quad (65)$$

2255 Following (Nesterov, 2021a; Doikov et al., 2024a), we can integrate this inequality and, using  
 2256 convexity, obtain, for an arbitrary directions  $\mathbf{v} \in \mathbb{R}^n$  and  $\mathbf{u} \in \mathbb{R}^n$ :

$$2257 \quad 0 \leq \langle \nabla^2 f(\mathbf{x} + \mathbf{v})\mathbf{h}, \mathbf{h} \rangle \leq \langle \nabla^2 f(\mathbf{x})\mathbf{h}, \mathbf{h} \rangle + \nabla^3 f(\mathbf{x})[\mathbf{h}, \mathbf{h}, \mathbf{v}] + \frac{L_{3,\nu}}{1+\nu} \|\mathbf{h}\|^2 \cdot \|\mathbf{v}\|^{1+\nu}.$$

2259 Now, substituting  $\mathbf{v} = \pm \tau \mathbf{u}$ , for some  $\tau > 0$  and  $\mathbf{u} \in \mathbb{R}^n$ , we get

$$2260 \quad |\nabla^3 f(\mathbf{x})[\mathbf{h}, \mathbf{h}, \mathbf{u}]| \leq \frac{1}{\tau} \langle \nabla^2 f(\mathbf{x})\mathbf{h}, \mathbf{h} \rangle + \tau^\nu \cdot \frac{L_{3,\nu}}{1+\nu} \|\mathbf{h}\|^2 \cdot \|\mathbf{u}\|^{1+\nu}.$$

2262 Balancing the right hand side, we can choose  $\tau := \left(\frac{(1+\nu) \langle \nabla^2 f(\mathbf{x})\mathbf{h}, \mathbf{h} \rangle}{L_{3,\nu} \|\mathbf{h}\|^2 \|\mathbf{u}\|^{1+\nu}}\right)^{\frac{1}{1+\nu}}$ , which gives:

$$2264 \quad |\nabla^3 f(\mathbf{x})[\mathbf{h}, \mathbf{h}, \mathbf{u}]| \leq 2 \cdot \left(\frac{L_{3,\nu}}{1+\nu}\right)^{\frac{1}{1+\nu}} \langle \nabla^2 f(\mathbf{x})\mathbf{h}, \mathbf{h} \rangle^{\frac{\nu}{1+\nu}} \cdot \|\mathbf{h}\|^{\frac{2}{1+\nu}} \cdot \|\mathbf{u}\|^{1+\nu} \quad (66)$$

$$2265 \quad = 2 \cdot \left(\frac{L_{3,\nu}}{1+\nu}\right)^{\frac{1}{1+\nu}} \|\mathbf{h}\|_{\mathbf{x}}^{\frac{2\nu}{1+\nu}} \cdot \|\mathbf{h}\|^{\frac{2}{1+\nu}} \cdot \|\mathbf{u}\|, \quad \mathbf{h}, \mathbf{u} \in \mathbb{R}^n.$$

2268 Then, using Taylor's formula for the gradient approximation, we obtain  
 2269

$$2270 \quad \|\nabla f(\mathbf{x} + \mathbf{h}) - \nabla f(\mathbf{x}) - \nabla^2 f(\mathbf{x})\mathbf{h} - \frac{1}{2}\nabla^3 f(\mathbf{x})[\mathbf{h}, \mathbf{h}]\|_* \stackrel{(65)}{\leq} \frac{L_{3,\nu}}{(1+\nu)(2+\nu)} \|\mathbf{h}\|^{2+\nu}. \\ 2271$$

2272 Hence, applying the triangle inequality and our bound (66), we conclude that  
 2273

$$2274 \quad \|\nabla f(\mathbf{x} + \mathbf{h}) - \nabla f(\mathbf{x}) - \nabla^2 f(\mathbf{x})\mathbf{h}\|_* \\ 2275 \quad \leq \frac{L_{3,\nu}}{(1+\nu)(2+\nu)} \|\mathbf{h}\|^{2+\nu} + \left(\frac{L_{3,\nu}}{1+\nu}\right)^{\frac{1}{1+\nu}} \|\mathbf{h}\|_{\mathbf{x}}^{\frac{2\nu}{1+\nu}} \cdot \|\mathbf{h}\|^{\frac{2}{1+\nu}}. \\ 2276$$

2277 Now, for an arbitrary  $\mathbf{g} \in \mathbb{R}^n$  and a fixed  $\gamma > 0$ , we consider only the directions  $\mathbf{h} \in B_\gamma \cap \mathcal{O}_{\mathbf{x}, \mathbf{g}}$ , i.e.  
 2278 it holds:  
 2279

$$2280 \quad \|\mathbf{h}\| \leq \gamma \quad \text{and} \quad \|\mathbf{h}\|_{\mathbf{x}}^2 \leq -\langle \mathbf{g}, \mathbf{h} \rangle \leq \|\mathbf{g}\|_* \|\mathbf{h}\|. \\ 2281$$

2281 For such directions, we can continue our bound, as follows:  
 2282

$$2283 \quad \|\nabla f(\mathbf{x} + \mathbf{h}) - \nabla f(\mathbf{x}) - \nabla^2 f(\mathbf{x})\mathbf{h}\|_* \leq \frac{L_{3,\nu}\gamma^{1+\nu}}{(1+\nu)(2+\nu)} \|\mathbf{h}\| + \left(\frac{L_{3,\nu}}{1+\nu}\right)^{\frac{1}{1+\nu}} \gamma^{\frac{1}{1+\nu}} \|\mathbf{g}\|_*^{\frac{\nu}{1+\nu}} \|\mathbf{h}\|. \\ 2284$$

2285 Now, we notice that to ensure  
 2286

$$2286 \quad \frac{L_{3,\nu}\gamma^{1+\nu}}{(1+\nu)(2+\nu)} + \left(\frac{L_{3,\nu}}{1+\nu}\right)^{\frac{1}{1+\nu}} \gamma^{\frac{1}{1+\nu}} \|\mathbf{g}\|_*^{\frac{\nu}{1+\nu}} \leq \frac{\|\mathbf{g}\|_*}{\gamma}, \\ 2287$$

2288 it is sufficient to choose  
 2289

$$2290 \quad \gamma := \left(\frac{1+\nu}{2^{1+\nu} L_{3,\nu}} \|\mathbf{g}\|_*\right)^{\frac{1}{2+\nu}}. \\ 2291$$

2291 Therefore, we finally conclude the following bound.

2292 **Proposition 2.** *Let  $f$  be convex and satisfy (65) for some  $\nu \in [0, 1]$  and  $L_{3,\nu} > 0$ . Then,*

$$2295 \quad \gamma_f(\mathbf{x}, \mathbf{g}) \geq \left(\frac{1+\nu}{2^{1+\nu} L_{3,\nu}} \|\mathbf{g}\|_*\right)^{\frac{1}{2+\nu}}. \\ 2296$$

2297 Using this estimate with Theorem 6, for convex problems ( $c = 0$ ), we get the complexity to find  
 2298 global solution in terms of the functional residual,  $F(\mathbf{x}_K) - F^* \leq \varepsilon$  of order  
 2299

$$2300 \quad K = O\left(\left[\frac{L_{3,\nu} D_0^{3+\nu}}{\varepsilon}\right]^{\frac{1}{2+\nu}}\right) \quad (68) \\ 2301$$

2302 for our algorithm. For  $\nu = 1$ , this gives  $O([1/\varepsilon]^{\frac{1}{3}})$ . This result recovers fast rates for the Super-  
 2303 Universal Newton method from (Doikov et al., 2024a). Note that our algorithms and theory generalize  
 2304 these rate to the case of inexact Hessian (see Corollaries 8 and 9).

### 2305 G.3 QUASI-SELF-CONCORDANT FUNCTIONS

2306 Important in applications with softmax problems, logistic and exponential regressions, matrix balancing  
 2307 and matrix scaling problems, are convex objectives that satisfy the following condition (Bach,  
 2308 2010; Sun & Tran-Dinh, 2018; Karimireddy et al., 2018; Carmon et al., 2020; Doikov, 2023), with  
 2309 some parameter  $M_1 \geq 0$ :

$$2312 \quad \langle \nabla^3 f(\mathbf{x})\mathbf{h}, \mathbf{h}, \mathbf{u} \rangle \leq M_1 \|\mathbf{h}\|_{\mathbf{x}}^2 \|\mathbf{u}\|, \quad \mathbf{x}, \mathbf{h}, \mathbf{u} \in \mathbb{R}^n. \quad (69)$$

2313 By integrating this inequality, we obtain (see, e.g., Lemma 2.7 in (Doikov, 2023)), for any  $\mathbf{x}, \mathbf{h} \in \mathbb{R}^n$ :

$$2315 \quad \|\nabla f(\mathbf{x} + \mathbf{h}) - \nabla f(\mathbf{x}) - \nabla^2 f(\mathbf{x})\mathbf{h}\|_* \leq M_1 \|\mathbf{h}\|_{\mathbf{x}}^2 \varphi(M_1 \|\mathbf{h}\|), \quad (70)$$

2316 where  $\varphi(t) := \frac{e^t - t - 1}{t^2} \geq 0$  is a convex and monotone function. Now, let us assume that  $\mathbf{h} \in$   
 2317  $B_\gamma \cap \mathcal{O}_{\mathbf{x}, \mathbf{g}}$ , for an arbitrary  $\gamma > 0$  and  $\mathbf{g} \in \mathbb{R}^n$ :

$$2319 \quad \|\mathbf{h}\| \leq \gamma \quad \text{and} \quad \|\mathbf{h}\|_{\mathbf{x}}^2 \leq -\langle \mathbf{g}, \mathbf{h} \rangle \leq \|\mathbf{g}\|_* \|\mathbf{h}\|. \quad (71)$$

2320 Substituting these bounds into (70), we get  
 2321

$$\|\nabla f(\mathbf{x} + \mathbf{h}) - \nabla f(\mathbf{x}) - \nabla^2 f(\mathbf{x})\mathbf{h}\|_* \leq M_1 \|\mathbf{g}\|_* \|\mathbf{h}\| \cdot \varphi(\gamma M_1),$$

2322 and for  $\gamma := \frac{1}{M_1}$  we ensure  $M_1\varphi(\gamma M_1) \leq \frac{1}{\gamma}$ . Hence, we have established the following result.  
 2323

2324 **Proposition 3.** *Let  $f$  be Quasi-Self-Concordant (69) for some  $M_1 > 0$ . Then,*

$$\gamma_f(\mathbf{x}, \mathbf{g}) \geq \frac{1}{M_1}.$$

2328 Using this bound on Gradient-Normalized Smoothness in our Theorem 6 for convex functions  
 2329 ( $c = 0$ ) immediately gives the global linear rate of convergence for our method, and to achieve  
 2330  $F(\mathbf{x}_K) - F^* \leq \varepsilon$ , it is enough to perform

$$K = O\left(M_1 D_0 \cdot \log \frac{F_0}{\varepsilon}\right)$$

2333 iterations of the algorithm.

2334 Note that this is the same rate established in (Doikov, 2023) for the Newton method with gradient  
 2335 regularization. This result shows that the Newton method can achieve a global linear rate of conver-  
 2336 gence without any additional assumptions of uniform or strong convexity on the objective. In contrast,  
 2337 first-order methods can attain only sublinear rates on these problems unless additional regularization  
 2338 is applied.

2339 In this work, we generalize this result to methods with an *inexact Hessian*. It appears that, as soon as  
 2340  $\mathbf{C}_1 \approx 0$  and  $\beta = 0$  in condition (12), the method with an inexact Hessian has *the same fast global*  
 2341 *rate* as the full Newton method. Remarkably, as we show, this holds—for example—for the logistic  
 2342 regression problem (Example 6), where the Fisher approximation of the Hessian yields  $\mathbf{C}_1 = f^*$  (the  
 2343 global optimum), which can be close to zero in well-separable case.

#### 2345 G.4 GENERALIZED SELF-CONCORDANT FUNCTIONS

2346 Combining the previous two examples, let us consider the following class of convex *Generalized*  
 2347 *Self-Concordant* functions (Sun & Tran-Dinh, 2018), for some degree  $0 \leq q < 2$  and  $G_q \geq 0$ :

$$\nabla^3 f(\mathbf{x})[\mathbf{h}, \mathbf{h}, \mathbf{u}] \leq G_q \|\mathbf{h}\|_{\mathbf{x}}^q \|\mathbf{h}\|^{2-q} \|\mathbf{u}\|, \quad \mathbf{x}, \mathbf{h}, \mathbf{u} \in \mathbb{R}^n. \quad (72)$$

2348 Note that  $q = 2$  corresponds to Quasi-Self-Concordant functions (69), and for the convex functions  
 2349 with Hölder continuous third derivative (66) of degree  $\nu \in [0, 1]$ , we have  $q = \frac{2\nu}{1+\nu}$ . Let us present  
 2350 the following example that provides us with all intermediate powers  $0 \leq q < 2$ .

2351 **Example 9.** *For  $p \geq 2$ , consider*

$$f(\mathbf{x}) = \frac{1}{p} \|\mathbf{x}\|^p.$$

2352 *Then, (72) is satisfied with  $q := \frac{2(p-3)}{p-2}$  and  $G_q := (p-1)(p-2)$ .*

2361 *Proof.* Indeed, for arbitrary  $\mathbf{h}, \mathbf{u} \in \mathbb{R}^n$ , we have:

$$\langle \nabla f(\mathbf{x}), \mathbf{h} \rangle = \|\mathbf{x}\|^{p-2} \langle \mathbf{Bx}, \mathbf{h} \rangle$$

$$\langle \nabla^2 f(\mathbf{x}) \mathbf{h}, \mathbf{h} \rangle = (p-2) \|\mathbf{x}\|^{p-4} \langle \mathbf{Bx}, \mathbf{h} \rangle^2 + \|\mathbf{x}\|^{p-2} \|\mathbf{h}\|^2 \geq \|\mathbf{x}\|^{p-2} \|\mathbf{h}\|^2,$$

$$\nabla^3 f(\mathbf{x})[\mathbf{h}, \mathbf{h}, \mathbf{u}] = 2(p-2) \|\mathbf{x}\|^{p-4} \langle \mathbf{Bx}, \mathbf{h} \rangle \langle \mathbf{Bu}, \mathbf{h} \rangle$$

$$+ (p-2)(p-4) \|\mathbf{x}\|^{p-6} \langle \mathbf{Bx}, \mathbf{u} \rangle \langle \mathbf{Bx}, \mathbf{h} \rangle^2$$

$$+ (p-2) \|\mathbf{x}\|^{p-4} \|\mathbf{h}\|^2 \langle \mathbf{Bxu} \rangle$$

$$\leq (p-1)(p-2) \|\mathbf{x}\|^{p-3} \|\mathbf{h}\|^2 \|\mathbf{u}\|$$

$$\leq (p-1)(p-2) \|\mathbf{h}\|_{\mathbf{x}}^{\frac{2(p-3)}{p-2}} \|\mathbf{h}\|^{\frac{2}{p-2}} \|\mathbf{u}\|,$$

2375 which is the required bound.  $\square$

Using direct computation, we also immediately obtain the following simple proposition.

**Proposition 4** (Affine Substitution). *Let  $f$  satisfy (72) for some  $0 \leq q < 2$  and  $G_q > 0$ . Then,  $g(\mathbf{x}) := f(\mathbf{Ax} - \mathbf{b})$  satisfy (72) with the same degree  $q$  and constant  $G_q$ , by correcting the global norm accordingly:  $\mathbf{B}' := \mathbf{A}^\top \mathbf{B} \mathbf{A}$ .*

Now, let us fix a point  $\mathbf{x} \in \mathbb{R}^n$ . For arbitrary given directions  $\mathbf{u}, \mathbf{h} \in \mathbb{R}^n$ , we denote the following univariate function

$$\varphi(\tau) := \frac{2}{2-q} \langle \nabla^2 f(\mathbf{x} + \tau \mathbf{u}) \mathbf{h}, \mathbf{h} \rangle^{\frac{2-q}{2}}.$$

Then,

$$|\varphi'(\tau)| = \left| \frac{\nabla^3 f(\mathbf{x} + \tau \mathbf{u})[\mathbf{h}, \mathbf{h}, \mathbf{u}]}{\nabla^2 f(\mathbf{x} + \tau \mathbf{u}) \mathbf{h}, \mathbf{h}} \right|^{\frac{2-q}{2}} \stackrel{(72)}{\leq} G_q \|\mathbf{h}\|^{2-q} \|\mathbf{u}\|. \quad (73)$$

Hence, for arbitrary  $\mathbf{x}, \mathbf{y}, \mathbf{h} \in \mathbb{R}^n$ , setting  $\mathbf{u} := \mathbf{y} - \mathbf{x}$ , we have

$$\|\mathbf{h}\|_{\mathbf{y}}^{2-q} - \|\mathbf{h}\|_{\mathbf{x}}^{2-q} = \frac{2-q}{2} (\varphi(1) - \varphi(0)) \stackrel{(73)}{\leq} \frac{2-q}{2} G_q \|\mathbf{h}\|^{2-q} \|\mathbf{y} - \mathbf{x}\|. \quad (74)$$

Therefore, for an arbitrary  $\mathbf{h} \in \mathbb{R}^n$  and  $\mathbf{u} \in \mathbb{R}^n$  such that  $\|\mathbf{u}\| = 1$  we have

$$\begin{aligned} \langle \nabla f(\mathbf{x} + \mathbf{h}) - \nabla f(\mathbf{x}) - \nabla^2 f(\mathbf{x}) \mathbf{h}, \mathbf{u} \rangle &= \int_0^1 (1-\tau) \nabla^3 f(\mathbf{x} + \tau \mathbf{h})[\mathbf{h}, \mathbf{h}, \mathbf{u}] d\tau \\ &\stackrel{(72)}{\leq} G_q \|\mathbf{h}\|^{2-q} \int_0^1 (1-\tau) \|\mathbf{h}\|_{\mathbf{x} + \tau \mathbf{h}}^q d\tau \\ &\stackrel{(74)}{\leq} G_q \|\mathbf{h}\|^{2-q} \int_0^1 (1-\tau) \left( \|\mathbf{h}\|_{\mathbf{x}}^{2-q} + \frac{2-q}{2} G_q \|\mathbf{h}\|^{3-q} \tau \right)^{\frac{q}{2-q}} d\tau \\ &\leq 2^{\frac{q}{2-q}} G_q \|\mathbf{h}\|^{2-q} \cdot \left[ \|\mathbf{h}\|_{\mathbf{x}}^q \int_0^1 (1-\tau) d\tau + \left( \frac{2-q}{2} G_q \right)^{\frac{q}{2-q}} \|\mathbf{h}\|^{\frac{q(3-q)}{2-q}} \int_0^1 (1-\tau) \tau^{\frac{q}{2-q}} d\tau \right] \\ &= 2^{\frac{2(q+1)}{2-q}} G_q \|\mathbf{h}\|^{2-q} \|\mathbf{h}\|_{\mathbf{x}}^q + \frac{(2-q)^{\frac{4-q}{2-q}}}{2 \cdot (4-q)} G_q^{\frac{2}{2-q}} \|\mathbf{h}\|^{\frac{4-q}{2-q}}. \end{aligned}$$

Therefore, we have proved the following bound.

**Proposition 5.** *Let  $f$  satisfy (72) for some  $0 \leq q < 2$  and  $G_q > 0$ . Then,*

$$\|\nabla f(\mathbf{x} + \mathbf{h}) - \nabla f(\mathbf{x}) - \nabla^2 f(\mathbf{x}) \mathbf{h}\|_* \leq c_1 \cdot G_q \|\mathbf{h}\|^{2-q} \|\mathbf{h}\|_{\mathbf{x}}^q + c_2 \cdot G_q^{\frac{2}{2-q}} \|\mathbf{h}\|^{\frac{4-q}{2-q}}, \quad (75)$$

$$\text{with } c_1 := 2^{\frac{2(q+1)}{2-q}} \text{ and } c_2 := \frac{(2-q)^{\frac{4-q}{2-q}}}{2 \cdot (4-q)}.$$

Note that in view of (66), this inequality recovers up to numerical constants the bound (67) for the convex functions with Hölder third derivative, which correspond to  $q := \frac{2\nu}{1+\nu}$ ,  $G_q := L_{3,\nu}^{1/(1+\nu)}$  and  $0 \leq \nu \leq 1$  covers the interval  $0 \leq q \leq 1$ .

It remains to establish the bound for the Gradient Normalized Smoothness  $\gamma(\cdot)$ . We fix an arbitrary  $\mathbf{g} \in \mathbb{R}^n$  and  $\gamma > 0$ , and consider the directions  $\mathbf{h} \in B_\gamma \cap \mathcal{O}_{\mathbf{x}, \mathbf{g}}$ , i.e.

$$\|\mathbf{h}\| \leq \gamma \quad \text{and} \quad \|\mathbf{h}\|_{\mathbf{x}}^2 \leq -\langle \mathbf{g}, \mathbf{h} \rangle \leq \|\mathbf{g}\|_* \|\mathbf{h}\|.$$

For such  $\mathbf{h}$ , our bound (75) leads to

$$\|\nabla f(\mathbf{x} + \mathbf{h}) - \nabla f(\mathbf{x}) - \nabla^2 f(\mathbf{x}) \mathbf{h}\|_* \leq c_1 G_q \cdot \gamma^{\frac{2-q}{2}} \cdot \|\mathbf{g}\|_*^{\frac{q}{2}} \cdot \|\mathbf{h}\| + c_2 G_q^{\frac{2}{2-q}} \cdot \gamma^{\frac{2}{2-q}} \cdot \|\mathbf{h}\|.$$

We notice that to ensure

$$c_1 G_q \cdot \gamma^{\frac{2-q}{2}} \cdot \|\mathbf{g}\|_*^{\frac{q}{2}} + c_2 G_q^{\frac{2}{2-q}} \cdot \gamma^{\frac{2}{2-q}} \leq \frac{\|\mathbf{g}\|_*}{\gamma},$$

it is sufficient to choose

$$\gamma := \left[ \frac{1}{2} \right]^{\frac{8+2q}{(2-q)(4-q)}} \cdot \left[ \frac{\|\mathbf{g}\|_*^{2-q}}{G_q^2} \right]^{\frac{1}{4-q}},$$

2430 and thus we establish the following result.  
 2431

2432 **Proposition 6.** *Let  $f$  satisfy (72) for some  $0 \leq q < 2$  and  $G_q > 0$ . Then,*

$$2434 \quad \gamma_f(\mathbf{x}, \mathbf{g}) \geq \left[ \frac{1}{2} \right]^{\frac{8+2q}{(2-q)(4-q)}} \cdot \left[ \frac{\|\mathbf{g}\|_*^{2-q}}{G_q^2} \right]^{\frac{1}{4-q}}. \\ 2435$$

2436 This bound generalizes that one from Proposition 2 as a particular case  $0 \leq q \leq 1$ . We also see that,  
 2437 ignoring the numerical constant and substituting formally  $q := 2$  provides us with the right power  
 2438 that corresponds to the Quasi-Self-Concordant functions from Proposition 3.  
 2439

2440 Using this bound in our Theorem 6 with  $\alpha := \frac{2-q}{4-q}$  for convex functions ( $c = 0$ ) immediately gives  
 2441 us the following complexity to find  $F(\mathbf{x}_K) - F^* \leq \varepsilon$  of order  
 2442

$$2443 \quad K = O\left(\left[\frac{G_q^{\frac{2}{2-q}} D_0^{\frac{6-2q}{2-q}}}{\varepsilon}\right]^{\frac{2-q}{4-q}}\right) \quad (76) \\ 2444 \\ 2445$$

2446 for our algorithm, minimizing Generalized Quasi-Self-Concordant functions (72) of degree  $0 \leq$   
 2447  $q < 2$ . To the best of our knowledge, this global complexity is completely new and has not been  
 2448 covered in the prior literature. This result recovers complexity (68) as a particular case and naturally  
 2449 interpolates the complexities for convex functions with Hölder continuous third derivative and  
 2450 Quasi-Self-Concordant functions (see also Table 1).  
 2451

2452 To illustrate the power of our results, we return to Example (9) to examine the direct consequences  
 2453 of our theory.  
 2454

2455 **Example 10.** *Let  $f(\mathbf{x}) = \frac{1}{p} \|\mathbf{Ax} - \mathbf{b}\|_2^p$ , for some  $p \geq 2$ , and  $\|\cdot\|_2$  is the standard Euclidean  
 2456 norm. Let us choose the norm in our space with  $\mathbf{B} := \mathbf{A}^\top \mathbf{A}$ , assuming  $\mathbf{B} \succ 0$ . Then, according  
 2457 to our previous observations, function  $f$  belongs to class (72) with*

$$2458 \quad q := \frac{2(p-3)}{p-2}, \quad \text{and} \quad G_q := (p-1)(p-2). \\ 2459 \\ 2460$$

2461 According to Proposition 6, the Gradient-Normalized Smoothness for this function is bounded as

$$2462 \quad \gamma_f(\mathbf{x}) \geq \frac{\|\nabla f(\mathbf{x})\|_*^\alpha}{M_{1-\alpha}}, \\ 2463$$

2464 with  $\alpha := \frac{2-q}{4-q} = \frac{1}{p-1}$  and  $M_{1-\alpha} := [(p-1)(p-2)2^{3p-7}]^{\frac{p-2}{p-1}}$ . At the same time, this objective  
 2465 is uniformly convex (55) of degree  $p$  with constant  $\sigma_p = 2^{2-p}$  (Doikov & Nesterov, 2021). Hence,  
 2466 the gradient-dominance condition (54) is satisfied with  
 2467

$$2468 \quad c := \frac{1}{p-1} \quad \text{and} \quad D_c := \frac{p-1}{p} \cdot 2^{\frac{p-2}{p-1}}. \\ 2469$$

2470 Therefore, since  $\alpha \equiv c$ , by Theorem 6, our algorithm has the global linear rate, and the number  
 2471 of iterations to achieve  $f(\mathbf{x}_K) - f^* \leq \varepsilon$  is bounded as

$$2473 \quad K = 8M_{1-\alpha}D_c \log \frac{f(\mathbf{x}_0) - f^*}{\varepsilon} = O\left(\log \frac{f(\mathbf{x}_0) - f^*}{\varepsilon}\right), \\ 2474$$

2475 where  $O(\cdot)$  hides a numerical constant that depends only on  $p$ .  
 2476  
 2477

## 2478 G.5 $(L_0, L_1)$ -SMOOTH FUNCTIONS

2481 Let us assume that  $f$  satisfies the following inequality (Zhang et al., 2019):  
 2482

$$2483 \quad \|\nabla^2 f(\mathbf{x})\| \leq L_0 + L_1 \|\nabla f(\mathbf{x})\|_*, \quad \mathbf{x} \in \mathbb{R}^n. \quad (77)$$

Then, for such functions, we have the following bound (see Lemma 2.5 in (Vankov et al., 2024)), for any  $\mathbf{x}, \mathbf{h} \in \mathbb{R}^n$ :

$$\begin{aligned} \|\nabla f(\mathbf{x} + \mathbf{h}) - \nabla f(\mathbf{x}) - \nabla^2 f(\mathbf{x})\mathbf{h}\|_* &\leq \|\nabla f(\mathbf{x} + \mathbf{h}) - \nabla f(\mathbf{x})\|_* + \|\nabla^2 f(\mathbf{x})\| \cdot \|\mathbf{h}\| \\ &\leq \left( L_0 + L_1 \|\nabla f(\mathbf{x})\|_* \right) \cdot \left[ \|\mathbf{h}\| + \frac{e^{L_1 \|\mathbf{h}\|} - 1}{L_1} \right] \\ &\leq \left( L_0 + L_1 \|\nabla f(\mathbf{x})\|_* \right) \cdot \|\mathbf{h}\| \cdot (1 + e^{L_1 \|\mathbf{h}\|}). \end{aligned}$$

We fix  $\gamma > 0$ ,  $\mathbf{g} \in \mathbb{R}^n$ , and consider  $\mathbf{h} \in B_\gamma$ . Then, we have an upper bound

$$\|\nabla f(\mathbf{x} + \mathbf{h}) - \nabla f(\mathbf{x}) - \nabla^2 f(\mathbf{x})\mathbf{h}\|_* \leq \frac{\|\mathbf{g}\|_* \|\mathbf{h}\|}{\gamma},$$

as soon as

$$\left( L_0 + L_1 \|\nabla f(\mathbf{x})\|_* \right) \cdot (1 + e^{L_1 \gamma}) \leq \frac{\|\mathbf{g}\|_*}{\gamma}.$$

It is easy to check that it is satisfied for  $\gamma := \frac{1}{1 + \exp(\|\mathbf{g}\|_* / \|\nabla f(\mathbf{x})\|_*)} \cdot \frac{\|\mathbf{g}\|_*}{L_0 + L_1 \|\nabla f(\mathbf{x})\|_*}$ . Therefore, we have established the following lower bound.

**Proposition 7.** *Let  $f$  satisfy (77) for some  $L_0, L_1 > 0$ . Then,*

$$\gamma_f(\mathbf{x}, \mathbf{g}) \geq \frac{\|\mathbf{g}\|_*}{L_0 + L_1 \|\nabla f(\mathbf{x})\|_*} \cdot \left( 1 + \exp\left(\frac{\|\mathbf{g}\|_*}{\|\nabla f(\mathbf{x})\|_*}\right) \right)^{-1},$$

and for  $\mathbf{g} := \nabla f(\mathbf{x})$ , we obtain

$$\gamma_f(\mathbf{x}) \geq \frac{\|\nabla f(\mathbf{x})\|_*}{\rho(L_0 + L_1 \|\nabla f(\mathbf{x})\|_*)},$$

where  $\rho := 1 + e \approx 3.718$ .

Using these bounds directly in our Theorems 1 and 2, we obtain the following complexity results:

- For unconstrained minimization of a non-convex function  $f(\cdot)$ , to achieve  $\|\nabla f(\mathbf{x}_K)\|_* \leq \varepsilon$  it is enough to perform

$$K = F_0 \cdot O\left(\frac{L_0}{\varepsilon^2} + \frac{L_1}{\varepsilon}\right)$$

iterations of our algorithm.

- For unconstrained minimization of a convex function  $f(\cdot)$ , to achieve  $f(\mathbf{x}_K) - f^* \leq \varepsilon$ , it is enough to perform

$$K = O\left(\left[\frac{L_0 D_0^2}{\varepsilon} + L_1 D_0\right] \log \frac{F_0}{\varepsilon}\right)$$

iterations of our algorithm.

Therefore, we see that our method has a global convergence guarantee, at least as strong as that of first-order methods on  $(L_0, L_1)$ -smooth functions. Moreover, these convergence rates are achieved automatically, and the actual speed of the method will be the best within these problem classes.

## G.6 SECOND-ORDER $(M_0, M_1)$ -SMOOTH FUNCTIONS

Following (Xie et al., 2024; Gratton et al., 2025), let us assume that  $f$  satisfies the following inequality:

$$\|\nabla^2 f(\mathbf{x}) - \nabla^2 f(\mathbf{y})\| \leq (M_0 + M_1 \|\nabla f(\mathbf{x})\|_*) \|\mathbf{x} - \mathbf{y}\|, \quad \mathbf{x}, \mathbf{y} \in \mathbb{R}^n, \quad (78)$$

for some constants  $M_0, M_1 \geq 0$ . Then, we have the bound, for all  $\mathbf{h} \in \mathbb{R}^n$

$$\|\nabla f(\mathbf{x} + \mathbf{h}) - \nabla f(\mathbf{x}) - \nabla^2 f(\mathbf{x})\mathbf{h}\|_* \leq \frac{M_0 + M_1 \|\nabla f(\mathbf{x})\|_*}{2} \|\mathbf{h}\|^2.$$

Restricting our direction onto a ball,  $\mathbf{h} \in B_\gamma$ , we have that

$$\|\nabla f(\mathbf{x} + \mathbf{h}) - \nabla f(\mathbf{x}) - \nabla^2 f(\mathbf{x})\mathbf{h}\|_* \leq \gamma \cdot \frac{M_0 + M_1 \|\nabla f(\mathbf{x})\|_*}{2} \|\mathbf{h}\| = \frac{\|\mathbf{g}\|_* \|\mathbf{h}\|}{\gamma},$$

where the last equation holds for the particular choice  $\gamma := \sqrt{\frac{2\|\mathbf{g}\|_*}{M_0 + M_1 \|\nabla f(\mathbf{x})\|_*}}$ . Therefore, we obtain the following statement.

2538  
2539  
2540  
2541  
2542  
2543  
2544  
2545  
2546  
2547  
2548  
2549  
2550  
2551  
2552  
2553  
2554  
2555  
2556  
2557  
2558  
2559  
2560  
2561  
2562  
2563  
2564  
2565  
2566  
2567  
2568  
2569  
2570  
2571  
2572  
2573  
2574  
2575  
2576  
2577  
2578  
2579  
2580  
2581  
2582  
2583  
2584  
2585  
2586  
2587  
2588  
2589  
2590  
2591

**Proposition 8.** Let  $f$  satisfy (78) for some  $M_0, M_1 > 0$ . Then,

$$\gamma_f(\mathbf{x}, \mathbf{g}) \geq \left( \frac{2\|\mathbf{g}\|_*}{M_0 + M_1 \|\nabla f(\mathbf{x})\|_*} \right)^{1/2}.$$

Using this bound in our Theorems 1 and 2, we obtain:

- For unconstrained minimization, in the non-convex case, to achieve  $\|\nabla f(\mathbf{x}_K)\|_* \leq \varepsilon$  it is enough to perform

$$K = F_0 \cdot O\left(\frac{M_0^{1/2}}{\varepsilon^{3/2}} + \frac{M_1^{1/2}}{\varepsilon}\right)$$

iterations of our algorithm.

- For unconstrained minimization, in the convex case, to achieve  $f(\mathbf{x}_K) - f^* \leq \varepsilon$ , it is enough to perform

$$K = O\left(\left[\left(\frac{M_0 D_0^3}{\varepsilon}\right)^{1/2} + M_1^{1/2} D_0\right] \log \frac{F_0}{\varepsilon}\right)$$

iterations of our algorithm.

We see that a stronger second-order  $(M_0, M_1)$ -smoothness condition allows for improved complexity results compared to first-order  $(L_0, L_1)$ -smooth functions. It is important that all these problem classes are covered by our framework, which also allows for inexact Hessians.

## H BOUNDS ON EFFECTIVE HESSIAN APPROXIMATIONS

### H.1 SOFT MAXIMUM

**Example 11** (Soft Maximum: Extended). *In applications with multiclass classification, graph problems, and matrix games, we have*

$$f(\mathbf{x}) := s(\mathbf{u}(\mathbf{x})),$$

where  $\mathbf{u} : \mathbb{R}^n \rightarrow \mathbb{R}^d$  is an operator (e.g. a linear or nonlinear model), and  $s(\mathbf{y}) := \log \sum_{i=1}^d e^{y_i}$  is the LogSumExp loss. Note that  $s(\cdot)$  is Quasi-Self-Concordant (Section G.3), and its gradient is the softmax:  $[\nabla s(\mathbf{y})]_i = e^{y_i} \cdot (\sum_{j=1}^d e^{y_j})^{-1}$ . Assume that

$$\|\nabla \mathbf{u}(\mathbf{x})\| \leq \xi_0, \quad \|\nabla^2 \mathbf{u}(\mathbf{x})\| \leq \xi_1, \quad \mathbf{x} \in \mathbb{R}^n,$$

for some  $\xi_0, \xi_1 \geq 0$ , and that operator  $\mathbf{u}(\cdot)$  is non-degenerate<sup>4</sup>, for some  $\mu > 0$ :

$$\nabla \mathbf{u}(\mathbf{x}) \mathbf{B}^{-1} \nabla \mathbf{u}(\mathbf{x})^\top \succeq \mu \mathbf{I}_d, \quad \mathbf{x} \in \mathbb{R}^n. \quad (79)$$

We introduce the following approximations and derive corresponding bounds:

- If  $\mathbf{H}(\mathbf{x}) := \nabla \mathbf{u}(\mathbf{x})^\top \nabla^2 s(\mathbf{u}(\mathbf{x})) \nabla \mathbf{u}(\mathbf{x}) \succeq \mathbf{0}$ , we have

$$\|\nabla^2 f(\mathbf{x}) - \mathbf{H}(\mathbf{x})\| \leq \frac{\xi_1}{\sqrt{\mu}} \|\nabla f(\mathbf{x})\|_*.$$

- If  $\mathbf{H}(\mathbf{x}) := \nabla \mathbf{u}(\mathbf{x})^\top \nabla \mathbf{u}(\mathbf{x}) \succeq \mathbf{0}$  (Gauss-Newton), we have

$$\|\nabla^2 f(\mathbf{x}) - \mathbf{H}(\mathbf{x})\| \leq \xi_0^2 + \left(\xi_0 + \frac{\xi_1}{\sqrt{\mu}}\right) \|\nabla f(\mathbf{x})\|_*.$$

- If  $\mathbf{H}(\mathbf{x}) := \nabla \mathbf{u}(\mathbf{x})^\top \text{Diag}(\nabla s(\mathbf{u}(\mathbf{x}))) \nabla \mathbf{u}(\mathbf{x}) \succeq \mathbf{0}$  (Weighted Gauss-Newton), we have

$$\|\nabla^2 f(\mathbf{x}) - \mathbf{H}(\mathbf{x})\| \leq \left(\xi_0 + \frac{\xi_1}{\sqrt{\mu}}\right) \|\nabla f(\mathbf{x})\|_*.$$

<sup>4</sup>This assumption can be relaxed. It holds, for example, when the model is overparametrized (i.e.  $n \gg d$ ).

2592 *Proof.* Note that

$$2593 \quad \nabla f(\mathbf{x}) = \nabla \mathbf{u}(\mathbf{x})^\top \nabla s(\mathbf{u}(\mathbf{x})),$$

2594 where  $\nabla \mathbf{u}(\mathbf{x}) \in \mathbb{R}^{d \times n}$  denotes the Jacobian of mapping  $\mathbf{u}$ , and

$$\begin{aligned} 2596 \quad \nabla^2 f(\mathbf{x}) &= \nabla \mathbf{u}(\mathbf{x})^\top \nabla^2 s(\mathbf{u}(\mathbf{x})) \nabla \mathbf{u}(\mathbf{x}) + \sum_{i=1}^d [\nabla s(\mathbf{u}(\mathbf{x}))]_i \nabla^2 u_i(\mathbf{x}) \\ 2597 &= \nabla \mathbf{u}(\mathbf{x})^\top \left( \text{Diag}(\nabla s(\mathbf{u}(\mathbf{x}))) - \nabla s(\mathbf{u}(\mathbf{x})) \nabla s(\mathbf{u}(\mathbf{x}))^\top \right) \nabla \mathbf{u}(\mathbf{x}) \\ 2598 &\quad + \sum_{i=1}^d [\nabla s(\mathbf{u}(\mathbf{x}))]_i \nabla^2 u_i(\mathbf{x}), \\ 2600 & \\ 2601 \end{aligned}$$

2602 where  $\nabla^2 \mathbf{u}(\mathbf{x})$  is the tensor of second derivatives of  $\mathbf{u}$ , which we assume to be bounded.

2603

2604 1. Consider the approximation

$$2605 \quad \mathbf{H}(\mathbf{x}) := \nabla \mathbf{u}(\mathbf{x})^\top \nabla^2(s(\mathbf{u}(\mathbf{x})) \nabla \mathbf{u}(\mathbf{x})) \succeq \mathbf{0}.$$

2606 Note that when operator  $\mathbf{u}(\cdot)$  is linear,  $\mathbf{H}(\mathbf{x})$  is the exact Hessian. In general non-linear case, we can  
2607 bound

$$\begin{aligned} 2609 \quad \|\nabla^2 f(\mathbf{x}) - \mathbf{H}(\mathbf{x})\| &= \left\| \sum_{i=1}^d [\nabla s(\mathbf{u}(\mathbf{x}))]_i \nabla^2 u_i(\mathbf{x}) \right\| \\ 2610 & \\ 2611 &\leq \xi_1 \|\nabla s(\mathbf{u}(\mathbf{x}))\|. \\ 2612 \end{aligned}$$

2613 On the other hand,

$$\begin{aligned} 2614 \quad \|\nabla f(\mathbf{x})\|_*^2 &:= \langle \nabla f(\mathbf{x}), \mathbf{B}^{-1} \nabla f(\mathbf{x}) \rangle = \langle \nabla \mathbf{u}(\mathbf{x}) \mathbf{B}^{-1} \nabla \mathbf{u}(\mathbf{x})^\top \nabla s(\mathbf{u}(\mathbf{x})), \nabla s(\mathbf{u}(\mathbf{x})) \rangle \\ 2615 & \\ 2616 &\geq \mu \|\nabla s(\mathbf{u}(\mathbf{x}))\|^2, \end{aligned}$$

2617 where in the last inequality we used the non-degeneracy condition and the standard Euclidean norm  
2618 in  $\mathbb{R}^d$ . Thus, we have the following bound  $\|\nabla s(\mathbf{u}(\mathbf{x}))\| \leq \frac{1}{\sqrt{\mu}} \|\nabla f(\mathbf{x})\|_*$ , that yields  
2619

$$2620 \quad \|\nabla^2 f(\mathbf{x}) - \mathbf{H}(\mathbf{x})\| \leq \frac{\xi_1}{\sqrt{\mu}} \|\nabla f(\mathbf{x})\|_*.$$

2621

2622

2623 2. Consider the approximation

$$2624 \quad \mathbf{H}(\mathbf{x}) := \nabla \mathbf{u}(\mathbf{x})^\top \nabla \mathbf{u}(\mathbf{x}) \succeq \mathbf{0}.$$

2625 Then, as in the previous case, we have:

$$\begin{aligned} 2626 \quad \|\nabla^2 f(\mathbf{x}) - \mathbf{H}(\mathbf{x})\| &= \left\| \nabla \mathbf{u}(\mathbf{x})^\top (\nabla^2 s(\mathbf{u}(\mathbf{x})) - \mathbf{I}_d) \nabla \mathbf{u}(\mathbf{x}) + \sum_{i=1}^d [\nabla s(\mathbf{u}(\mathbf{x}))]_i \nabla^2 u_i(\mathbf{x}) \right\| \\ 2627 & \\ 2628 &\leq \|\nabla \mathbf{u}(\mathbf{x})^\top (\nabla^2 s(\mathbf{u}(\mathbf{x})) - \mathbf{I}_d) \nabla \mathbf{u}(\mathbf{x})\| + \frac{\xi_1}{\sqrt{\mu}} \|\nabla f(\mathbf{x})\|_*, \\ 2629 & \\ 2630 & \\ 2631 & \\ 2632 \end{aligned}$$

2633 and it remains to bound the following term:

$$\begin{aligned} 2634 \quad \|\nabla \mathbf{u}(\mathbf{x})^\top (\nabla^2 s(\mathbf{u}(\mathbf{x})) - \mathbf{I}_d) \nabla \mathbf{u}(\mathbf{x})\| & \\ 2635 & \\ 2636 &= \left\| \nabla \mathbf{u}(\mathbf{x})^\top [\text{Diag}(\nabla s(\mathbf{u}(\mathbf{x}))) - \mathbf{I}_d] \nabla \mathbf{u}(\mathbf{x}) - \nabla \mathbf{u}(\mathbf{x})^\top \nabla s(\mathbf{u}(\mathbf{x})) \nabla s(\mathbf{u}(\mathbf{x}))^\top \nabla \mathbf{u}(\mathbf{x}) \right\| \\ 2637 & \\ 2638 &\leq \left\| \nabla \mathbf{u}(\mathbf{x})^\top [\text{Diag}(\nabla s(\mathbf{u}(\mathbf{x}))) - \mathbf{I}_d] \nabla \mathbf{u}(\mathbf{x}) \right\| + \left\| \nabla f(\mathbf{x})^\top \nabla f(\mathbf{x}) \right\|. \\ 2639 & \\ 2640 & \end{aligned}$$

2641 The first term can be bounded as follows:

$$2642 \quad \|\nabla \mathbf{u}(\mathbf{x})^\top [\text{Diag}(\nabla s(\mathbf{u}(\mathbf{x}))) - \mathbf{I}_d] \nabla \mathbf{u}(\mathbf{x})\| \leq \|\nabla \mathbf{u}(\mathbf{x})\|^2 \|\text{Diag}(\nabla s(\mathbf{u}(\mathbf{x}))) - \mathbf{I}_d\| \leq \xi_0^2,$$

2643 where we used the fact that  $\max_{1 \leq i \leq d} |[\nabla s(\mathbf{u}(\mathbf{x}))]_i - 1| \leq 1$  and our assumption regarding the bound-  
2644 edness of  $\|\nabla \mathbf{u}(\mathbf{x})\|$ . For the second term, we notice that  
2645

$$\|\nabla f(\mathbf{x})\|_* \leq \|\nabla \mathbf{u}(\mathbf{x})\| \cdot \|\nabla s(\mathbf{u}(\mathbf{x}))\| \leq \xi_0,$$

2646 since  $\nabla s(\mathbf{u}(\mathbf{x}))$  is from the simplex. Hence,

$$2647 \quad \|\nabla f(\mathbf{x})^\top \nabla f(\mathbf{x})\| = \|\nabla f(\mathbf{x})\|_*^2 \leq \xi_0 \|\nabla f(\mathbf{x})\|_*,$$

2648 and we finally obtain the following bound:

$$2649 \quad \|\nabla^2 f(\mathbf{x}) - \mathbf{H}(\mathbf{x})\| \leq \xi_0^2 + \left( \xi_0 + \frac{\xi_1}{\sqrt{\mu}} \right) \|\nabla f(\mathbf{x})\|_*.$$

2653 3. Consider the approximation

$$2654 \quad \mathbf{H}(\mathbf{x}) := \nabla \mathbf{u}(\mathbf{x})^\top \text{Diag}(\nabla s(\mathbf{u}(\mathbf{x}))) \nabla \mathbf{u}(\mathbf{x}) \succeq \mathbf{0}.$$

2656 Repeating the reasoning from the previous case, it follows immediately that

$$2657 \quad \|\nabla^2 f(\mathbf{x}) - \mathbf{H}(\mathbf{x})\| \leq \left( \xi_0 + \frac{\xi_1}{\sqrt{\mu}} \right) \|\nabla f(\mathbf{x})\|_*,$$

2659 which is the required bound.  $\square$

## 2661 H.2 NONLINEAR EQUATIONS

2663 **Example 12** (Nonlinear Equations: Extended). *Let  $\mathbf{u} : \mathbb{R}^n \rightarrow \mathbb{R}^d$  be a nonlinear operator, and set*

$$2665 \quad f(\mathbf{x}) := \frac{1}{p} \|\mathbf{u}(\mathbf{x})\|^p = \frac{1}{p} \langle \mathbf{G}\mathbf{u}(\mathbf{x}), \mathbf{u}(\mathbf{x}) \rangle^{\frac{p}{2}},$$

2667 for some  $\mathbf{G} = \mathbf{G}^\top \succ \mathbf{0}$ , and  $p \geq 2$ . Note that  $\frac{1}{p} \|\cdot\|^p$  is a generalized self-concordant loss function (Section G.4). As in the previous example, we assume that

$$2669 \quad \|\nabla \mathbf{u}(\mathbf{x})\| \leq \xi_0, \quad \|\nabla^2 \mathbf{u}(\mathbf{x})\| \leq \xi_1, \quad \mathbf{x} \in \mathbb{R}^n,$$

2671 for some  $\xi_0, \xi_1 \geq 0$ , and that the operator is non-degenerate, for some  $\mu > 0$ :

$$2672 \quad \nabla \mathbf{u}(\mathbf{x}) \mathbf{B}^{-1} \nabla \mathbf{u}(\mathbf{x})^\top \succeq \mu \mathbf{G}^{-1}, \quad \mathbf{x} \in \mathbb{R}^n. \quad (80)$$

2674 We introduce the following approximations and derive corresponding bounds:

2675 • If  $\mathbf{H}(\mathbf{x}) := \|\mathbf{u}(\mathbf{x})\|^{p-2} \nabla \mathbf{u}(\mathbf{x})^\top \mathbf{G} \nabla \mathbf{u}(\mathbf{x}) + \frac{p-2}{\|\mathbf{u}(\mathbf{x})\|^p} \nabla f(\mathbf{x}) \nabla f(\mathbf{x})^\top \succeq \mathbf{0}$ , we have

$$2677 \quad \|\nabla^2 f(\mathbf{x}) - \mathbf{H}(\mathbf{x})\| \leq \frac{\xi_1}{\sqrt{\mu}} \|\nabla f(\mathbf{x})\|_*.$$

2680 • If  $\mathbf{H}(\mathbf{x}) := \|\mathbf{u}(\mathbf{x})\|^{p-2} \nabla \mathbf{u}(\mathbf{x})^\top \mathbf{G} \nabla \mathbf{u}(\mathbf{x}) \succeq \mathbf{0}$ , we have

$$2682 \quad \|\nabla^2 f(\mathbf{x}) - \mathbf{H}(\mathbf{x})\| \leq (p-2) \xi_0^{\frac{p}{p-1}} \|\nabla f(\mathbf{x})\|_*^{\frac{p-2}{p-1}} + \frac{\xi_1}{\sqrt{\mu}} \|\nabla f(\mathbf{x})\|_*.$$

2684 • If  $\mathbf{H}(\mathbf{x}) := \frac{p-2}{\|\mathbf{u}(\mathbf{x})\|^p} \nabla f(\mathbf{x}) \nabla f(\mathbf{x})^\top \succeq \mathbf{0}$  (Fisher-type), we have

$$2686 \quad \|\nabla^2 f(\mathbf{x}) - \mathbf{H}(\mathbf{x})\| \leq \xi_0^2 \mu^{\frac{2-p}{2(p-1)}} \|\nabla f(\mathbf{x})\|_*^{\frac{p-2}{p-1}} + \frac{\xi_1}{\sqrt{\mu}} \|\nabla f(\mathbf{x})\|_*.$$

2689 *Proof.* Note that

$$2690 \quad \nabla f(\mathbf{x}) = \|\mathbf{u}(\mathbf{x})\|^{p-2} \nabla \mathbf{u}(\mathbf{x})^\top \mathbf{G} \mathbf{u}(\mathbf{x}),$$

2691 where  $\nabla \mathbf{u}(\mathbf{x}) \in \mathbb{R}^{d \times n}$  denotes the Jacobian matrix of mapping  $\mathbf{u}$ , and, for any direction  $\mathbf{h} \in \mathbb{R}^n$ ,  
2692 we have

$$2693 \quad \begin{aligned} \langle \nabla^2 f(\mathbf{x}) \mathbf{h}, \mathbf{h} \rangle &= \|\mathbf{u}(\mathbf{x})\|^{p-2} \langle \mathbf{G} \nabla \mathbf{u}(\mathbf{x}) \mathbf{h}, \nabla \mathbf{u}(\mathbf{x}) \mathbf{h} \rangle + \|\mathbf{u}(\mathbf{x})\|^{p-2} \langle \mathbf{G} \mathbf{u}(\mathbf{x}), \nabla^2 \mathbf{u}(\mathbf{x})[\mathbf{h}, \mathbf{h}] \rangle \\ &+ (p-2) \|\mathbf{u}(\mathbf{x})\|^{p-4} \langle \mathbf{G} \mathbf{u}(\mathbf{x}), \nabla \mathbf{u}(\mathbf{x}) \mathbf{h} \rangle^2, \end{aligned}$$

2696 where  $\nabla^2 \mathbf{u}(\mathbf{x})$  is the tensor of second derivatives of  $\mathbf{u}$ , which we assume to be bounded.

2698 1. Consider the approximation

$$2699 \quad \mathbf{H}(\mathbf{x}) := \|\mathbf{u}(\mathbf{x})\|^{p-2} \nabla \mathbf{u}(\mathbf{x})^\top \mathbf{G} \nabla \mathbf{u}(\mathbf{x}) + \frac{p-2}{\|\mathbf{u}(\mathbf{x})\|^p} \nabla f(\mathbf{x}) \nabla f(\mathbf{x})^\top \succeq \mathbf{0}. \quad (81)$$

2700 Note that it resembles a combination of the Gauss-Newton and Fisher approximation matrices, and  
 2701 for  $p = 2$  it gives the classic Gauss-Newton approximation. Moreover, when the operator  $\mathbf{u}$  is linear,  
 2702 the problem is convex, and  $\xi_1 = 0$ . Thus (81) gives us exact Hessian in this case. Let us consider  
 2703

$$\begin{aligned} 2704 \quad |\langle \nabla^2 f(\mathbf{x}) \mathbf{h}, \mathbf{h} \rangle - \langle \mathbf{H}(\mathbf{x}) \mathbf{h}, \mathbf{h} \rangle| &= \|\mathbf{u}(\mathbf{x})\|^{p-2} |\langle \mathbf{G}\mathbf{u}(\mathbf{x}), \nabla^2 \mathbf{u}(\mathbf{x}) [\mathbf{h}, \mathbf{h}] \rangle| \\ 2705 &\leq \|\mathbf{u}(\mathbf{x})\|^{p-2} \|\mathbf{u}(\mathbf{x})\| \|\nabla^2 \mathbf{u}(\mathbf{x})\| \|\mathbf{h}\|^2, \end{aligned}$$

2706 therefore

$$\begin{aligned} 2707 \quad \|\nabla^2 f(\mathbf{x}) - \mathbf{H}(\mathbf{x})\| &:= \max_{\mathbf{h}: \|\mathbf{h}\|=1} |\langle (\nabla^2 f(\mathbf{x}) - \mathbf{H}(\mathbf{x})) \mathbf{h}, \mathbf{h} \rangle| \\ 2708 &\leq \xi_1 \|\mathbf{u}(\mathbf{x})\|^{p-1} = \xi_1 (p f(\mathbf{x}))^{\frac{p-1}{p}}. \end{aligned}$$

2712 Using our non-degeneracy condition, we can further bound

$$\begin{aligned} 2713 \quad \|\nabla f(\mathbf{x})\|_*^2 &= \|\mathbf{u}(\mathbf{x})\|^{2(p-2)} \|\nabla \mathbf{u}(\mathbf{x})^\top \mathbf{G}\mathbf{u}(\mathbf{x})\|_*^2 \\ 2714 &= \|\mathbf{u}(\mathbf{x})\|^{2(p-2)} \langle \mathbf{G}\mathbf{u}(\mathbf{x}), \nabla \mathbf{u}(\mathbf{x}) \mathbf{B}^{-1} \nabla \mathbf{u}(\mathbf{x})^\top \mathbf{G}\mathbf{u}(\mathbf{x}) \rangle \\ 2715 &\stackrel{(80)}{\geq} \mu \|\mathbf{u}(\mathbf{x})\|^{2(p-1)}. \end{aligned}$$

2719 Thus, we have  $\|\mathbf{u}(\mathbf{x})\|^{p-1} \leq \frac{1}{\sqrt{\mu}} \|\nabla f(\mathbf{x})\|_*$ , which gives us the following bound on the approxima-  
 2720 tion error:

$$2722 \quad \|\nabla^2 f(\mathbf{x}) - \mathbf{H}(\mathbf{x})\| \leq \frac{\xi_1}{\sqrt{\mu}} \|\nabla f(\mathbf{x})\|_*.$$

2724 2. Consider the approximation

$$2726 \quad \mathbf{H}(\mathbf{x}) := \|\mathbf{u}(\mathbf{x})\|^{p-2} \nabla \mathbf{u}(\mathbf{x})^\top \mathbf{G} \nabla \mathbf{u}(\mathbf{x}) \succeq \mathbf{0}.$$

2728 Using observations from the previous step,

$$\begin{aligned} 2729 \quad \|\nabla^2 f(\mathbf{x}) - \mathbf{H}(\mathbf{x})\| &:= \max_{\mathbf{h}: \|\mathbf{h}\|=1} |\langle (\nabla^2 f(\mathbf{x}) - \mathbf{H}(\mathbf{x})) \mathbf{h}, \mathbf{h} \rangle| \\ 2730 &\leq (p-2) \|\mathbf{u}(\mathbf{x})\|^{p-4} \max_{\mathbf{h}: \|\mathbf{h}\|=1} \langle \mathbf{G}\mathbf{u}(\mathbf{x}), \nabla \mathbf{u}(\mathbf{x}) \mathbf{h} \rangle^2 \\ 2731 &\quad + \|\mathbf{u}(\mathbf{x})\|^{p-2} \max_{\mathbf{h}: \|\mathbf{h}\|=1} |\langle \mathbf{G}\mathbf{u}(\mathbf{x}), \nabla^2 \mathbf{u}(\mathbf{x}) [\mathbf{h}, \mathbf{h}] \rangle| \\ 2732 &\leq (p-2) \|\mathbf{u}(\mathbf{x})\|^{p-4} \max_{\mathbf{h}: \|\mathbf{h}\|=1} \langle \mathbf{G}\mathbf{u}(\mathbf{x}), \nabla \mathbf{u}(\mathbf{x}) \mathbf{h} \rangle^2 + \frac{\xi_1}{\sqrt{\mu}} \|\nabla f(\mathbf{x})\|_*. \end{aligned}$$

2736 It remains to notice that, for  $\|\mathbf{h}\| = 1$ , we have:

$$\begin{aligned} 2740 \quad \|\mathbf{u}(\mathbf{x})\|^{p-4} \langle \mathbf{G}\mathbf{u}(\mathbf{x}), \nabla \mathbf{u}(\mathbf{x}) \mathbf{h} \rangle^2 &= \|\mathbf{u}(\mathbf{x})\|^{p-4} |\langle \mathbf{G}\mathbf{u}(\mathbf{x}), \nabla \mathbf{u}(\mathbf{x}) \mathbf{h} \rangle|^{\frac{p}{p-1}} |\langle \mathbf{G}\mathbf{u}(\mathbf{x}), \nabla \mathbf{u}(\mathbf{x}) \mathbf{h} \rangle|^{\frac{p-2}{p-1}} \\ 2741 &= \frac{1}{\|\mathbf{u}(\mathbf{x})\|^{\frac{p}{p-1}}} |\langle \mathbf{G}\mathbf{u}(\mathbf{x}), \nabla \mathbf{u}(\mathbf{x}) \mathbf{h} \rangle|^{\frac{p}{p-1}} |\langle \nabla f(\mathbf{x}), \mathbf{h} \rangle|^{\frac{p-2}{p-1}} \\ 2742 &\leq \xi_0^{\frac{p}{p-1}} \|\nabla f(\mathbf{x})\|_*^{\frac{p-2}{p-1}}, \end{aligned}$$

2745 which gives the desired bound.

2749 3. Consider the approximation

$$2750 \quad \mathbf{H}(\mathbf{x}) := \frac{p-2}{\|\mathbf{u}(\mathbf{x})\|^p} \nabla f(\mathbf{x}) \nabla f(\mathbf{x})^\top \succeq \mathbf{0}.$$

2752 Note this matrix can be equivalently represented as

$$2753 \quad \mathbf{H}(\mathbf{x}) = (p-2) \|\mathbf{u}(\mathbf{x})\|^{p-4} \nabla \mathbf{u}(\mathbf{x})^\top \mathbf{G} \mathbf{u}(\mathbf{x}) \mathbf{u}(\mathbf{x})^\top \mathbf{G} \nabla \mathbf{u}(\mathbf{x}).$$

2754 Therefore, we have

$$\begin{aligned}
 \|\nabla^2 f(\mathbf{x}) - \mathbf{H}(\mathbf{x})\| &\leq \max_{\mathbf{h}: \|\mathbf{h}\|=1} \|\mathbf{u}(\mathbf{x})\|^{p-2} \langle \mathbf{G} \nabla \mathbf{u}(\mathbf{x}) \mathbf{h}, \nabla \mathbf{u}(\mathbf{x}) \mathbf{h} \rangle + \frac{\xi_1}{\sqrt{\mu}} \|\nabla f(\mathbf{x})\|_* \\
 &\leq \xi_0^2 \|\mathbf{u}(\mathbf{x})\|^{p-2} + \frac{\xi_1}{\sqrt{\mu}} \|\nabla f(\mathbf{x})\|_* \\
 &\leq \xi_0^2 \mu^{\frac{2-p}{2(p-1)}} \|\nabla f(\mathbf{x})\|_*^{\frac{p-2}{p-1}} + \frac{\xi_1}{\sqrt{\mu}} \|\nabla f(\mathbf{x})\|_*.
 \end{aligned}$$

2762  $\square$

2763

### 2764 H.3 SEPARABLE OPTIMIZATION

2766 **Example 13** (Separable Optimization: Extended). *Consider the following structure of the*  
 2767 *objective,*

$$f(\mathbf{x}) := \sum_{i=1}^d f_i(\mathbf{x}),$$

2771 where  $f_i(\mathbf{x}) := \ell(u_i(\mathbf{x}))$ , for a convex nonnegative loss function  $\ell$  and mappings  $u_i : \mathbb{R}^n \rightarrow \mathbb{R}$ .  
 2772 Consider logistic regression,  $\ell(t) := \log(1 + \exp(t))$ , and the following Fisher-type Hessian  
 2773 approximation:

$$\mathbf{H}(\mathbf{x}) := \sum_{i=1}^d \nabla f_i(\mathbf{x}) \nabla f_i(\mathbf{x})^\top \succeq \mathbf{0},$$

2776 • Let each  $u_i$  be a nonlinear mapping, and  $f$  be a gradient-dominated (54) function. Assume  
 2777 that, for some  $\xi_0, \xi_1 \geq 0$ :  $\|\nabla u_i(\mathbf{x})\| \leq \xi_0$ ,  $\|\nabla^2 u_i(\mathbf{x})\| \leq \xi_1$ ,  $\forall 1 \leq i \leq d$ . Then, we have

$$\|\nabla^2 f(\mathbf{x}) - \mathbf{H}(\mathbf{x})\| \leq (\xi_0^2 + \xi_1) (f^* + D_c \|\nabla f(\mathbf{x})\|_*^{1+c}).$$

2780 • If the mappings  $u_i(\mathbf{x}) := \langle \mathbf{a}_i, \mathbf{x} \rangle - b_i$  are linear models, then, by setting  $\mathbf{B} := \sum_{i=1}^n \mathbf{a}_i \mathbf{a}_i^\top$ , we  
 2781 have

$$\|\nabla^2 f(\mathbf{x}) - \mathbf{H}(\mathbf{x})\| \leq f(\mathbf{x}) \leq f^* + D \|\nabla f(\mathbf{x})\|,$$

2784 for  $\mathbf{x} \in \mathcal{F}_0$ .

2785

2786 *Proof.* Note that

$$\nabla f(\mathbf{x}) = \sum_{i=1}^d \nabla f_i(\mathbf{x}) = \sum_{i=1}^d \ell'(u_i(\mathbf{x})) \nabla u_i(\mathbf{x}),$$

2790 and

$$\nabla^2 f(\mathbf{x}) = \sum_{i=1}^d [\ell''(u_i(\mathbf{x})) \nabla u_i(\mathbf{x}) \nabla u_i(\mathbf{x})^\top + \ell'(u_i(\mathbf{x})) \nabla^2 u_i(\mathbf{x})].$$

2794 Consider approximation

$$\mathbf{H}(\mathbf{x}) := \sum_{i=1}^d \nabla f_i(\mathbf{x}) \nabla f_i(\mathbf{x})^\top = \sum_{i=1}^d \ell'(u_i(\mathbf{x}))^2 \nabla u_i(\mathbf{x}) \nabla u_i(\mathbf{x})^\top \succeq \mathbf{0}.$$

2797

2798 Then, we have

$$\begin{aligned}
 &\|\nabla^2 f(\mathbf{x}) - \mathbf{H}(\mathbf{x})\| \\
 &= \left\| \sum_{i=1}^d \left[ (\ell''(u_i(\mathbf{x})) - \ell'(u_i(\mathbf{x}))^2) \nabla u_i(\mathbf{x}) \nabla u_i(\mathbf{x})^\top + \ell'(u_i(\mathbf{x})) \nabla^2 u_i(\mathbf{x}) \right] \right\| \\
 &= \left\| \sum_{i=1}^d \left[ \ell'(u_i(\mathbf{x})) (1 - 2\ell'(u_i(\mathbf{x}))) \nabla u_i(\mathbf{x}) \nabla u_i(\mathbf{x})^\top + \ell'(u_i(\mathbf{x})) \nabla^2 u_i(\mathbf{x}) \right] \right\| \\
 &\leq \sum_{i=1}^d \left[ \ell'(u_i(\mathbf{x})) |1 - 2\ell'(u_i(\mathbf{x}))| \|\nabla u_i(\mathbf{x})\|^2 \right] + \sum_{i=1}^d \ell'(u_i(\mathbf{x})) \|\nabla^2 u_i(\mathbf{x})\|,
 \end{aligned}$$

2808 where we used that  $\ell''(t) = \ell'(t) \cdot (1 - \ell'(t))$  and  $\|\nabla u_i(\mathbf{x}) \nabla u_i(\mathbf{x})^\top\| = \|\nabla u_i(\mathbf{x})\|^2$ .  
 2809

2810 Applying our bounds on  $\|\nabla u_i(\mathbf{x})\|$  and  $\|\nabla^2 u_i(\mathbf{x})\|$  for any  $i$ , and using the fact that  $|1 - 2\ell'(t)| < 1$   
 2811 for any  $t$ , we have

$$2812 \quad \|\nabla^2 f(\mathbf{x}) - \mathbf{H}(\mathbf{x})\| \leq (\xi_0^2 + \xi_1) \sum_{i=1}^d \ell'(u_i(\mathbf{x})) \leq (\xi_0^2 + \xi_1) f(\mathbf{x}),$$

2813 where in the last inequality we used that  $\ell'(t) < \ell(t)$  for all  $t$ . Now, consider two important cases.  
 2814

2815 1. Let  $u_i(\mathbf{x})$  be non-linear mappings and let  $f(\mathbf{x})$  be gradient-dominated, i.e., condition  
 2816 (54) holds. Then, we have the bound:  
 2817

$$2818 \quad \|\nabla^2 f(\mathbf{x}) - \mathbf{H}(\mathbf{x})\| \leq (\xi_0^2 + \xi_1) f(\mathbf{x}) \leq (\xi_0^2 + \xi_1) [f^* + D_c \|\nabla f(\mathbf{x})\|_*^{1+c}], \quad 0 \leq c \leq 1.$$

2819 2. Another important case is when  $u_i := \langle \mathbf{a}_i, \mathbf{x} \rangle - b_i$  are linear models, where  $\{\mathbf{a}_i, b_i\}_{i=1}^d$  are given  
 2820 data. Note that in this case, the *Gauss-Newton matrix* is constant, and we can set  
 2821

$$2822 \quad \mathbf{B} := \sum_{i=1}^d \nabla u_i(\mathbf{x}) \nabla u_i(\mathbf{x})^\top = \sum_{i=1}^d \mathbf{a}_i \mathbf{a}_i^\top \succeq \mathbf{0},$$

2823 and it is natural to use it as our choice of the Euclidean norm. At the same time, our *Fisher  
 2824 approximation* becomes

$$2825 \quad \mathbf{H}(\mathbf{x}) := \sum_{i=1}^d \nabla f_i(\mathbf{x}) \nabla f_i(\mathbf{x})^\top = \sum_{i=1}^d \ell'(u_i(\mathbf{x}))^2 \mathbf{a}_i \mathbf{a}_i^\top \succeq \mathbf{0}.$$

2826 Therefore, we result in bound  
 2827

$$2828 \quad \begin{aligned} \|\nabla^2 f(\mathbf{x}) - \mathbf{H}(\mathbf{x})\| &= \left\| \sum_{i=1}^d (\ell''(u_i(\mathbf{x})) - \ell'(u_i(\mathbf{x}))) \mathbf{a}_i \mathbf{a}_i^\top \right\| \\ 2829 &\leq \sum_{i=1}^d \ell'(u_i(\mathbf{x})) |1 - 2\ell'(u_i(\mathbf{x}))| \leq \sum_{i=1}^d \ell'(u_i(\mathbf{x})) \leq f(\mathbf{x}), \end{aligned}$$

2830 which corresponds to the previous case with  $\xi_0 = 1$  and  $\xi_1 = 0$ . Due to convexity of  $f$ , we have  
 2831

$$2832 \quad \|\nabla^2 f(\mathbf{x}) - \mathbf{H}(\mathbf{x})\| \leq f(\mathbf{x}) \leq f^* + D_0 \|\nabla f(\mathbf{x})\|_*,$$

2833 for all points from the initial sublevel set:  $\mathbf{x} \in \mathcal{F}_0$ , where all iterates of our algorithm belong to.  $\square$   
 2834

#### 2835 H.4 RECOVERING COMPLEXITIES FOR PRACTICAL APPROXIMATIONS

2836 **Contribution of the Degrees of  $\pi$ .** As we saw, the general form of our lower bound is given by  
 2837 structural assumption (10), for all problem cases, it appears to be the harmonic mean of simple  
 2838 monomials:  $\pi(t)^{-1} = \sum_{i=1}^d M_{1-\alpha_i} t^{-\alpha_i}$ , where  $\alpha_i \in [0, 1]$  are some degrees that depend on  
 2839 the problem class and on the level of Hessian approximation  $\beta$ . For example, let us assume that  
 2840  $\pi(t)$  is the harmonic mean of two monomials (as, e.g. for  $(L_0, L_1)$ -functions (77)):  $\pi(t) =$   
 2841  $(M_1 t^{-\alpha_1} + M_2 t^{-\alpha_2})^{-1}$ , for some  $M_1, M_2 > 0$  and  $0 \leq \alpha_1, \alpha_2 \leq 1$ . Then, for the non-convex case,  
 2842 the global complexity of the method is (Corollary 1):  $K = O(F_0 \cdot [\frac{M_1}{\varepsilon^{1+\alpha_1}} + \frac{M_2}{\varepsilon^{1+\alpha_2}}])$  iterations to  
 2843 solve the problem, where  $\varepsilon > 0$  is the target accuracy for the gradient norm. We show that the fastest  
 2844 possible rate corresponds to the smallest degree,  $\alpha := \min_{1 \leq i \leq d} \alpha_i$ , while the other exponents correspond  
 2845 to additional slow terms. Notably, our proof is based on first selecting the smallest  $\alpha$ , to establish the  
 2846 progress, which highlights its importance.

2847 **The definition of  $\pi(\cdot)$ .** This paragraph is an extended version of a short note in Section 5. The notion  
 2848 of  $\pi$  (10) is a structural assumption on the global behavior of the Gradient-Normalized Smoothness  
 2849  $\gamma(\cdot)$ . It is needed to translate our knowledge of a problem class to the complexity bounds in their  
 2850 standard form. Formally there could be many choices for  $\pi$ , while  $\gamma(\cdot)$  is defined in a unique way.  
 2851 However, it is important that our method does not need to know the particular problem class or the  
 2852 particular  $\pi$ , and by implementing a simple adaptive search (Algorithm 3) the method becomes  
 2853

parameter-free. Let us consider several important examples of known structures of the lower bound  $\pi$ .

- Function with  $L$ -Lipschitz Hessian (Example 1 with  $\nu = 1$ ). Then,  $\gamma(x) \geq (\frac{2}{L} \|\nabla f(x)\|)^{1/2}$ . Hence,  $\pi(t) = (\frac{2}{L} t)^{1/2}$ , and the corresponding global complexity in the convex case (Theorem 2) is

$$O\left(\sqrt{\frac{LD^3}{\varepsilon}}\right),$$

where  $\varepsilon > 0$  is the target accuracy for the functional residual, and  $D$  is the diameter of the initial sublevel set.

- Convex functions with  $L$ -Lipschitz Third Derivative (Example 2 with  $\nu = 1$ ). Then,  $\gamma(x) \geq (\frac{1}{2L} \|\nabla f(x)\|)^{1/3}$ . Hence,  $\pi(t) = (\frac{1}{2L} t)^{1/3}$ . The corresponding complexity of the method (Theorem 2) is

$$O\left(\left[\frac{LD^4}{\varepsilon}\right]^{1/3}\right).$$

- Quasi-Self-Concordant functions (Example 3). Then,  $\gamma(x) \geq \frac{1}{M}$ . Hence,  $\pi(t) \equiv \frac{1}{M}$ , and the corresponding complexity (Theorem 2) is

$$O\left(MD \log \frac{1}{\varepsilon}\right) \quad (\text{global linear rate of convergence}).$$

- $(L_0, L_1)$ -smooth functions (Example 4). Then,  $\gamma(x) \geq \frac{1}{1+e} \frac{\|\nabla f(x)\|}{L_0 + L_1 \|\nabla f(x)\|}$ . Hence,  $\pi(t) = \frac{1}{1+e} \left[ \frac{L_0}{t} + L_1 \right]^{-1}$ . Note that this expression also matches the structural assumption on  $\pi$  in (10). And the corresponding complexity of the method becomes (Theorem 2):

$$O\left((L_1 D + \frac{L_0 D^2}{\varepsilon}) \log \frac{1}{\varepsilon}\right).$$

We see that we recover the right complexities in all known special cases. Every particular problem class leads to the specific structure of the lower bound  $\pi(\cdot)$ . However, the power of our result is that we do not need to know and fix the problem class in the method, adapting to the best possible bound. One interesting example follows from the basic properties of  $\gamma$  under simple operations (Section 2). Let us assume that our objective is represented as a finite sum of functions:  $f(x) = \frac{1}{n} \sum_{i=1}^n f_i(x)$ . Every function in the sum might belong to a different problem class, and therefore, every function  $f_i$  might have a different lower bound  $\pi_i(t)$  (e.g. as in the above examples). In this case, the whole objective does not belong to any 'standard' problem class, and therefore, simple assumptions such as Lipschitzness of the Hessian are not applicable in this case. However, the lower bound  $\pi(\cdot)$  for the whole objective can be computed as the Harmonic mean of the lower bounds for the components:

$$\pi(t) \geq \left( \sum_{i=1}^n \pi_i(t) \right)^{-1}$$

**The effect of inexact Hessian.** This paragraph is also an extension of Section 5, designed to show how we derive complexities for a method with inexact Hessian using condition (12). If we assume (12), then the Gradient-Normalized Smoothness, when using the Hessian approximation, is bounded according to our rules, as:

$$\gamma(\mathbf{x}) \geq (\gamma_1(\mathbf{x})^{-1} + \frac{\mathbf{C}_1}{\|\nabla f(\mathbf{x})\|} + \frac{\mathbf{C}_2}{\|\nabla f(\mathbf{x})\|^\beta})^{-1},$$

where  $\gamma_1(\mathbf{x})$  is the Gradient-Normalized Smoothness for the exact Hessian. In other words, if we know the lower bound  $\pi(\cdot)$  for the exact Hessian (e.g. any of the problem classes above), then  $\pi(\cdot)$  for the method with inexact Hessian can be computed in a form that satisfies the structural assumption 10:

$$\pi(t) = \left( \frac{1}{\pi_1(t)} + \frac{\mathbf{C}_1}{t} + \frac{\mathbf{C}_2}{t^\beta} \right)^{-1}.$$

2916 And we immediately obtain the complexity result for the method with inexact Hessian (Corollaries 2  
 2917 and 3). We see that the total complexity of the method becomes the sum of the complexity for the  
 2918 exact case plus two additional terms that depend on  $\mathbf{C}_1$ ,  $\mathbf{C}_2$ , and the degree of approximation  $\beta$ .  
 2919

2920 One important consequence of our theory is that when  $\mathbf{C}_1 \approx 0$  is very small or zero, and  $\beta < \alpha$ ,  
 2921 where  $\alpha$  is the minimal degree of the monomial in the expression for  $\pi$ , then the rate of convergence  
 2922 is not affected by the Hessian inexactness (see also Figure 1). We see that these conditions hold, e.g.,  
 2923 for the Fisher and Gauss-Newton approximations in several applications (Examples 6, 7, 8), where  
 2924 we have  $\beta = 0$ . Therefore, in these applications, the use of the inexact Hessian will give us *the same*  
 2925 *global rate* as the exact Newton method, while computation of every step is much more efficient.  
 2926

2927 Let us consider the concrete example with the logistic regression problem and the Fisher approxima-  
 2928 tion matrix (3). The logistic regression is Quasi-Self-Concordant, and hence  $\pi_1(t) \equiv \frac{1}{M}$  (Example 3),  
 2929 where  $\pi_1(t)$  is the bound for the Gradient-Normalized Smoothness with exact Hessian. When using  
 2930 the Fisher approximation, we have (12) satisfied with  $\mathbf{C}_1 = f^*$ ,  $\mathbf{C}_2 = D$ , and  $\beta = 0$  (Example 6).  
 2931 Therefore, the Gradient-Normalized Smoothness for the Fisher approximation is bounded as:  
 2932

$$\gamma(\mathbf{x}) \geq \pi(\|\nabla f(\mathbf{x})\|), \quad \text{with } \pi(t) = \left(M + D + \frac{f^*}{t}\right)^{-1},$$

2933 and the corresponding complexity becomes:

$$O\left(\left[MD + D^2 + \frac{f^* D^2}{\varepsilon}\right] \cdot \log \frac{1}{\varepsilon}\right).$$

2934 If  $f^* \approx 0$  (well separated data), this gives a very fast global linear rate. To the best of our knowledge,  
 2935 we are the first to establish such a rate for the inexact Newton method with the Fisher approxima-  
 2936 tion matrix. Similar reasoning also work for applications with Nonlinear Equations (Example 7) and Soft  
 2937 Maximum (LogSumExp) (Example 8) with Gauss-Newton approximations.  
 2938

2939 Below, we present a formal statement, serving as a good example of the practical applicability of our  
 2940 notion. In Proposition 9, we show that our method (1) achieves a global linear rate of convergence on  
 2941 the logistic regression problem.  
 2942

2943 **Proposition 9** (A global linear rate of convergence for the inexact Hessian.) *Consider the logistic  
 2944 regression objective  $f(\mathbf{x}) = \sum_{i=1}^n f_i(\mathbf{x})$ , where  $f_i(\mathbf{x}) := \log(1 + \exp(\langle \mathbf{a}_i, \mathbf{x} \rangle - b_i))$ . Then,  
 2945 for Algorithm 1 with*

$$\mathbf{H}(\mathbf{x}) := \sum_{i=1}^n \nabla f_i(\mathbf{x}) \nabla f_i(\mathbf{x})^\top \succeq \mathbf{0}, \quad (\text{Fisher approximation matrix})$$

2946 the corresponding complexity is

$$O\left(\left[MD + D^2 + \frac{f^* D^2}{\varepsilon}\right] \cdot \log \frac{1}{\varepsilon}\right).$$

2947 *If the data is well separated ( $f^* \approx 0$ ), this gives a global linear rate.*

2948 *Proof.* Assuming (12), the Gradient-Normalized Smoothness when using the inexact Hessian is  
 2949 bounded as

$$\gamma(\mathbf{x}) \geq (\gamma_1(\mathbf{x})^{-1} + \frac{\mathbf{C}_1}{\|\nabla f(\mathbf{x})\|} + \frac{\mathbf{C}_2}{\|\nabla f(\mathbf{x})\|^\beta})^{-1}, \quad (\text{The "Hessian inexactness" property})$$

2950 where  $\gamma_1(\mathbf{x})$  is the Gradient-Normalized Smoothness for the exact Hessian. Since  $f(\mathbf{x})$  is Quasi-Self-  
 2951 Concordant,  $\gamma_1(\mathbf{x}) \geq \frac{1}{M}$ . According to Example 6,  $\mathbf{H}(\mathbf{x})$  satisfies condition (12) with  $\mathbf{C}_1 = f^*$ ,  
 2952  $\mathbf{C}_2 = D$ , and  $\beta = 0$ . Then, we result in the following bound:  
 2953

$$\gamma(\mathbf{x}) \geq \left(M + D + \frac{f^*}{\|\nabla f(\mathbf{x})\|}\right)^{-1}.$$

2954 According to Corollary 2, complexity for the method with inexact Hessian becomes:

$$K = O\left(\left[MD + D^2 + \frac{f^* D^2}{\varepsilon}\right] \cdot \log \frac{1}{\varepsilon}\right).$$

2955 Here, the term  $MD \cdot \log \frac{1}{\varepsilon}$  corresponds to the previously established complexity for the method with  
 2956 exact Hessian (see Table 1). When the optimal value  $f^* \approx 0$ , we result in the global linear rate of  
 2957 converge.  $\square$